

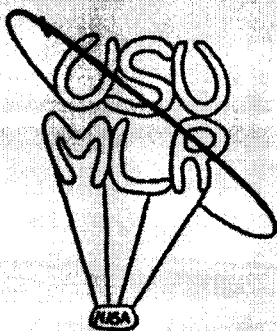
NGT 21-002-080

1N-85-CR

128702

1229

INTERIM REPORT
MARS LANDER/ROVER VEHICLE DEVELOPMENT
An Advanced Space Design Project
for
USRA and NASA/OAST
WINTER 1987



UTAH STATE UNIVERSITY
Logan, Utah

(NASA-CR-182562) MARS LANDER/ROVER VEHICLE
DEVELOPMENT: AN ADVANCED SPACE DESIGN
PROJECT FOR USRA AND NASA/OAST Interim
Report (Utah State Univ.) 122 p CSCL 134

H38-20226

Unclass

11/85 0123702

INTERIM REPORT
(Winter Quarter)

1.0	Introduction.....	1
2.0	Environment and Trajectory Group.....	2
3.0	Payload Subsystem Group.....	20
4.0	Ground Systems Group.....	29
5.0	Balloon System Group.....	56
6.0	Conclusion.....	68
	Appendices.....	69

1.0 Introduction

1.1 Report Objective

This report delineates and explains the accomplishments of the Utah State University (USU) Mars Lander/Rover (MLR) Design class during Winter Quarter 1987. This segment of the course built upon the achievements of the previous quarter, resulting in the more defined, realistic system presented in the following pages.

1.2 Operational Scenario

The baseline for this project has been derived from various sources, most notably the National Commission on Space Report. This information, combined with the decision that delivering the payload to Mars orbit would not be considered within the scope of this study, resulted in the following overall mass constraint. It was assumed that future launch vehicles would be capable of delivering 5000 kg to the surface of Mars. Further, it was decided that this mass would be made up of five separate lander vehicles. Each of these vehicles consists of a lander ship (termed the "mother ship"), a local sample acquisition rover (SAR), and an airborne balloon rover. This system was selected from a group of candidates, having been viewed the most feasible and effective method of accomplishing the goal of wide-scale characterization of Mars.

1.3 Organization of Report

The balance of the report is divided into sections pertaining to various aspects of the system development. Each is presented as a complete sub-element of this document, and consequently, may be read in a different order if desired. References are found at the end of each section. Supporting appendices are located in a separate section at the end of the document, and are numbered corresponding to the respective sections of text.

1.4 Goals

During this quarter it was intended that the overall Mars Lander/Rover (MLR) system be more clearly defined, as well as the further development of solutions to the challenges involved in this mission. This then provided a sound basis for the selection of certain components of the MLR design for in-depth development during Spring Quarter, the final phase of this design course. These objectives were accomplished and the results comprise the following sections.

2.0 Environment and Trajectory Group

2.1 Introduction

The purpose of this report is to summarize the progress made by the Environment and Trajectory group since the beginning of Winter Quarter, 1987 in the Mars Lander/Rover design class. Included are a description of our goals, a brief statement of the problems unique to our group, the assumptions made in attacking the problem, and the methods with their subsequent results.

2.2 Goals

The Environment and Trajectory group is responsible for providing trajectory information for a given Mars lander configuration and operational scenario. These calculations are based on a suitable choice of Mars atmospheric model, and simplifying assumptions on the geometry of the lander. The results of these computations include position, velocity, mass, and acceleration of the vehicle as a function of time. Since the Viking mission was a proven success, many of its features were incorporated into our model.

The basic assumption as a foundation for our calculations is that it will be possible in the future to put 5,000 kg on the surface of Mars. We further assume this mass will be distributed: 1,000 kg will be landed at five different locations on the Martian surface. These locations will be detailed in Section 2.5 of this report. Thus, the problem that we must attack is to determine the masses of each of the five Lander/Rovers before they are launched from the Orbiter.

Several simplifications were employed in preparation of the model to calculate entry and landing trajectories in light of time available for this project. It is structured, however, to allow parts of it to be easily changed when more precision is required.

2.3 Operational Scenario for the Orbiter/Lander/Rover System

The calculations to be presented here are modeled, in part, after the Viking mission, in which a spacecraft consisting of an orbiter and a lander was sent to Mars for the purpose of scientific investigation of its atmosphere and surface. Upon arrival near the planet, a thruster firing placed the spacecraft in a synchronous, elliptical orbit about Mars. After separation of the Viking lander from the orbiter, a retrograde burn was effected for de-orbit of the lander. The vehicle entered the Martian atmosphere being slowed initially by atmospheric drag only. As Viking neared the surface to about 5.8 km altitude, its "aeroshell" was ejected and a parachute was deployed to further slow the vehicle; at about 1.2 km altitude, the parachute was ejected and, during the final descent, the retro-rockets were fired for soft landing.

2.3.1 The Mars Orbiter

Initially, the five Lander/Rovers will be attached to an Orbiter which is in an elliptical orbit about Mars roughly in the plane of the ecliptic. The purpose of the Orbiter is to relay communications from Lander/Rovers within reasonable time intervals. The parameters of this orbit have not yet been determined.

To estimate the mass of the Orbiter, we have assumed that it will be roughly the same as that of the Viking (2,325 kg with fuel, 902 kg without), with a conservative added-mass allowance of 400 kg for hardware to attach the five Lander/Rovers, and an allocation of roughly 6,100 kg extra rocket fuel, to be used for orbital insertion about Mars. The value for this extra rocket fuel mass was estimated by linear scaling, using the Viking orbiter fuel to total Viking system mass ratio of 0.4, and assuming that the total mass of the five Lander/Rovers attached to the Orbiter will be no greater than 10,000 kg. Therefore, an upper limit for the mass of the entire Mars Orbiter/Lander/Rover system before insertion into orbit about Mars is 18,833 kg; i.e., 8,833 kg for the Orbiter and 10,000 kg for the Lander/Rovers. In the sections below, detailed analyses and calculations are presented with the purpose of modifying the 10,000 kg initial estimate for the total mass of the Lander/Rovers attached to the Orbiter.

2.3.2 The Mars Lander/Rovers

The five Lander/Rovers attached to the Orbiter in orbit about Mars, will be deployed at various locations on the planet's surface. Thus, each of the Lander/Rovers must be equipped with an amount of fuel sufficient to maneuver to the proper orbital inclination and, then, effect the proper retrograde burn to de-orbit and land at its target site. Furthermore, each of the Lander/Rovers will be equipped with scientific instrumentation specific to its landing site. For example, one of the Lander/Rovers will land at the northern ice cap; it must have extra fuel to get into a high latitude orbit, and be outfitted with instruments to conduct analyses of the ice.

The phases in the mission scenario for each of the Lander/Rovers from Orbiter to ground are:

- 1) Separation from Orbiter/Lander/Rover system
- 2) Change orbital inclination (if necessary)
- 3) Fire retrograde thrusters for de-orbit
- 4) Eject "aeroshell" - deploy parachute (5.8 km)
- 5) Eject parachute - fire descent propulsion (1.2 km)
- 6) Touchdown

2.4 Lander/Rover Trajectory Calculations

We have chosen to do the entry and landing trajectory calculations using a two-dimensional, polar (r , θ) coordinate, inertial system in a given orbital plane. By standard convention, $\theta = 0^\circ$ defines the periapsis of the lander orbit about Mars. We assume that the lander is initially in a closed orbit about Mars, where the initial conditions and other details of its motion can be obtained using Kepler's equations. If the orbital inclination of a given Lander/Rover must be changed, it will be accomplished by an instantaneous delta-vee rocket burn at the apoapsis of the elliptical orbit. For all rocket fuel calculations, we assumed hydrazine ($I_{sp}=235$). In addition, we assume the lander has a given mass and that it has a spherical shape of given radius.

2.4.1 Orbital Plane Changes

The additional fuel required for changes in the orbital plane of a

given Lander/Rover was calculated for the standard Viking orbit; i.e., periapsis = 4.9×10^6 m, apoapsis = 3.6×10^7 m. The computations were carried out assuming an instantaneous burn at apoapsis, where the required fuel is expected to be a minimum, for an initial Lander/Rover mass in the range 1,500 kg to 2,100 kg. The results are shown in Figure 2.4.1.

2.4.2 Mars Entry Vehicle De-Orbit Burn

Design of the Mars entry vehicle required a knowledge of the amount of fuel necessary to alter the orbit so that the vehicle will enter the atmosphere at a flight path angle dictated by the aerodynamic characteristics of the vehicle. In conducting an investigation of the fuel consumption, several assumptions were made:

- 1) The vehicle is initially in an orbit of eccentricity, $e=.75$, and semi-major axis of $a=19,654$ km (initial orbit of Viking I). Mission requirements may force selection of a different initial orbit, but it is reasonable to consider this orbit because a highly elliptical orbit uses less fuel in the Mars capture burn than would a more circular orbit, and it has a period of nearly 1 sol, so that the orbiter passes over a point on the surface at the same time of day every orbit.
- 2) The total entry vehicle mass initially equals 1,400 kg.
- 3) The propellant is hydrazine ($I_{sp}=235s$).
- 4) The thrust is always oriented to directly oppose the velocity.
- 5) The vehicle is considered to have entered the atmosphere at an altitude of 250 km.

To find the fuel consumption, a 4th order Runge-Kutta algorithm integrated the equations of motion for an orbiting body acted upon by a thrust. The orbit parameters were checked each iteration, and when the periapsis altitude was found to have dropped to the planet's surface, the program ended. Elapsed burn time, fuel used, and descent orbit parameters were then outputted. The accompanying graphs display the effect of fuel burn rate and true anomaly at the de-orbit burn start, on fuel efficiency and other parameters.

2.4.3 Vehicle Drag Due to the Martian Atmosphere

The drag force on the lander due to atmospheric friction is given by:

$$f = (\pi/2)a^2C_D\rho v^2 \quad (1)$$

where a is the radius of the lander, C_D is the coefficient of drag, ρ is given by equation 2 below, and v is the lander velocity [Swanson, 1970]. The coefficient of drag is well-known as a function of Reynolds number N_{RE} (see Figure 2.4-8). We have used an interpolation routine to compute C_D from tabulated experimental data for $N_{RE} < 2 \times 10^5$, and we have assumed $C_D=0.4$, for Reynolds numbers greater than 2×10^5 .

For the parachute calculations, we assumed a flat-plate model of a given radius and a coefficient of drag of 0.55, corresponding to that of a disk-gap band parachute as used on Viking. This added force term due to parachute drag comes in to the calculations only when the Lander/Rover is between 5.8 and 1.2 km high.

In order to justify our simplifying assumption on the Lander/Rover geometry for entry and landing calculations, the remainder of this subsection is devoted to a comparison of the drag coefficients of a sphere and the Viking aeroshell.

The computer generated model developed by our trajectory, environment, and landing sub-group used drag-coefficient data derived from classical geometrical drag models for spheres. This data is based on fundamental fluid mechanics and is shown in Figure 2.4-8.

Actual Viking I data, while largely based on pressure, acceleration, and mass spectrometer measurements, is similarly matched to experimental drag-coefficient data for spherical models in the Reynold's number range of 10 to 10^2 . In other words, measured data had to be supplemented by experimental data to construct the Viking I drag-coefficient curves. This actual drag-coefficient data from Viking I is shown in Figure 2.4-9.

Our model has provided a valid approximation for Mars entry calculations. Preliminary data runs of our program have shown any error to be conservative in drag-coefficient determination. This error is conservative in the range of ten to thirty percent (C_D error of .1 to 1). These error bounds give our model both a reasonable result and a desirable conservative range.

2.4.4 Model Atmosphere for Mars

To keep the entry and landing calculations simple, we have assumed that the Martian atmosphere is composed of pure carbon dioxide gas with a density, ρ , that varies exponentially in altitude, z , with a constant scale height, H , as follows:

$$\rho = \rho_0 e^{(-z/H)} \quad (2)$$

where $H = k_B T / mg = 11.28$ km, k_B is Boltzmann's constant, $T = 220$ K is the temperature, $g = 3.73$ m/sec², and m is the mass of a CO₂ molecule. $\rho_0 = 1.426 \times 10^{-2}$ kg/m³ was computed assuming that the Martian surface pressure is 6 mbar.

2.4.5 Descent Propulsion Calculations

To calculate the fuel burn rate (kg of fuel per second) and burn time (the thrusters firing is assumed to occur in the time interval from when the parachute is ejected to touchdown on the Martian surface) for the terminal descent propulsion system to soft-land the Lander/Rover, the equations of motion were written for a one-dimensional Cartesian coordinate system, where the forces considered were constant terms, one for gravity near the Martian surface and the other for rocket engine thrust. In this calculation, drag due to atmospheric friction is small and, therefore, was neglected. Thus, equations for the velocity and position can be solved for in closed form, being functions of the burn rate and burn time. Using initial and final conditions (that is, at the start and the end of the burn), for position and velocity, the resulting transcendental equations can be inverted for burn rate and burn time.

2.4.6 Computer Code for Entry and Landing Trajectory

The force term given by equation (1) was incorporated into the equations

of motion for the lander entry. The variables to be integrated in time, and the parameters that must be assumed or determined from the trajectory are:

- 1) Position coordinates, r and θ
- 2) Velocities in the r and θ directions, v_r and v_θ
- 3) Fuel mass required for de-orbit
- 4) Initial position of de-orbit
- 5) "Aeroshell" drag characteristics
- 6) Parachute diameter
- 7) Parachute terminal velocity
- 8) Fuel mass required for final soft-landing
- 9) Maximum design loads encountered

These are solved numerically using a predictor-corrector method, which has been fully tested and yields satisfactory results. The programs, presented in the Appendix, are well documented and can be easily followed.

2.4.7 Numerical Calculations

The initial conditions, as input for the computer programmed simulations in the model calculation presented here, are as follows:

- 1) Vehicle radius is 2 m
- 2) Initial orbit: $r=4.9 \times 10^6$ m (periapsis)
 $r=3.5 \times 10^7$ m (apoapsis)
- 3) Parachute radius is 14 m
- 4) "Aeroshell" ejection (192 kg ejected) at 5.8 km
- 5) Parachute deployment at an altitude of 5.8 km
- 6) Parachute ejection altitude (50 kg ejected) is 1.2 km

Using the above parameters, several runs were made, varying initial Lander/Rover mass M_i , (kg), (after optional change of orbital plane), position of de-orbit burn, θ_i (degrees), and change in velocity at de-orbit, Δv (m/sec). At $\theta_i=200^\circ$, the landing time was about 6.5 hours; at $\theta_i=230^\circ$, the landing time was about 2.5 hours. For all cases, the parachute terminal velocity was about 45 m/sec. The remaining important results from the calculations, namely the final mass, M_f (kg), the maximum loads (which always occurred when the parachute was deployed), L_{\max} (m/sec²), and the final position on the surface, θ_f (degrees), are tabulated below for a given M_i , θ_i , and Δv :

Run	Δv	M_i	M_f	L_{\max}	θ_i	θ_f
A	150	1500	1054	*	200	340
B	150	1450	1011	1104	200	340
C	200	1450	984	490	200	315
D	250	1450	957	786	200	300
E	200	1475	1005	491	200	315
F	300	1475	952	1637	230	361
G	300	1550	1013	1298	230	261
H	200	1475			230	**

* Not computed for this run

** Δv was too small - Lander/Rover "skipped" off atmosphere

For $\theta_i=230^\circ$, higher design loads were encountered and more Δv (meaning more rocket fuel) was required. For $\theta_i=200^\circ$, the amount of Δv affected the design loads experienced, as well as the angle of entry into the atmosphere, and final value for θ_f . Run C gives the lowest value for L_{max} .

From the above results, the initial mass of each Lander/Rover must be in the range 1450-1850 kg, depending on whether a change in orbital-plane is necessary. This is close to our estimate of $M_i=2000$ kg from scaled Viking data.

Table 2.4-1

Orbit Parameters Before De-Orbit Burn

semi-major axis:	19,653.75 km
eccentricity:	0.749 95
argument of periapsis:	0.0

Orbit Parameters After Retro Burn

true anomaly at burn start:	205	225
fuel used (kg):	94.5	159.4
burn duration (sec):	945.0	1,594.0
semi-major axis (km):	17,248.1	14,147.9
eccentricity:	0.803	0.760
argument of periapsis (deg):	8.98	17.34
flight path angle at entry (250 km):	-14.32	-14.09
entry velocity (km/sec):	4.59	4.53

LIST OF FIGURES

- Figure 2.4-1 Orbital plane change versus hydrazine fuel required for various values of the initial Lander/Rover mass.
- Figure 2.4-2 De-orbit Fuel Consumption. A low thrust burn uses less fuel than a high thrust burn if it starts before the true anomaly reaches 180 degrees. Beyond apoapsis, a high thrust burn is more efficient. However, in the range of 45 degrees either side of apoapsis, the differences become so little that the problem may be treated as an instantaneous burn and an instantaneous change of velocity. Fuel consumed is therefore given by: $M_f = M_0(1 - \ln(-(V_0 - V)/I_{sp} * 9.8))$.
- Figure 2.4-3 De-orbit Duration. The burn time is directly proportional to the fuel mass used for constant thrust:
$$t_b = M/(\Delta M/\Delta t)$$
- Figure 2.4-4 Semi-major Axis of Entry Ellipse. Since the energy of an orbit is inversely proportional to its semi-major axis, burning at periapsis will use the least amount of fuel.
- Figure 2.4-5 Eccentricity at De-orbit Burn End. Burning near apoapsis increases the eccentricity of the orbit slightly, causing a steeper angle of entry.
- Figure 2.4-6 Periapsis Angle of Descent Ellipse. This shows the effect of the starting position on the final orientation of the argument of periapsis. A burn beginning anywhere other than at apoapsis of the original orbit will rotate the line of apsides of the descent ellipse with respect to the former. For a synchronous primary orbit, the periapsis of the orbiter would not be directly over the landing site if the periapsis rotates.
- Figure 2.4-7 Entry Flight Path Angle. This is the governing parameter for an aerodynamic entry. When the lift and thermal characteristics of the entry vehicle are understood, the optimal entry angle can be chosen. This in turn indicates the true anomaly at which the de-orbit burn should start.

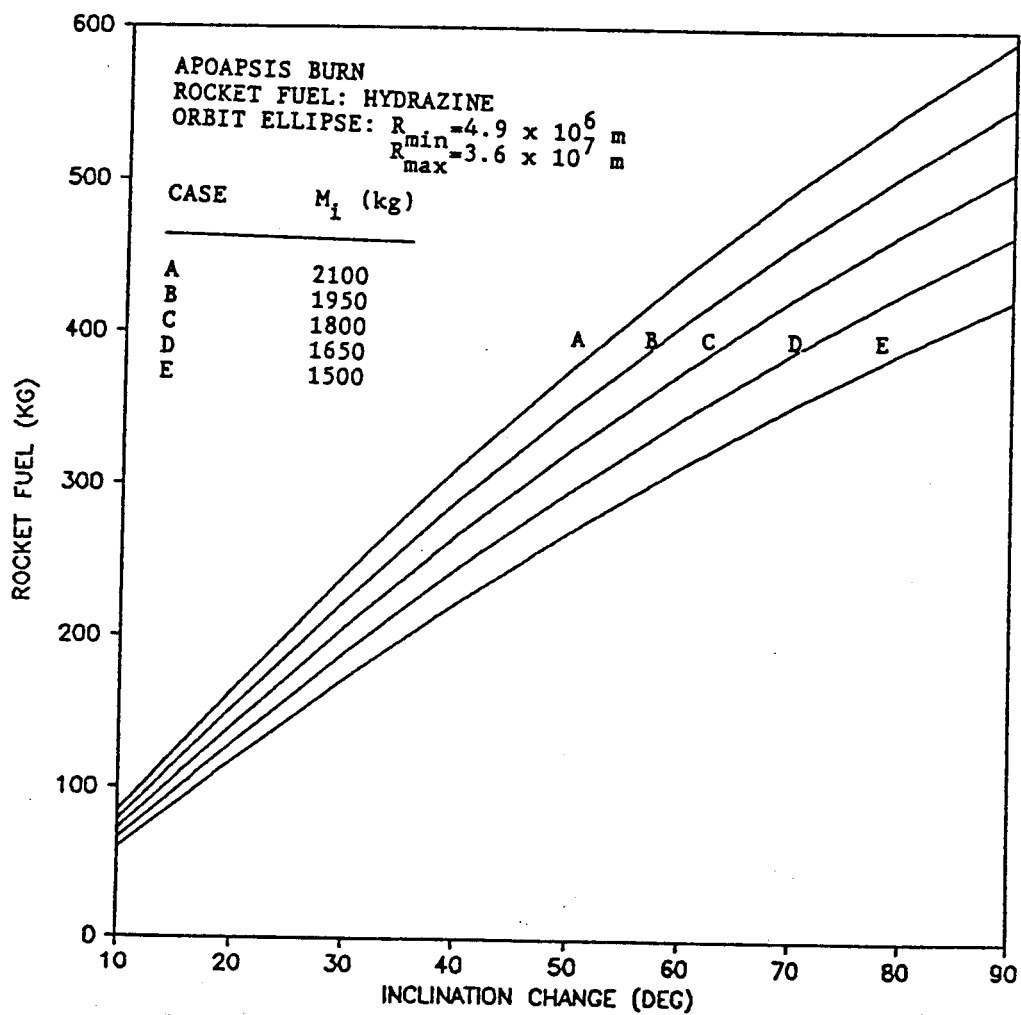


Figure 2.4-1

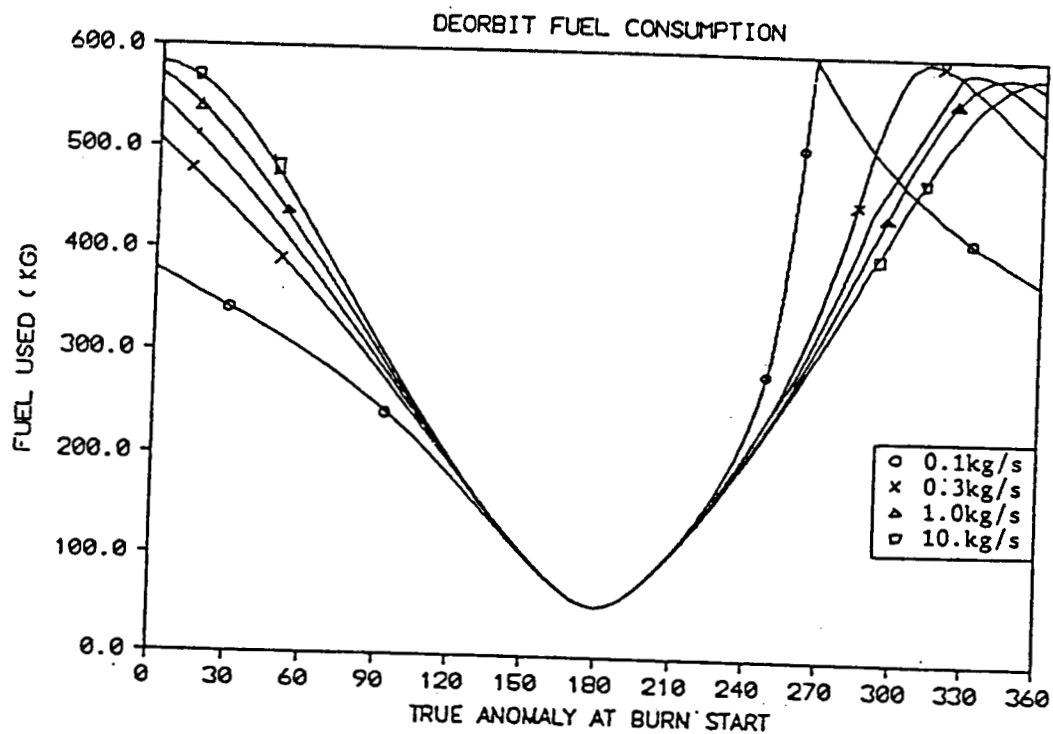


Figure 2.4-2

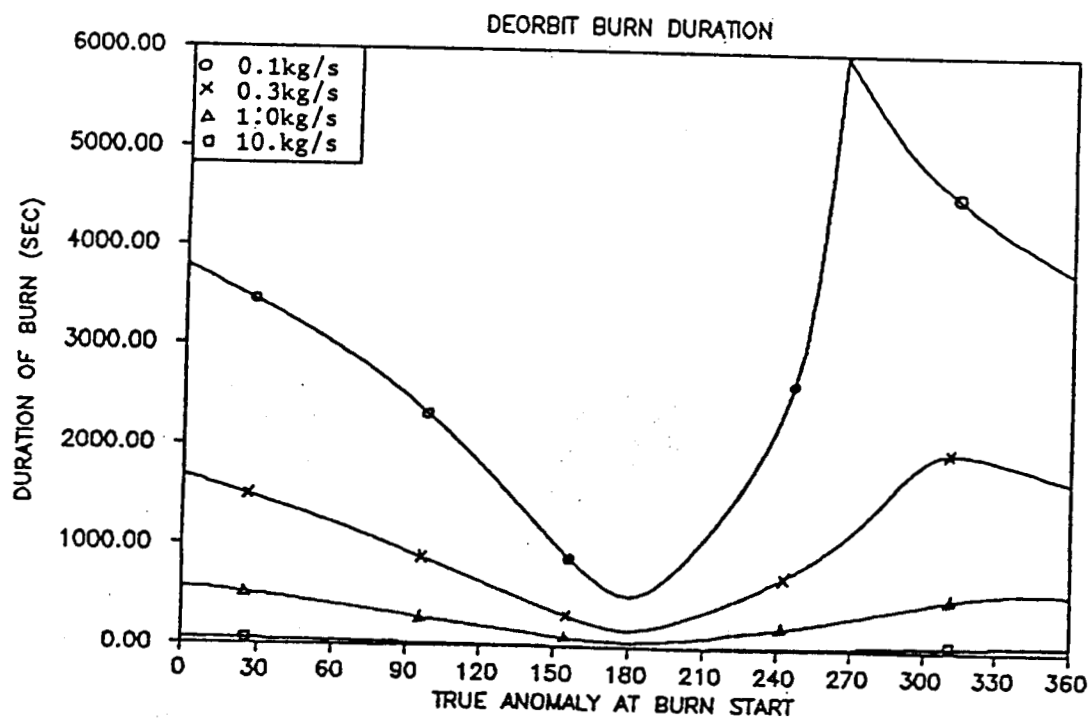


Figure 2.4-3

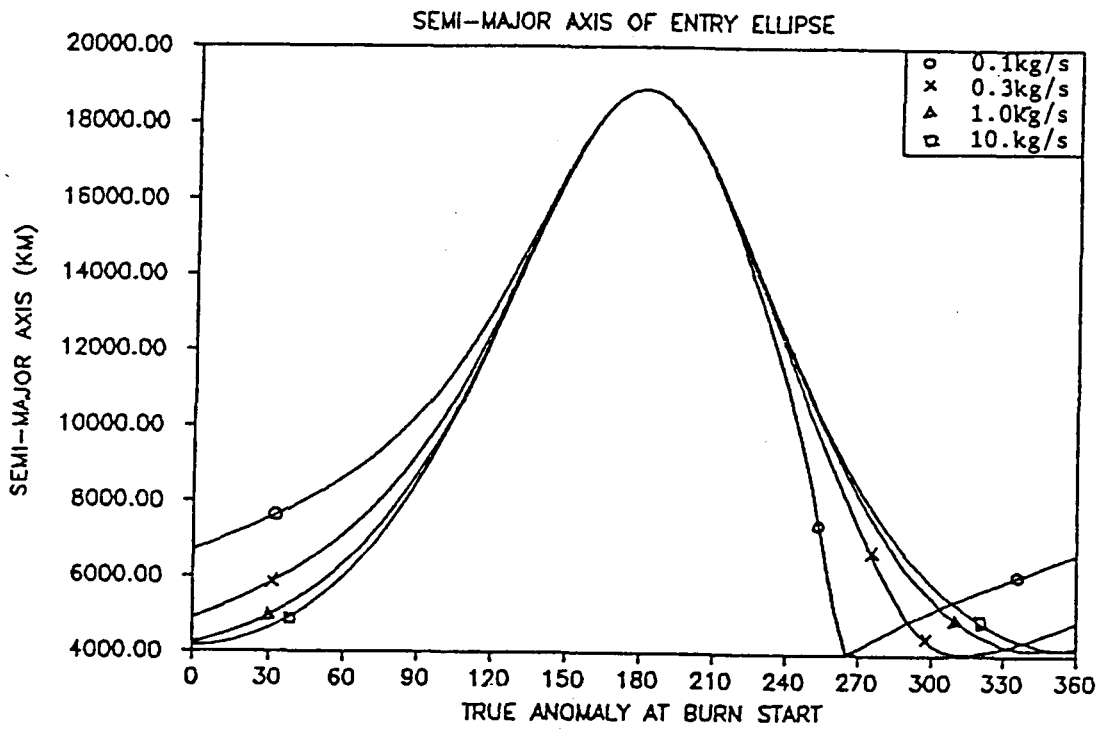


Figure 2.4-4

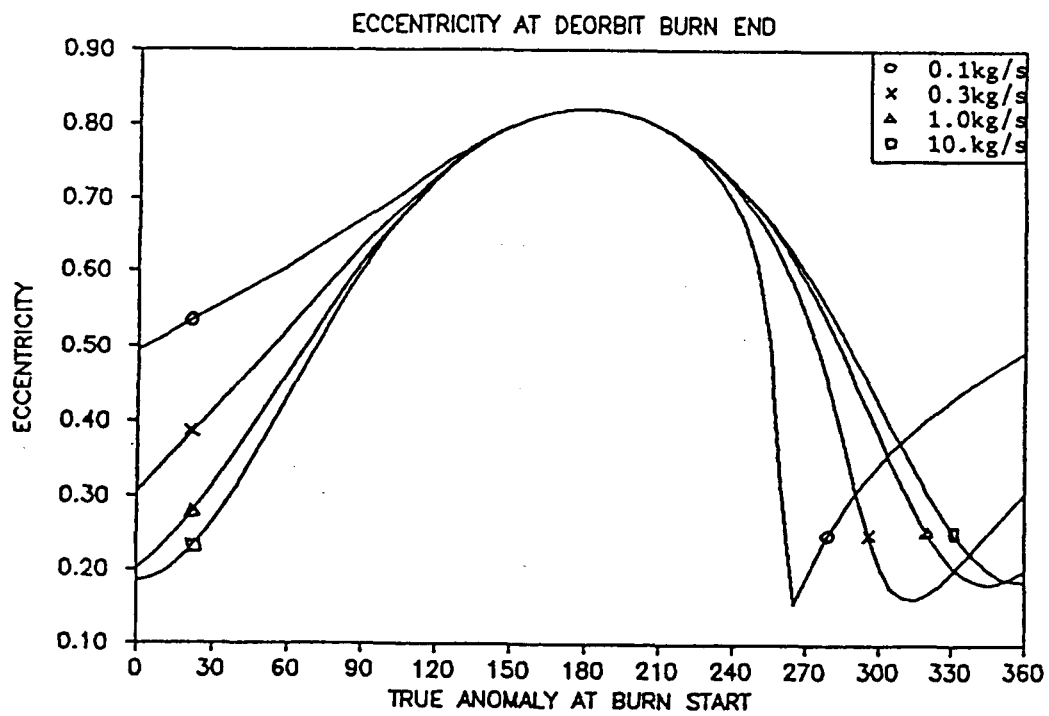


Figure 2.4-5

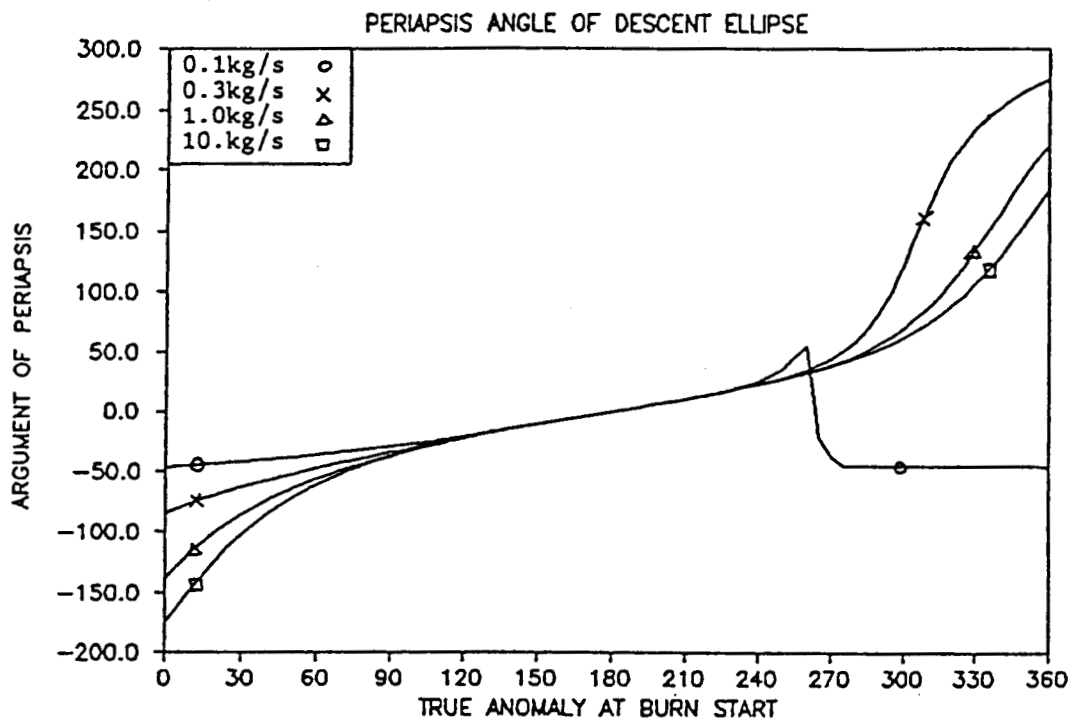


Figure 2.4-6

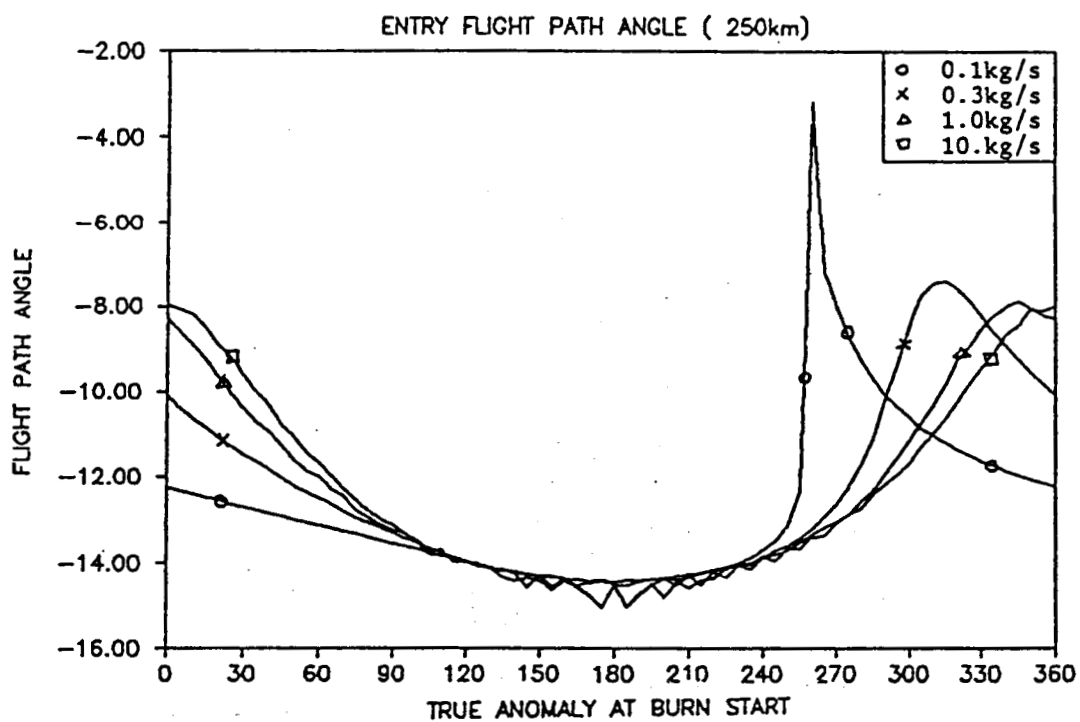


Figure 2.4-7

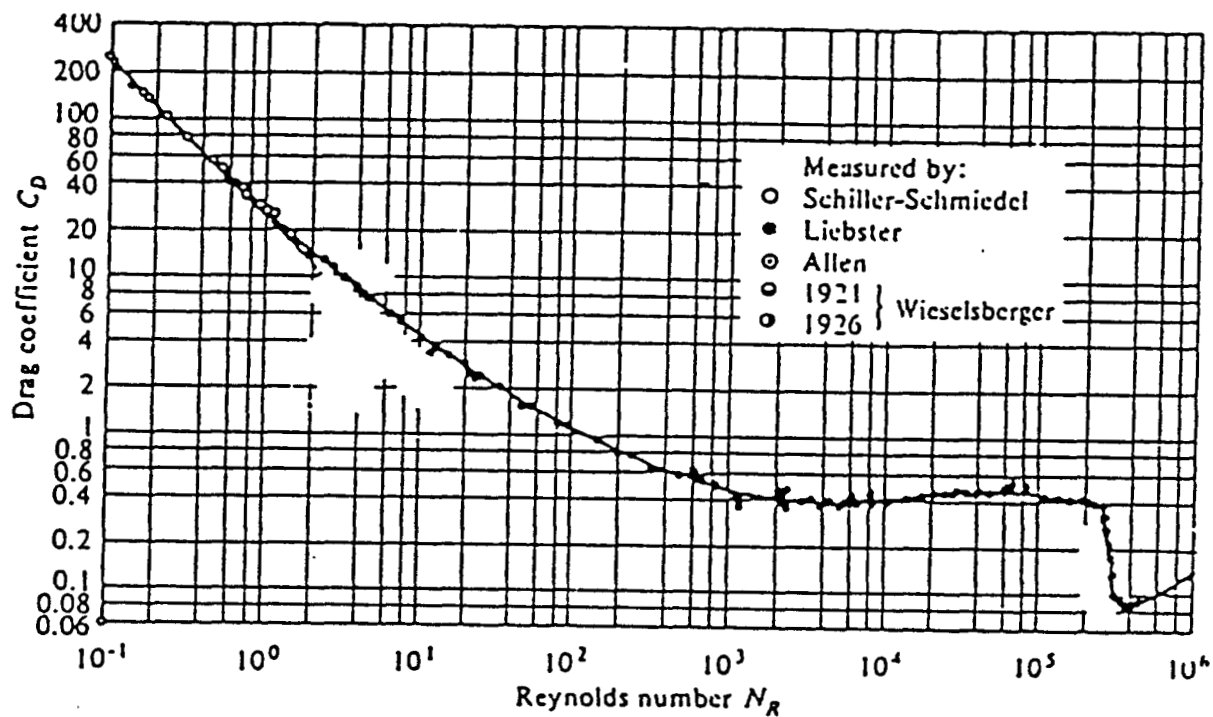


Figure 2.4-8 Drag Coefficient as a Function of Reynolds Number for Spheres.

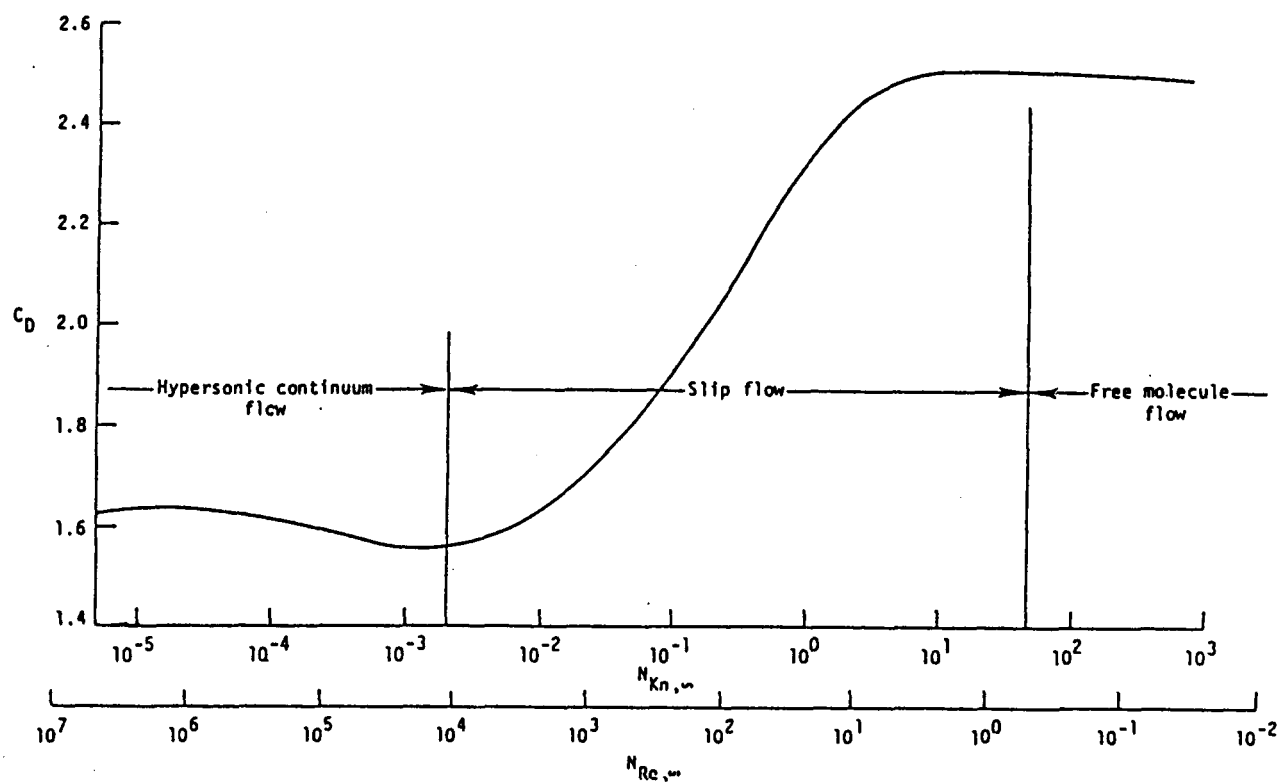


Figure 2.4-9 Low-Density Flow Regimes and Drag Coefficient for Viking Lander Capsule.

2.5 Mars Landing Sites

2.5.1 Selection Process

The selection of landing sites on the surface of Mars involves several parameters which must be considered in order to obtain a variety of data while ensuring the life of the lander and durability of the rover. The preliminary requirements for landing site selection must include the following:

- 1) Location: The Visual Imaging System of the lander must be able to recognize landmarks to correct attitude during descent to steer the craft to its final landing site. This is critical as smaller landing ellipse sizes are proposed. The Viking landing ellipse size was approximately 100 km x 300 km, while current sizes are at 50 km x 80 km and projected sizes go as small as 10 km x 10 km. These sizes are dependent upon orbiter camera resolutions, the camera's ability to see individual rocks and small craters, and the lander's ability to guide itself to its landing site.
- 2) Altitude: Since the Martian atmosphere is very thin, the maximum amount of aerobraking is required to use the least amount of fuel for descent and to maximize payload. Viking altitude parameters were set at less than 4.25 km above the average surface level. This gives the lander sufficient time to slow down to the touchdown velocity.
- 3) Slopes: To prevent the lander from tumbling down a slope, its grade must be limited. Although the Viking parameter was restricted to less than 19°, this parameter is dependent upon lander design, center of gravity, and lander leg configuration. Much of the terrain to be studied is on slopes, valleys, or craters, so this parameter must be set and landing sites altered slightly after landing site data is obtained by the orbiter.
- 4) Protruberances: To protect the bottom plate of the lander, a limit on rock size must be given for the site specification. This is also dependent on the lander design and site location. The distribution occurrences of rock size must be studied for each site to reduce the possibility of bottom plate puncture and possible lander disablement.
- 5) Winds and Dust Storms: To enhance trajectory performance and lander stability, winds must be taken into account for entry into the Martian atmosphere. With smaller landing ellipse sizes, winds become a critical factor in the accuracy of lander placement. Although global dust storms occur on a regular basis, usually during summer in the southern hemisphere, minor dust storms can

also occur and alter the flight path. Once the lander has arrived at its site, dust storms must also be considered in the Lander/Rover deployment and use. Frosting of the camera lenses due to sand blasting must be minimized. This may not be a significant problem as per Viking data.

With these parameters taken into account, several landing sites have been selected. These are:

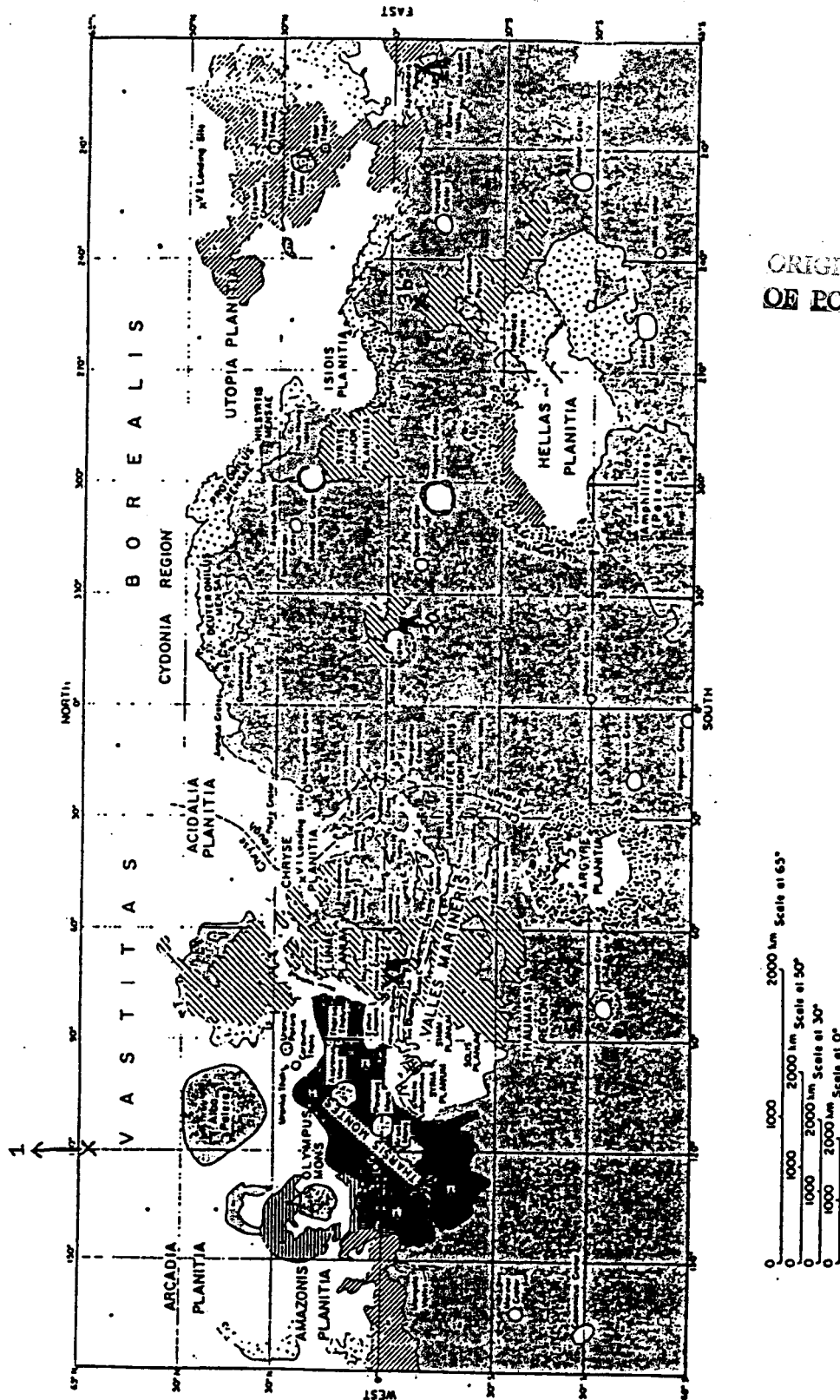
- 1) The North Pole: It has been hypothesized that water might exist at the north pole more so than at the south. The sublimation temperature of CO₂ at 6.1 mb is 148 K. In the northern summer, temperatures rise to as much as 235 K, well above the temperature to keep CO₂ in a solid phase. Yet, it is observed that ice is still present at this pole. Large amounts of water vapor are also observed in the atmosphere at the pole at between 80 and 100 precipitable microns.
- 2a) Arsia Mons West, 8°S, 132.5°W: This is an area of young volcanic rock. It is one of several large volcanoes in a chain at Tharsis Montes. Its peak is 27 km above the Mars datum, eliminating this as a landing site even though the caldera is 120 km across. Landing near the base is more feasible and also includes a larger variety of terrain for study.
- 2b) Apollinaris Patera, 5°S, 190°W: This would be a suitable backup site as it is at approximately the same latitude as Arsia Mons. It includes eolian sediments, young volcanic rock, plains, and knobby terrain.
- 3a) Schiaparelli Basin, 8°S, 336°W: Contains the oldest Martian crustal rocks from ancient cratered terrain. It also has ridged plains, mountainous terrain and heavily cratered uplands.
- 3b) Tyrrhena Terra, 7°S, 243°W: At about the same latitude as Schiaparelli Basin, it could be a suitable backup site. It contains much of the same terrain but also includes old volcanic rock above ancient crust.

- 4) Candor Chasma, 6.3°S , 73.8°W and Hebes Chasma, 7°S , 77°W :

These two chasms make up part of the large system of canyons of Valles Marineris. One lander with two rovers could explore these sites. The terrain includes layered rock with ridged plains surrounding it. These sites could have been caused by great floods of liquid water billions of years past.

- 5) Argyre Planitia, 45°S , 40°W : This very large crater appears to have been caused by the impact of a large meteor or comet. This area contains a large plain in its center and mountainous terrain surrounding it. Some very interesting data could result from soil samplings in this crater.

The proposed landing sites have been plotted in Figure 2.5-1.



ORIGINAL PAGE IS
OF POOR QUALITY

Figure 2.5-1

REFERENCES

NASA/JPL, "Viking-Mars: Anatomy of Success," Mission Status Bulletin, No. 46, October 31, 1978.

Corliss, W. R., "The Viking Mission to Mars," NASA-SP334, Scientific and Technical Information Office, NASA, Washington, D.C., 1974.

Blanchard, R. C. and G. D. Walberg, "Determination of the Hypersonic Continuum/Rarefied Flow Drag Coefficients of the Viking Lander Capsule I Aeroshell from Flight Data," NASA Technical Paper 1793, December, 1980.

Swanson, W. M., Fluid Mechanics, Holt, Reinhart, and Winston, New York, 1970.

JPL Report No. 715-23, Jet Propulsion Laboratory, Pasadena, California, 1980.

Carr, M. H., "The Surface of Mars," Yale University, 1980.

Baker, V. R., "The Channels of Mars," University of Texas, 1982.

3.0 Conceptual Design of a Scientific Payload for the USU Mars Lander/Rover

Payload Subsystem Group

3.1 Introduction

The overall design of the Mars Lander has been an interactive process by which the various design groups imposed constraints on each other. These constraints dealt with specific physical parameters such as size, mass, volume, and power consumption, and with conceptual limitations such as mission sequence, purpose of the scientific mission, deployment considerations and interfacing of the scientific payload with the MLR.

Because the nature of the MLR has changed several times in order to accommodate all the design constraints, several options are presented. Initially, it was assumed that the 5000 kg landed mass would be divided into five independent lander/rovers, each moving about the planet by means of a balloon. Because of balloon performance estimates, the final configuration for each Lander/Rover consists of three separate components: a fixed lander supported by a mobile land rover and a smaller balloon rover. Thus, the scientific payload design had to accommodate these changes by adjusting the scientific mission of each independent rover.

The sizing of the scientific payload has been based on Viking-type mass/volume ratios and information supplied by JPL. It must be noted that it is difficult to estimate the volume and mass of any scientific instrument without actually designing it. The approach used is as follows: the masses and volumes of several modern instruments were obtained from scientific catalogs. The payload mass and volume predicted from these numbers would be unacceptable due to their magnitude and because they do not include an estimate of the structural mass necessary to withstand 5 m/s impacts. The final estimate was made by using mass and volume estimates of instruments found aboard Viking, information supplied by JPL and information found in the Planetary Spacecraft Systems Technology Report (Tables 3.1 and 3.2).

3.2 Scientific Mission Objectives

The science mission sequence is patterned after the Viking mission. Re-entry, surface and balloon scientific payloads have been designed to meet the conceptual constraints imposed by the purpose of the mission. A list of these objectives is presented:

- Characterize the internal structure, dynamics, and physical state of the planet.
- Characterize the chemical composition and mineralogy of surface and near surface materials on a global and regional basis.
- Determine the chemical composition, distribution, and transport of compounds that relate to the formation and chemical evolution of the atmosphere.
- Characterize the dynamics of the atmosphere on a global scale.
- Characterize the processes that have produced the landforms of the planet.

Mission Scenario

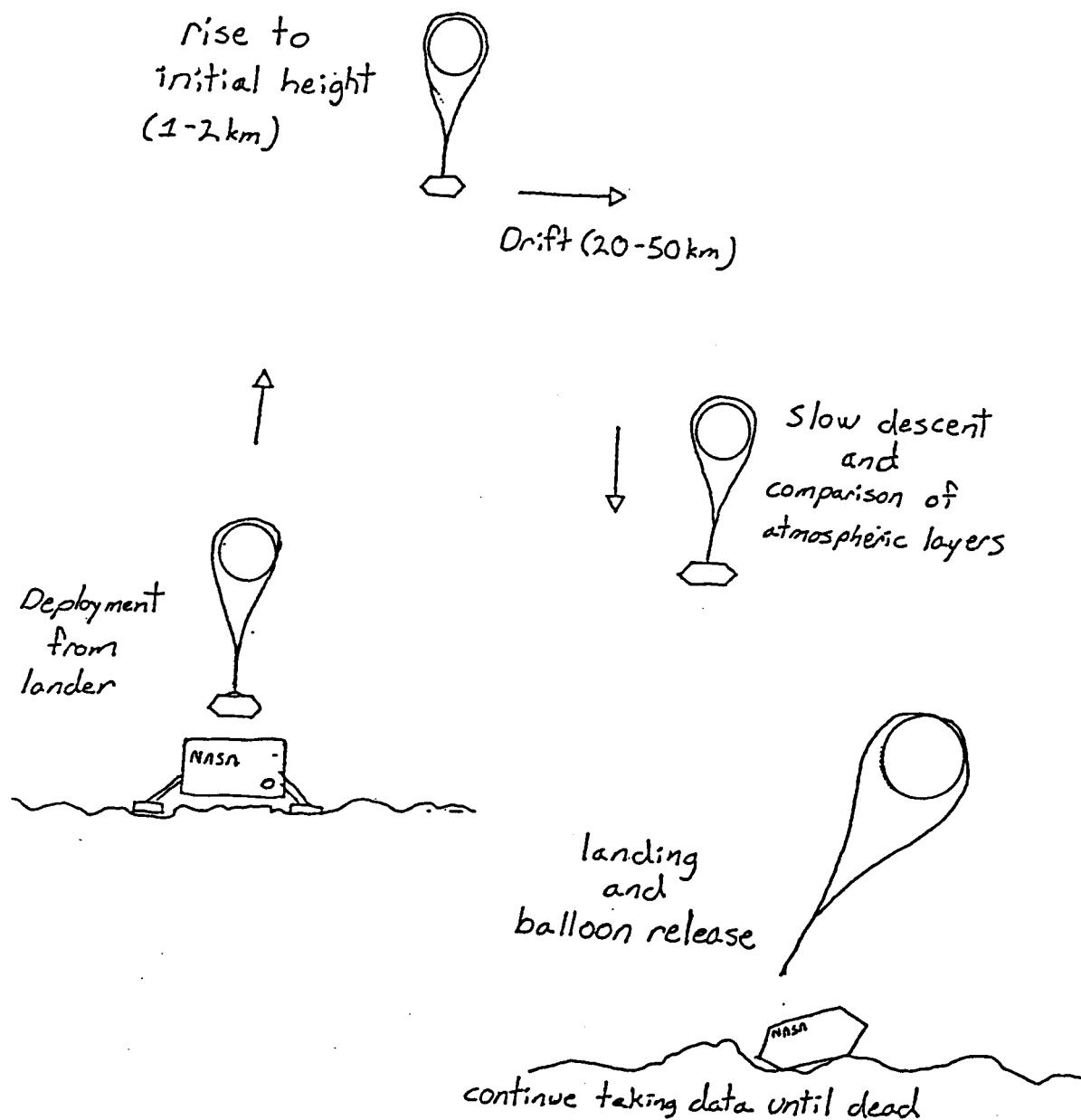


Figure 3.1

TABLE 3.1: MASS, VOLUME, AND POWER CHARACTERISTICS OF INSTRUMENTATION

#	Entry Science	Mass (kg)	Volume (m ³)	Power (W)
1	Retarding Potential Anal.	1.4	.004	3.0
1	Upper Atmos. Mass Spect.	6.8	.020	14.0
x	P, T, Accelerom. Sensors	2.5	.008	1.0
1	Altimeter Radar	6.0	.018	5.0
#	Surface Science	Mass (kg)	Volume (m ³)	Power (W)
2	Facsimile Cameras	1.0	.003	0.1
1	Electron Microscope	10.0	.030	30.0
1	Neutron Backscatter Device	2.0	.006	1.0
1	Volatile Detector	1.0	.003	5.0
1	Mineral Analysis Device	5.0	.015	10.0
1	Proximity Sensor	3.0	.009	2.0
1	Sun Sensor			
	Electronics	1.4	-	-
	Sensor	0.4	-	-
1	Gyrocompass	4.5	.014	-
1	Inclinometer	0.8	.002	-
1	X-Ray Fluorometer	2.0	.006	3.5
1	Meteorology Boom	5.5	.015	10.0
1	Seismometer	2.5	.007	10.0
#	Communications	Mass (kg)	Volume (m ³)	Power (W)
1	X-Band System			
	Emergency Uplink	2.0	-	5.0
	X-Band Antenna	1.0	-	-
#	Computers/Data Storage	Mass (kg)	Volume (m ³)	Power (W)
1	Vision	3.0	-	25.0
1	Sampling System	3.0	-	15.0
1	Science	3.0	-	15.0
1	Common Data Storage	10.0	-	18.0
1	Data Handling	27.0	-	12.0
#	Sampling Hardware	Mass (kg)	Volume (m ³)	Power (W)
1	Manipulator/Scoop	30.0	.100	Shared
1	Rock Crusher	11.0	.034	Shared
1	Data Handling Interface	1.5	-	1.0
1	Camera Pointing Platform	4.0	.012	2.0

TABLE 3.2: SCIENCE PAYLOAD MASS, VOLUME, AND POWER BUDGETS

	<u>MASS (KG)</u>	<u>VOLUME (m³)</u>	<u>POWER (Continuous) (W)</u>
<u>Entry Science:</u>	17	.005	14
<u>Surface Science:</u>	86	.300	128
<u>Balloon Rover:</u>	15	.050	10-20
<u>Surface Science and Computers/Data Storage:</u>	155	.350	128

- Determine the quantity of polar ice and estimate the quantity of permafrost.
- An in-depth search for life on Mars is not recommended until a thorough characterization of the planet's surface chemistry is made.
- The main purpose of this study is to accommodate the hardware requirements of the scientific objectives within the mass constraints of the mission.
- Characterize the interface of a science payload to a deployable remote sensing balloon.

The Viking Lander has demonstrated that a planetary probe can be built with regional planetary exploration capabilities. The size of the region studied was limited to the immediate vicinity of the lander. In order to accomplish the above-mentioned scientific objectives, it is necessary to increase the scale of the exploration capabilities of the probe being designed. The global scale exploration capability can be achieved by increasing the number of landing sites and by including a deployable balloon rover in the lander. The landing site region exploration is extended by including a land rover (<1 km).

The scientific instruments presented were selected so that a great variety of chemical characterization techniques are available for the subsequent design of specific experiments at a later time. The payloads will all contain facsimile cameras, a science computer, and a meteorology device. The particular science mission sequence will be evaluated later. What can be said for now is that the operation sequence will be complex due to the availability of power and communications.

3.3 Mission Sequence Scenarios

The mass for the mission was selected by the Environment and Trajectory Group to be 5,000 kg landed on the surface of the planet at five different landing sites. The Scientific Payload Group worked with the Ground Systems Group and the Balloon Group in order to size a given scientific payload within the possible lander/rover mass budgets.

3.3.1 Case 1

It was assumed initially that each 1,000 kg lander/rover structure or mothership would land at a velocity of 5 m/s. The re-entry sequence is like that of Viking, so that atmospheric monitoring will be similar. After landing, a balloon would be deployed and the mothership would hop about the planet flying during the day and landing at night. So as to decrease the weight to be carried about, some ballast could be discarded in flight. This approach helps to increase the lifetime of the balloon in the air and provides an efficient method of distributing several types of sensors; i.e., seismometers. The mothership could also be anchored during day periods so that a land rover could explore the immediate vicinity. The mothership would thus be capable of exploring both the atmosphere and surface of the planet on both a regional and global scale.

3.3.2 Case 2

Re-entry and initial landing would be the same as the Viking mission and Case 1. Landing would be followed by deployment of a balloon carrying meteorological and imaging devices and a long range surface rover (>10 km) with surface analysis capabilities. The lofted mass would be reduced compared to Case 1 because the descent propulsion sub-system and land rover would not be carried along.

3.3.3 Case 3

A Viking type landing sequence. A balloon is deployed with a meteorology/imaging payload. The mothership, in turn, deploys a short-range land rover. The rover would retrieve samples to be analyzed in the mothership labs. A typical mission could consist of sampling during daylight and analysis of samples at night.

The selection between these three cases was made in conjunction with the other design groups. Case 1 was discarded because a great deal of the mass would be spent in the massive landing structure necessary to survive multiple landings. Also, the tremendous balloon size required to loft the payload was deemed unacceptable. Case 2 was discarded because, although the descent propulsion subsystem is left behind, significant mass would be needed for the individual landing structures of each rover. Also, the surface rovers of the 1990's are expected to be of limited autonomy; thus, implementing a >10 km roving capability might be possible, but very complex.

The chosen scenario was Case 3. This option accommodated the sum total of the constraints imposed by the various design groups. Centralizing the analysis portion of the ground mission at the initial landing site avoids potential damage to, or loss of, delicate scientific instrumentation. The mass penalties of carrying the descent propulsion subsystem and of reinforced landing structures are eliminated and reduced, respectively. Furthermore, the mothership can be adequately supported by a 1990's surface rover. The adopted scenario provides both regional and global characterization capabilities.

3.4 Mass Budget and Constraints

The mass constraints for each 5,000 kg of landed mass are:

5 Lander/Rovers	at five different landing sites w/1,000 kg each:
Mothership	: 400 kg (structure/rover/science payload)
Balloon	: 300 kg (balloon/structure/science payload)
Reserve	: 300 kg (unassigned)

These constraints were most restrictive in the case of the balloon subsystem. The total non-balloon mass would be limited to 60 kg, which means that only 15 kg are available for a scientific payload. The mass constraints are not crucial to the science payload on the mothership because there is ample room and the only moving structure is the surface acquisition rover.

3.5 Mothership Mission

The mothership mission is composed of two parts:

- Part A - Entry Science
- Part B - Surface Science

3.5.1 Part A - Entry Science

- The purpose of the entry science is to study the upper atmosphere of Mars (>100 km).
- The hardware will be contained within the aeroshell during entry (i.e., Viking type hardware).
- The core of the study consists of determining the composition and structure of the upper atmosphere.

3.5.2 Part B - Surface Science

- The purpose of the surface science mission is to characterize the geology and surface composition of terrain immediate (<1 km radius) to the landing site. Also, a long-term local environment characterization will be possible with an on-board meteorology station.
- An important element of the surface mission will be to interface the sample acquisition and sample analysis hardware.
- Sample acquisition hardware will consist of a mobile surface rover that can be programmed by an Earth-based operator. The mobile rover will be used to obtain core samples, rock/soil samples, and surface images.
- Sample analysis hardware will consist of a stationary, fully automated laboratory capable of analyzing the various samples obtained by the surface rover.
- Apart from sample analysis the mothership can perform global seismic studies of the planet when coordinating with the other four motherships.

3.5.3 Balloon Rover Mission

- The purpose of the balloon rover is to extend the global remote sensing capabilities of the mission and to study a larger cross-section of the lower Martian atmosphere. Also, it will extend the local environment (i.e., meteorology) characterization capabilities by providing a secondary ground-based meteorology station once the balloon rover lands.
- Further, the balloon rover can relate high altitude imaging of the terrain immediate to the landing site during deployment. These images can be relayed to an Earth operator to aid in the selection of planned paths for the surface acquisition rover (SAR). This type of hazard avoidance/determination capability is reason enough to spend 3/10 of the landed mass on the balloon rover.
- Hardware will consist of a balloon carrying a 60 kg support payload (Structure/Communications/Power) including a 15 kg Science payload.
- The balloon payload scientific instrumentation will include the following: an atmospheric spectrometer, a volatile detection device, a neutron backscatter device, altimeter radar, 2 down-looking facsimile cameras, irradiance sensors, and a meteorology boom.

3.6 Extended Balloon Rover Payload Description

The mission of the balloon rover begins with deployment from the mothership, from where it will rise to its cruising altitude of 1-2 km, depending on balloon design and local atmospheric conditions. The on-board imaging devices will characterize the landing site as the balloon reaches its maximum altitude. The balloon rover will then travel with the Martian winds for the duration of its flight. It is hoped that the balloon rover can fly 2-3 days.

During flight the balloon loses lift due to diffusion of the lifting gas, resulting in a slow descent to the ground. During all phases of the mission, the payload will be gathering data constantly. From this information a detailed profile of the lower atmospheric layers of Mars may be developed. Also, detailed aerial photography of the planet's surface will be possible.

In the final stages of the descent phase, the rover will lose enough to make its landing at a projected 2-5 m/s velocity. The balloon, no longer having the necessary buoyancy to lift the payload, will be detached, leaving the instruments permanently grounded. Once landed, the rover will continue its meteorological studies as long as the power source permits.

The scientific payload is estimated to have an approximate volume of 0.05 m^3 , and mass of 15 kg. The payload will consume from 17-35 watts of power at any given time. The instruments will alternate operation in order to reduce the power requirement. The power needs at any given time depend on which instruments are in use. During flight, the cameras and the altimeter will run constantly, requiring that the cameras be equipped for 'night vision' (IR). The irradiance sensors will operate throughout, and, thus, may be used as a switch to regulate certain systems.

The operation sequence and positioning of the remaining instruments is yet to be determined. The landing structure and communications network of the balloon rover is not known, so it is difficult to specify the mission sequence at this time.

REFERENCES

- Klein, G., Planetary Spacecraft Systems - Final Report, 1986, JPL.
- Instrument sizes provided by J. Burke, JPL.
- A Handful of Mars, A Sample Return Mission to the Red Planet, etc.
- Corliss, W. R., "The Viking Mission to Mars," NASA-SP334, Scientific and Technical Information Office, NASA, Washington, D.C., 1974.
- The Viking Mission to Mars - Vol. 3, NASA.
- Soffen G: "The Viking Project," J. Geophysics Research, Vol. 82, No. 28, pp. 3959-3970, 1977.
- Nier, O.: "Composition and Structure of Mars' Upper Atmosphere: Results from the Neutral Mass Spectrometers On Viking 1 and 2," J. Geophysics Research, Vol. 82, No. 28, pp. 4341-4343, 1977.
- Horowitz, N. H., G. L. Hobby: "Viking on Mars: The Carbon Assimilation Experiments," J. Geophysics Research, Vol. 82, No. 28, pp. 4659-4662, 1977.
- Biemann, K., et.al.: "The Search for Organic Substances and Inorganic Volatile Compounds in the Surface of Mars," J. Geophysics Research, Vol. 82, No. 28, pp. 4641-4658, 1977.
- Toulmin, P., et.al.: "Geochemical and Minealogical Interpretation of the Viking Inorganic Chemical Results," J. Geophysics Research, Vol. 82, No. 28, pp. 4625-4634, 1977.

4.0 Ground Systems

Objectives: The purpose of the Ground Systems group is threefold:

- 1) to develop preliminary concepts and ideas pertaining to the surface operations of a planetary exploration of Mars
- 2) to evaluate these options based on a set of criteria determined by the needs of the mission
- 3) to narrow these ideas and concepts into one workable system based on the research of the Ground Systems group and the three other groups in the Mars Land Rover design class.

Mission Scenarios: During the course of the academic quarter, several different ideas for the overall exploration of the planet were considered. Among the most favored concepts were the following:

- 1) the overall mission being carried out by a balloon rover
- 2) the mission being carried out by both a balloon rover and a surface rover deployed from a common mothership

The balloon rover/surface rover mission was adopted by the class as a whole and is used as the baseline mission in this section.

4.1 Landing Systems

The landing system, being vital to the success of the mission, was the first component to be considered. Given the scenario of the hybrid mission, the need for two separate and distinct landing systems is apparent. The first of these landers, called the initial lander, applies to the landing of the mothership. The second lander, called the balloon lander, applies to the landing of the balloon payload. In the following sections, the two landing systems are covered as well as a variation on the balloon payload lander capable of repeated landings.

4.1.1 Initial Landing System

The initial landing system had the following requirements placed upon it:

- 1) land 1,000 kg payload
- 2) impact velocities up to 5 m/s
- 3) impart less than 30 g's to the payload
- 4) minimum system mass
- 5) minimum storage mass
- 6) payload protection during landing
- 7) stable landing on inclined surfaces
- 8) incorporation of descent thrusters in design

The first three of these requirements were used as design parameters while the last five were used as criteria for the evaluation and comparison of the candidate systems.

Three candidate systems for the initial landing systems were considered. Figure 4.1 shows candidate system 1, a pressure bladder lander. In this system, the pressurized cavity absorbs the impact energy

of the payload by compressing the gas which acts as a variable rate spring. Figure 4.2 shows candidate system 2, a crushable landing system. In this system, the payload impact energy is absorbed by a lightweight crushable material that surrounds the payload. Figure 4.3 shows candidate system 3, a Viking style, multi-legged lander. In this landing system, the kinetic energy of the payload is absorbed by crushing a honeycomb-like material located in its outermost legs.

Of the three landing systems considered, the Viking type proved to be the best choice for the initial lander. The legs on the Viking-style lander offer the best ground clearance of the three systems, as well as the possibility of folding its legs for storage purposes. The other two systems offer virtually no ground clearance and are based on a large volume, thus complicating their storage in the aeroshell during atmospheric descent. With respect to landing stability, the Viking system is better than the other candidate systems. This is due mostly to the Viking's multi-legged arrangement. The landing legs will conform individually to the contour, or slope, of the landing surface, resulting in a more level and stable payload orientation. In addition, descent thrusters are easily deployed on the Viking system due to ground clearance, while the incorporation of descent thrusters on either the pressure bladder lander or the crushable lander would be a major engineering challenge. With respect to the mass fraction of the landing system, the Viking lander mass fraction is very small. For the purpose of estimating the mass of the Viking legs, a rough design of these components was performed and appears in appendix 4.1. This design showed the mass of three legs and disks to be approximately 24 kg. It is unlikely, based on preliminary estimates, that the mass fraction of either the pressure bladder lander or the crushable lander could better that of the Viking lander. Finally, the technology of the multi-legged landing system is simple, well understood, and is a proven technology by virtue of two successful Viking missions to Mars. A preliminary sketch of the lander is shown in Figure 4.4.

4.1.2 Balloon Payload Lander

The balloon payload landing system is very different from the initial landing system due to dissimilar landing conditions and payload requirements. The initial landing system, complete with its scheme of aerobraking, parachutes, and descent thrusters can exercise a degree of control over landing velocities and locations. The balloon payload lander, in contrast, has no control over its landing conditions. The terrain it will encounter may vary considerably and winds are inevitable, which will cause a horizontal landing velocity. These conditions, along with a small balloon payload capacity, pose unique design problems. A logical design philosophy for this system is one of resilience. From this philosophy, the following requirements were developed:

- 1) land a 50 kg or smaller payload
- 2) land at velocities up to 5 m/s
- 3) payload deceleration of 30 g's
- 4) land in the presence of wind
- 5) varied landing terrain
- 6) protect payload from impact damage
- 7) stable landing dynamics

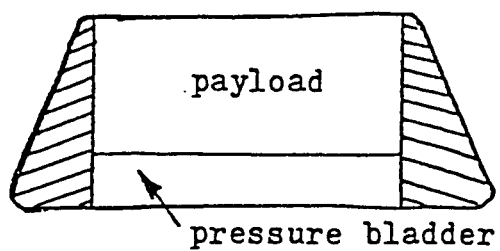


Figure 4.1 Pressure Bladder Lander

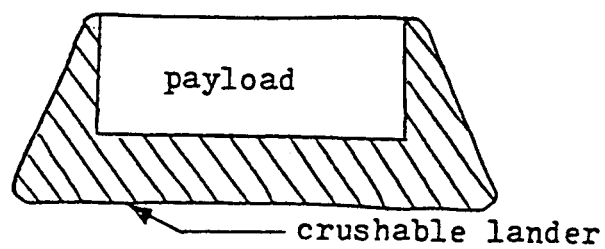


Figure 4.2 Crushable Lander

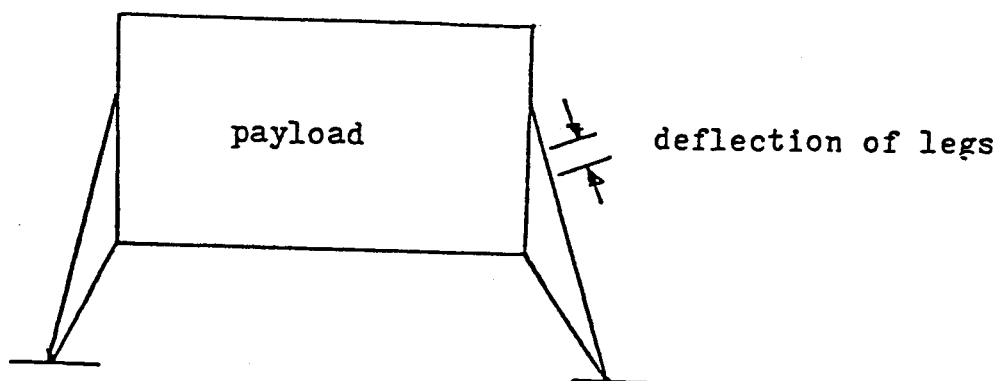


Figure 4.3 Viking Style Lander

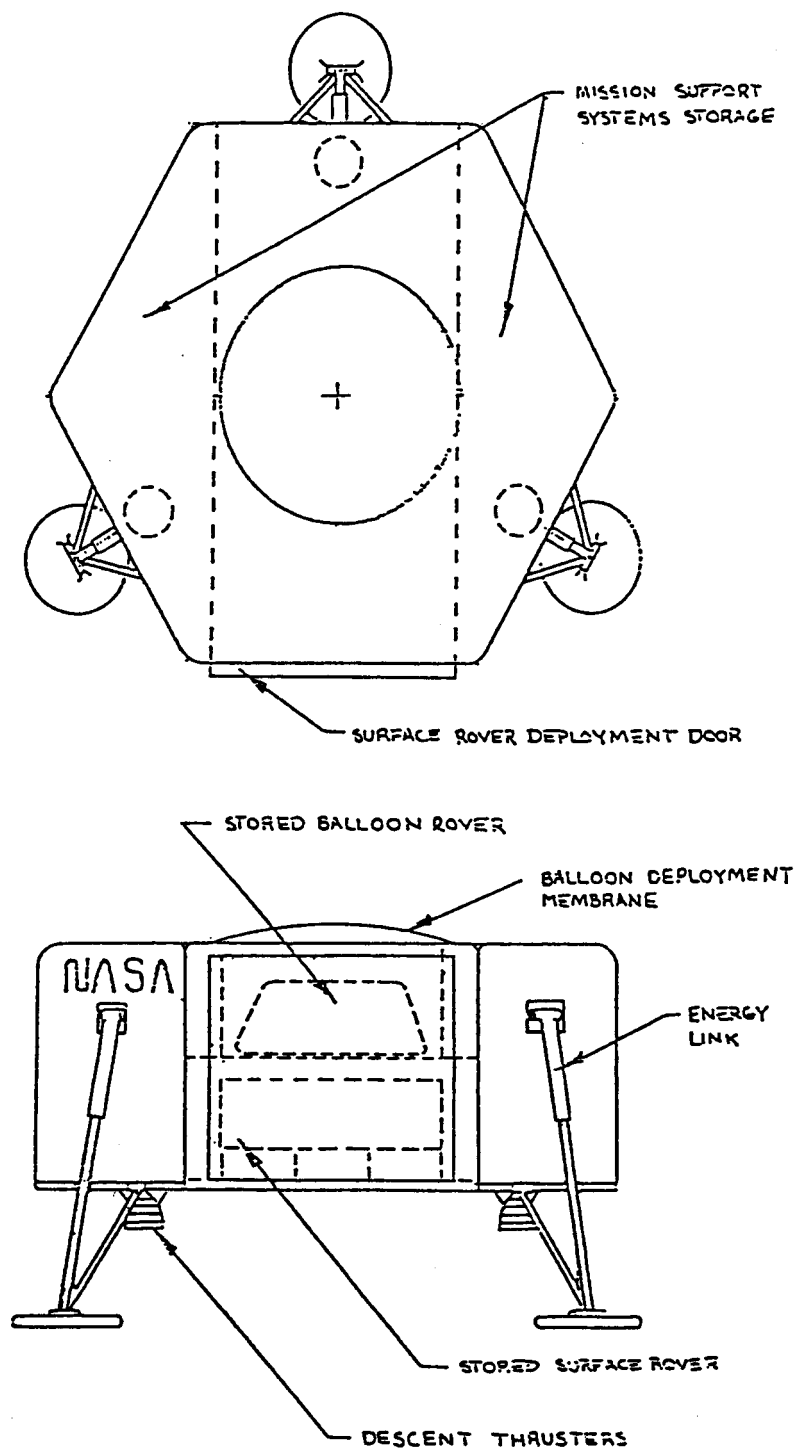


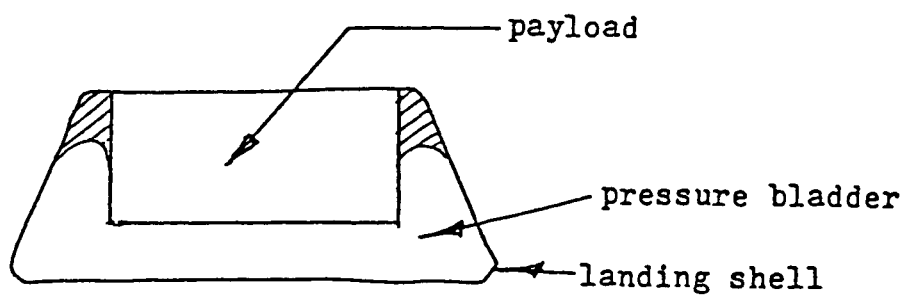
Figure 4.4 Mothership and Initial Lander

The first three requirements were considered as system design parameters, while the last four were used to develop and evaluate candidate systems.

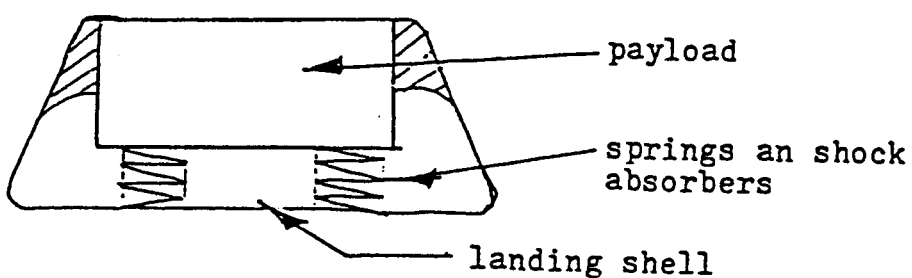
Four different concepts were considered for the balloon payload landing system. Figure 4.5 shows the candidates for this system, a pressure bladder lander, a spring/shock absorber lander, a crushable lander, and a Viking-style lander. In the first system, the lander absorbs the payload kinetic energy upon impact by the deflection of the pressurized bag. In addition, this bladder is protected from the landing surface by a shell. This shell might consist of a resilient material, such as a hard rubber or an impact plastic, or it may consist of a lightweight and rigid material such as a metallic alloy. The spring/shock absorber lander is similar conceptually to the pressure bladder lander but differs in its energy absorption technique. Here the pressure bladder is replaced by an array of springs and shock absorbers. This array is surrounded by a landing shell much the same shape and material composition as the pressure bladder landing system. The third landing concept is the crushable landing system. Here the payload is surrounded by a low strength, crushable material that yields to absorb impact energy and to protect the payload. The fourth system, a Viking-style lander, is the same conceptually as the initial landing system. Here the landing legs support the payload and absorb impact energy.

Of the four concepts considered, the pressure bladder system is the best choice for a balloon payload lander. The Viking-style lander, although used in the landing of the mothership, is not viable here due to the varied landing terrains and the presence of horizontal landing velocity components. These conditions alone would present major obstacles to maintaining the structural integrity of the landing legs. The spring/shock absorber lander has, when compared to the pressure bladder lander, a higher mass fraction due to its heavy spring and shock absorber system. In addition to a high mass fraction, the spring/shock system suffers from concentrated loads on the landing shell during impact, thus requiring a potentially heavier landing shell. The pressure bladder lander, on the other hand, has a more uniform pressure distribution on the shell and the mass of the gas is almost negligible. In one design, the gas mass was on the order of several hundred grams. The crushable lander suffers from large storage size requirements and structural integrity problems. The crushable material, being of a low yield strength, requires a potentially large volume for landings in the 30 g range. An analysis performed in Appendix 4.2 shows a storage volume of $.25 \text{ m}^3$. This volume is regarded as being too large to be stored in the mothership prior to balloon rover deployment. The uninflated pressure bladder, on the other hand, has the potential to be deflated during storage, thus limiting its storage size to slightly more than the payload volume. The structural integrity of a crushable lander is a serious problem. The crushable material, a low yield strength material, is not likely to have a high ultimate strength. If the lander should impact a surface obstacle, such as a rock, during landing with any horizontal velocity component, the crushable portion is in danger of being removed, in whole or in part, from the payload. This would then leave the payload vulnerable to damage.

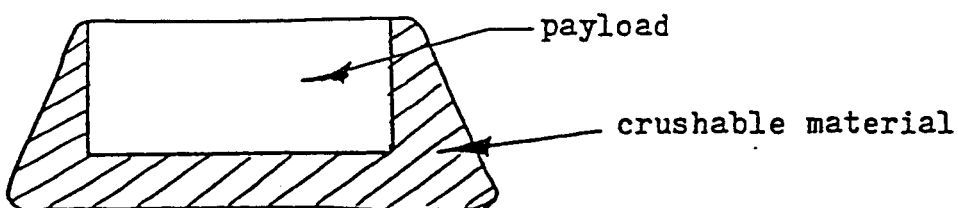
With the adoption of the pressure bladder system, the design philosophy of resilience can be maintained. A great deal of this resilience is due to a sleek shape and rigid construction of the shell. The shape can allow the shell to easily deflect over and around surface obstructions, thus minimizing the impacts. The selection of shell



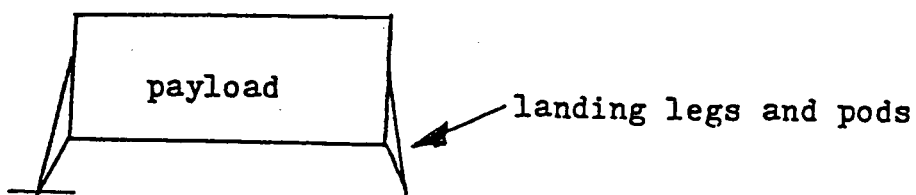
A. Pressure Bladder Lander



B. Spring/Shock Absorber Lander



C. Crushable Lander



D. Viking Style Lander

Figure 4.5 Balloon Payload Lander Candidate Systems

material and the design of the shell both have a tremendous influence on the mass fraction of the lander system. Ideally, the shell could be constructed of a material that has a high strength/mass ratio, a smooth surface finish, and good low temperature stability. In addition, the material must be immune to chemical reactions with the Martian surface. The lander shell design and the material selection has not yet been performed and represents an area for further research.

4.1.3 Pressure Bladder Performance

A model for the performance of the pressure bladder system, in terms of volumes and pressures, was developed assuming an ideal bladder gas such as He or CO₂. A relationship of work, pressure, and volume can be established using the ideal gas law and the First Law of Thermodynamics. This relationship is:

$$W_{12} = P_1 V_1 \ln(V_2/V_1)$$

where: W_{12} is the work done by the pressure bladder
 P_1 is the initial pressure of the closed system
 V_1 is the initial volume of the closed system
 V_2 is the final volume of the closed system

(see Appendix 4.3 for derivation)

From this mathematical relationship, Figure 4.6 was produced. Here a graphical relationship between the variables V_1 , P_1 , and P_2 is shown. From this, it can be seen that the final bladder pressure, affecting the design stresses of the system, is traded with the initial volume of the system. In general, peak bladder pressures are quite small, often less than 64 kPa. Figure 4.7 was derived from a mathematical relationship shown in Appendix 4.4. Here, the relationship between the initial volume and the maximum payload deceleration is shown. For the landings of a 50 kg payload in the 30 g range, a minimum volume for the system is approximately .1 m³. Neither the minimum volume constraint nor the peak bladder pressure is unreasonable. This serves to reinforce the feasibility of this system for small payloads like that of the balloon rover.

Problems of payload vibration with the pressure bladder system are likely to occur due to the low bladder gas pressures and the spring-like nature of gases. Some sort of damping scheme is needed to prevent severe payload oscillations. Some possible solutions to this problem may include: a 'slow release' shock absorber, a stress relief that blows out at peak pressure, or a ratchet mechanism to restrain payload movement. At present, no in-depth analysis of this problem has been performed. This, too, represents an area for further research.

4.1.4 Repeatable Balloon Payload Lander

Early in the development of the balloon payload lander, a system capable of repeated landings was sought. Even though the current payload lander is used for one landing only, considerable effort was directed toward the development of a repeatable landing system and its application to a balloon rover mission. The following is a noteworthy analysis of

Pressure Bladder Performance

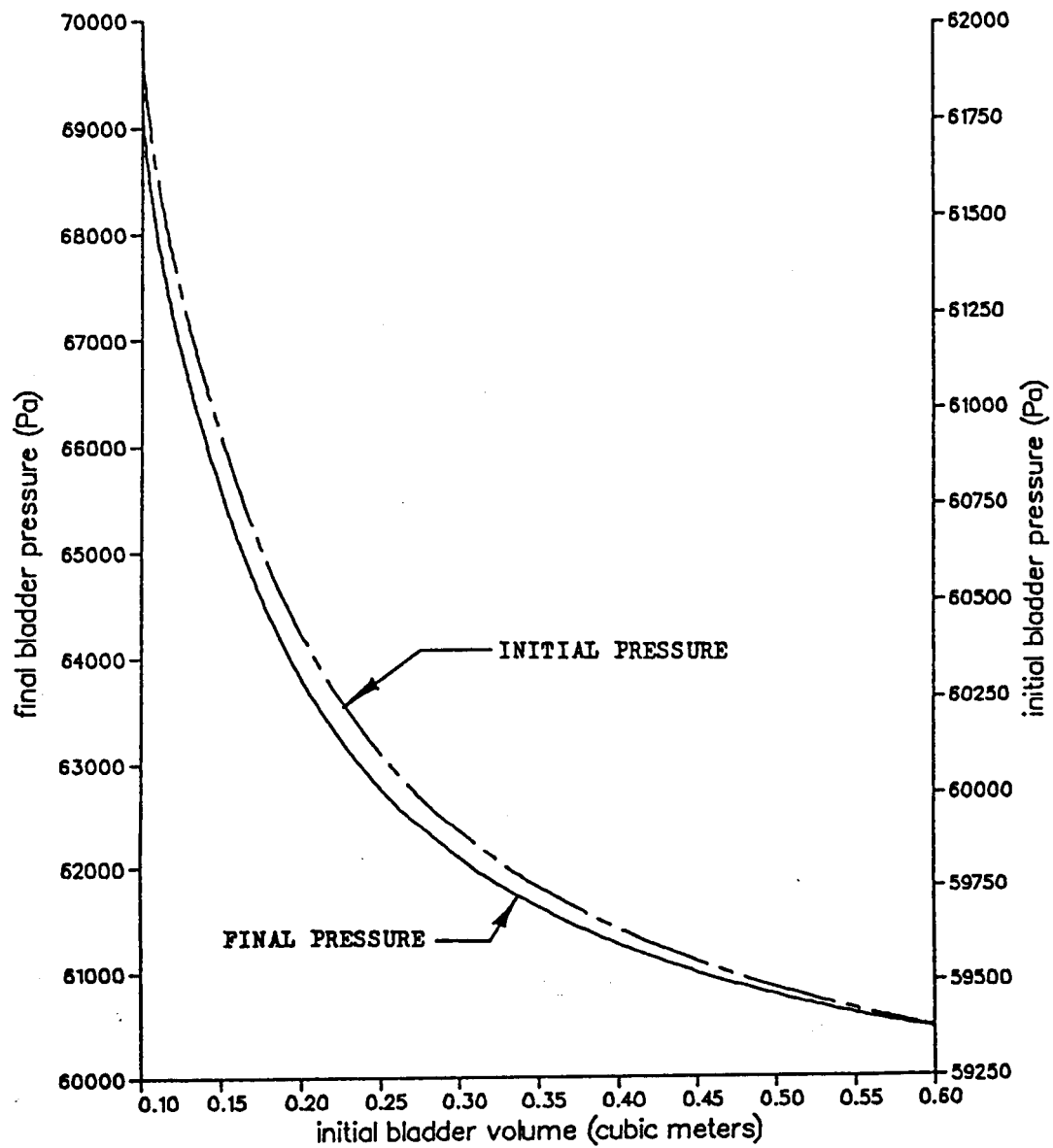


Figure 4.6

PRESSURE BLADDER V1-AMAX

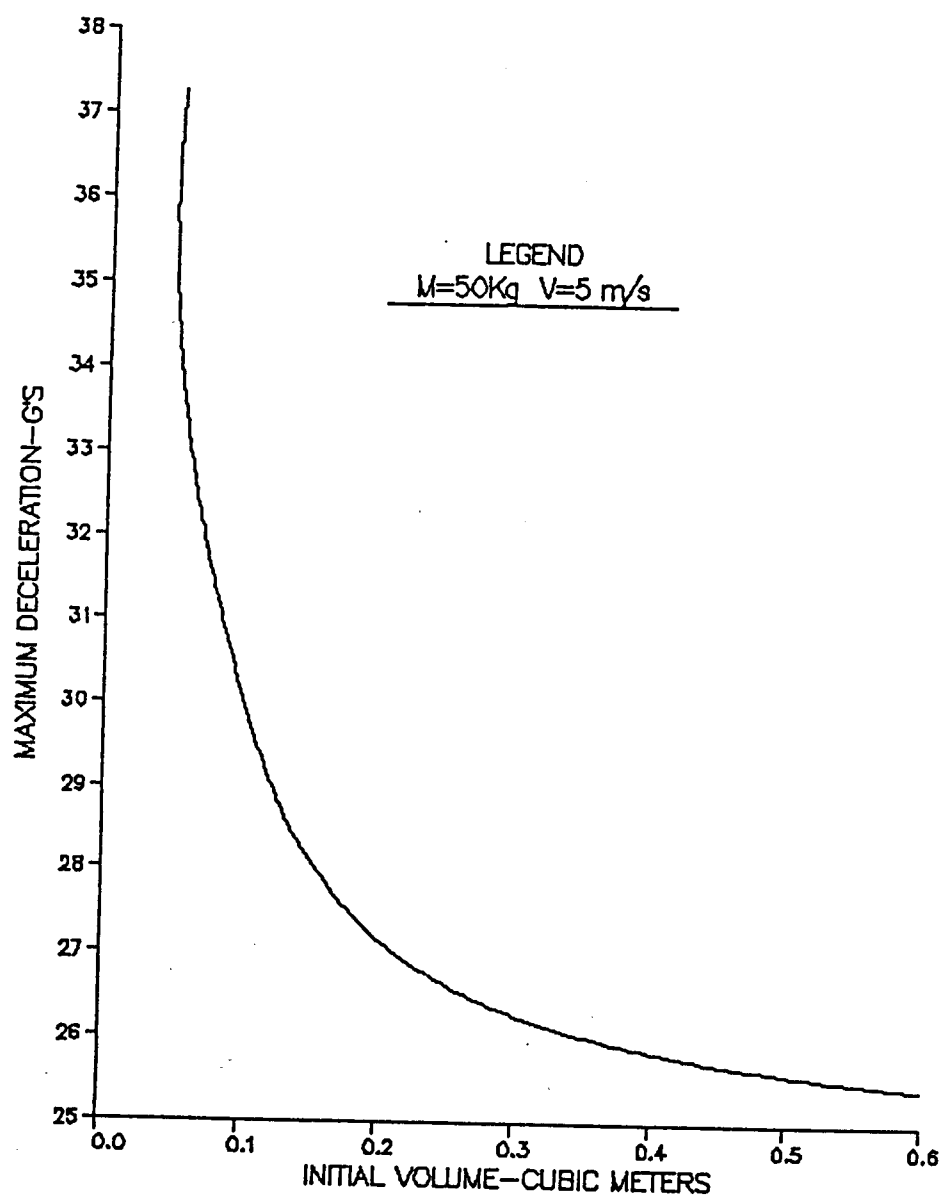


Figure 4.7

the performance of a repeatable, pressure bladder style balloon payload lander.

The philosophy of this system, once again, is one of resilience. The system requirements for this system are as they were for the single landing system discussed earlier. For the sake of clarity, they are repeated here. The system requirements are:

- 1) land a 50 kg or smaller payload
- 2) land at velocities up to 5 m/s
- 3) payload deceleration of less than 30 g's
- 4) land in the presence of winds
- 5) varied landing terrain
- 6) protect payload from damage
- 7) stable landing dynamics

Some additional problems must be addressed, such as payload dragging at night and during balloon ascent. During these times, very serious problems like payload snagging on surface obstructions can occur. A system resilient to impact and snagging needs to be developed.

Figure 4.8 shows the basic system concept. The impact energy absorption technique is accomplished by the pressure bladder system. The landing shell surrounding the bladder is much the same as that previously discussed for the non-repeatable lander. The characteristics of this system that distinguishes it from the other system is its balloon tethering method and the placement of its center of mass.

The balloon tether is connected to the payload via a gimbal mechanism shown in Figure 4.9. This gimbal is free to rotate independent of the payload orientation and the balloon tether is free to move along the rail of the gimbal. This is used in conjunction with an offset center of mass to obtain the desired lander orientation.

The lander orientation during flight, landing, and ascent is illustrated in Figures 4.10, 4.11, and 4.12, respectively. The advantage of this attitude is apparent when payload dragging across the surface is an issue. Ideally, it impacts between surface obstacles, and the payload shock is minimized in order to insure payload survival. This lander attitude allows it to deflect over and around surface obstructions, thus minimizing the impact.

The inclined lander orientation is a physically stable attitude due to the combination of the gimbal and the offset center of mass. Figure 4.10 shows the steady state orientation of the lander during flight. By the rotation and translation of the balloon cable fixture and the gimbal, the center of mass is "forced" to follow the direction of travel. When the balloon system descends and lands, the lander encounters the ground at the flight angle and, then rotates down to full contact with the surface. During ascent, the center of mass and the lander attitude will reorient themselves for renewed obstacle avoidance.

4.2 Sample Acquisition Rover Power Requirements/Mission Power Systems

4.2.1 Introduction

The sample acquisition rover (SAR) is a surface rover dedicated to collecting Martian surface samples, storing them, and returning them to the mothership. The SAR is conceptually an "extended arm" of the

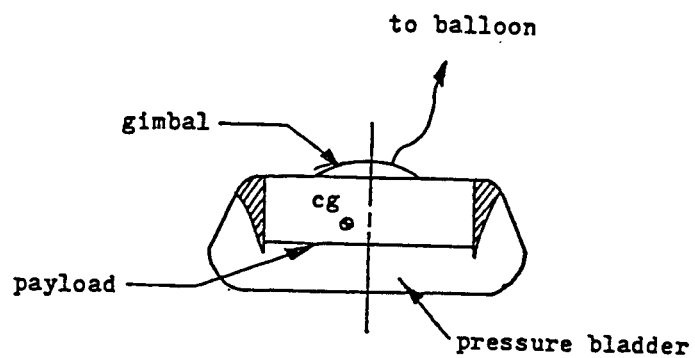


Figure 4.8 Repeatable Lander Configuration

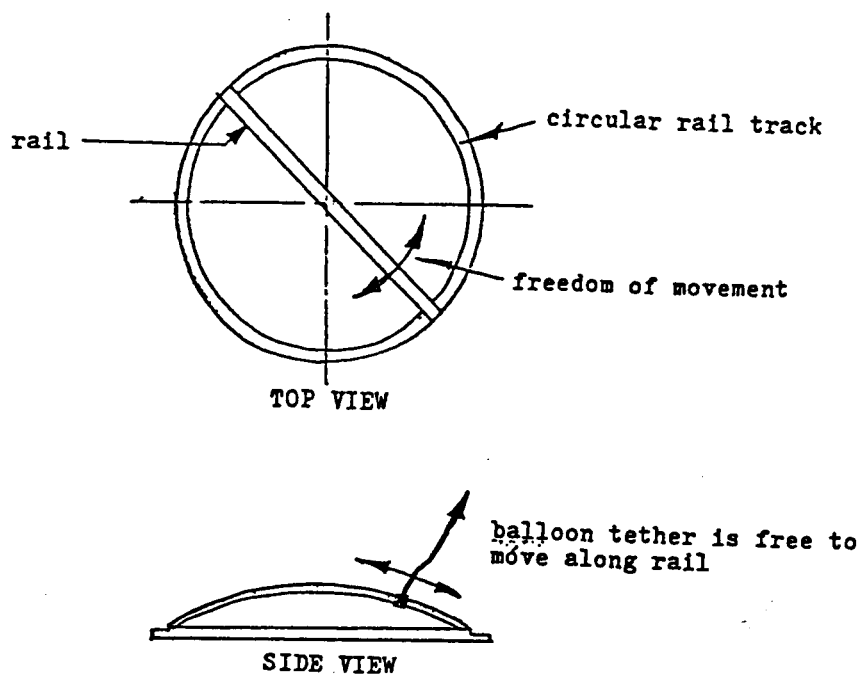


Figure 4.9 Gimbal Mechanism

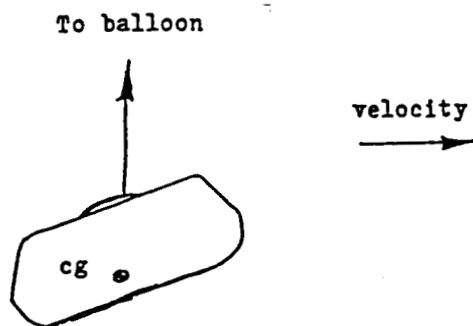


Figure 4.10 Flight Orientation

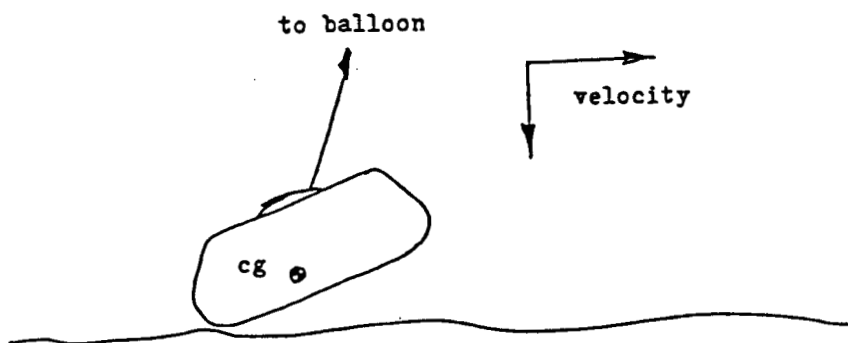


Figure 4.11 Landing Orientation

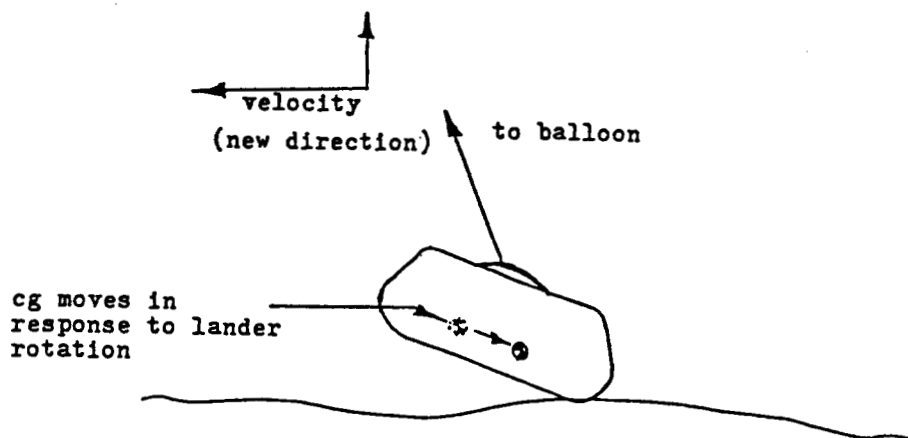


Figure 4.12 Ascent Orientation

mothership. Thus, its mission is limited to the area near the landing site. In this section, the locomotion power requirements and possible power systems are analyzed. In the following sections, communication, autonomy, and mobility concerns pertaining to the SAR are discussed.

4.2.2 Locomotion Power Requirements

Locomotion power, defined as the net power input to the mobility elements, is analyzed based on the following assumptions:

- 1) average traverse slope = 5°
- 2) maximum traverse slope = 35°
- 3) Mars gravitational field = 3.79 m/sec^2
- 4) six-wheeled mobility system
- 5) steady state conditions
- 6) overall efficiency of 45%

From these assumptions and the mathematical relationship derived in Appendix 4.5, Figures 4.13 and 4.14 resulted. Figure 4.13 shows the average steady state power requirements for several different rover masses. These power consumption figures are quite reasonable, generally less than 25 watts for traverses under 20 cm/second. However, Figure 4.14 shows that peak power requirements are around 120 watts. These figures are quite high when compared to the average power consumption. Different methods of coping with peak requirements may include the use of batteries to supplement power under peak demands and/or slower traverse speeds.

4.2.3 Power System Options

Figure 4.15 shows various power system options and their respective characteristics. Each of the three systems (the mothership, the SAR, and the balloon rover) require a separate, tailored power system. The mothership requires a large, reliable, and indefinite power system, while the balloon rover requires a small, finite, light-weight power supply. The SAR requires a combination of these two systems.

RTG's, radioisotope thermo-electric generators, are a rugged and reliable power source. They are also heavy and expensive. In addition, questions have recently arisen concerning the safety of earth-launching these radioactive systems. Despite these drawbacks, RTG's remain a good choice for heavy duty power systems like that required by the mothership and the SAR. Photovoltaic arrays, seemingly a good source at first glance, are intermittent and offer no significant weight advantage over the RTG.

Of the two battery types listed in Figure 4.15, lithium batteries offer the best power to mass ratio but are of a finite life. Ni-Cad cells, on the other hand, are heavier but have a much longer life span. For the balloon rover, the choice of lithium batteries is logical, and, for the SAR, the choice of Ni-Cad cells for supplementary power is equally logical.

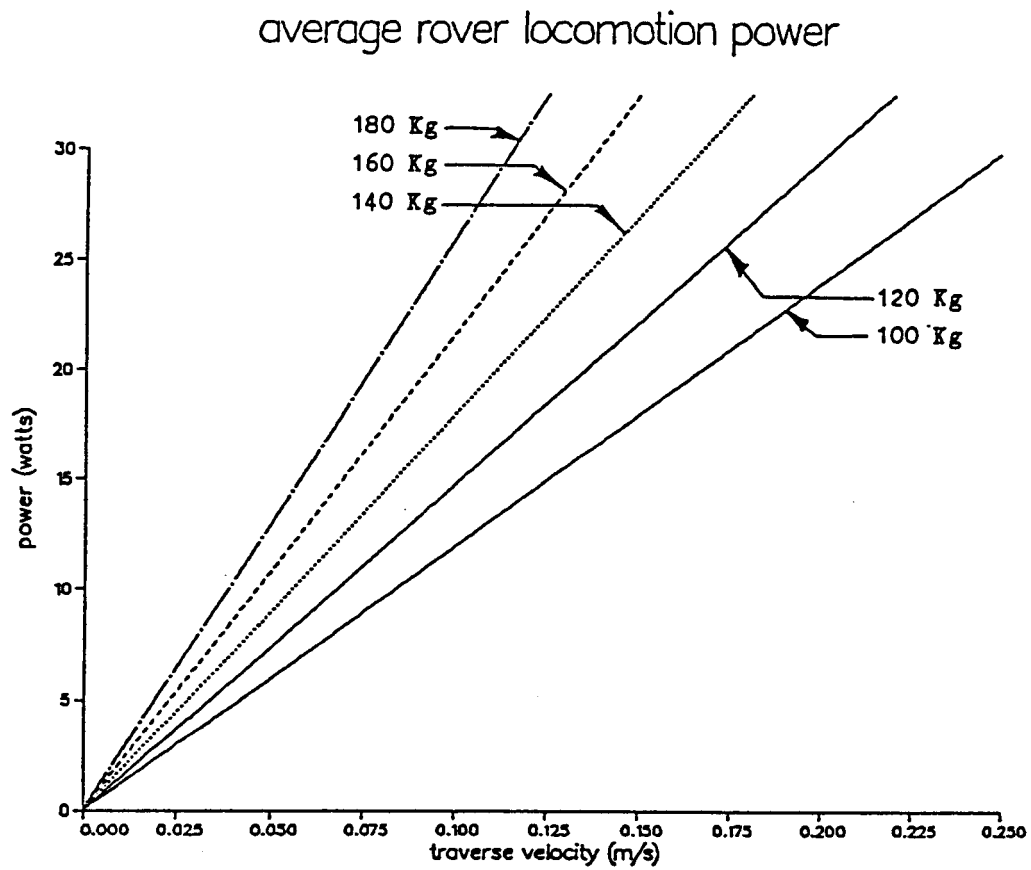


Figure 4.13

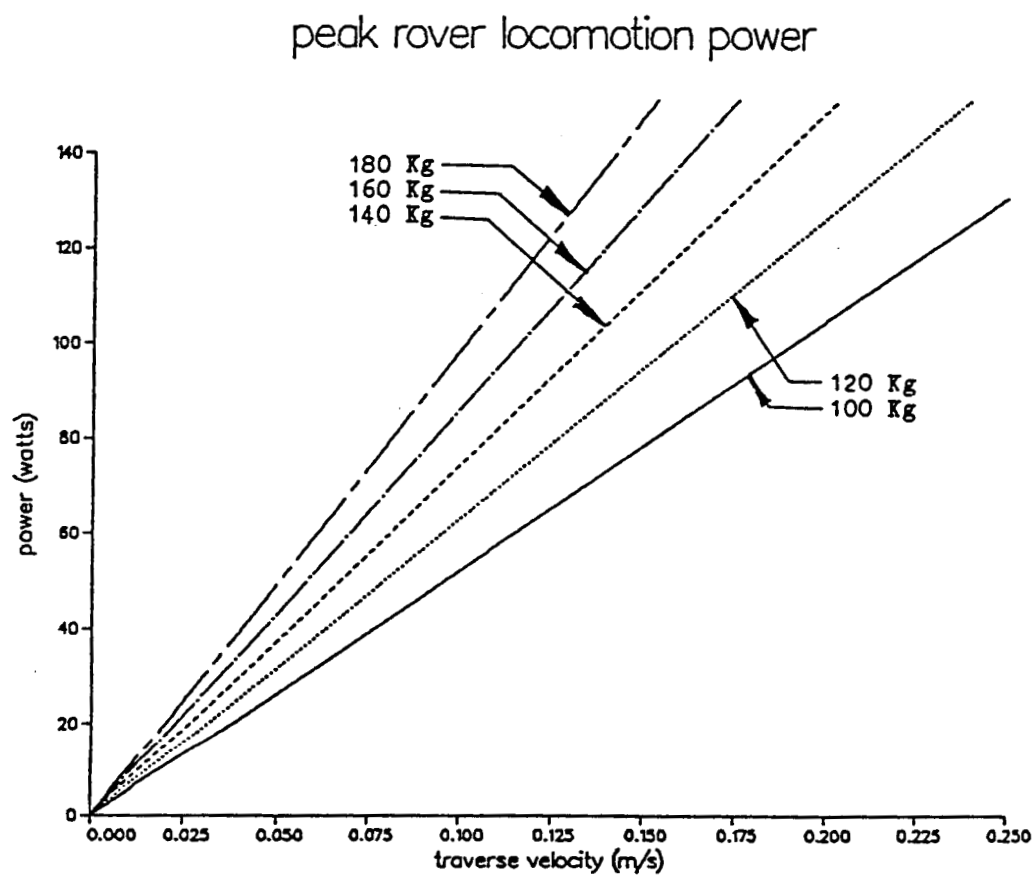


Figure 4.14

MISSION POWER SYSTEMS

Type	Specifications
RTG	5 watts/kg
Photovoltaic Arrays*	37.5 watts/m ²
	1.5 kg/m ²
array support structure	3.0 kg/m ²
total power/mass ratio	8.3 watts/kg
Lithium Batteries	250 watt·hr/kg
Rechargeable Ni-Cad Batteries	30 watt·hr/kg

* assumed under ideal Martian conditions

Figure 4.15: Power Systems

4.3 Rover System

4.3.1 Guidance Systems

Objective: the Ground System group's main objective during this phase of the class was to decide what degree of autonomy would be required for each of the possible rover/lander configurations and to gather information on the feasibility of meeting those requirements.

Options: the possible lander/rover configurations were divided into three general groups:

- 1) A short range system in which the Sample Acquisition Rover (SAR) would remain close to the initial lander. The range of this rover from the initial lander was set at 1 km. Samples would be returned to the initial lander for analysis.
- 2) A medium range system in which the SAR would remain within a 5 km range of the initial lander. The SAR would return to the initial lander to deposit samples which it collected, and the sample analysis would be done in the initial lander.
- 3) A long range system in which the SAR would not be limited by any specific range and would not be required to return samples to the initial lander for analysis. All the scientific payload would be carried on board the SAR.

Requirements: the requirements of each of the three general lander/rover configurations are considered below.

- 1) Short Range System: The requirements of the short range system include the ability on the part of ground control to operate the SAR remotely. By mounting a 3-D camera system on both the rover and on the lander it would be possible to guide the SAR totally by remote control. This would be accomplished by studying photographs sent back by both the initial lander and the SAR and plotting a course for the SAR on the basis of the three dimensional photographs received. The SAR would then be programmed remotely to follow that course.
- 2) Medium Range System: The requirements of this system differ from the short range system only in the possible need for some autonomy on the part of the SAR in order to avoid obstacles. In this case, the SAR would be programmed to follow a course determined by ground control on the basis of three dimensional pictures sent to Earth from cameras mounted on the SAR. Some degree of autonomy would help to protect the SAR in case of an undetected obstacle or a programming error on the part of ground control.
- 3) Long Range System: The requirements of the long range system differ greatly from the requirements of the short and medium range systems. Since this system would be carrying all the scientific payload on board, it would have to be larger and would require more power. It would have to communicate directly with the orbiter as compared to communicating through the initial lander to the orbiter. Because of a desire to cover a large amount of territory, the possibility of a fully autonomous SAR was considered.

Evaluation: one of the first things considered was the feasibility of a fully autonomous system for the SAR. In order for the system to be fully autonomous, it would have to know where it is with respect to its destination at all times. It would have to be able to plan a path and also to modify that path depending upon what obstacles in the path were met. A general path plan would be given to the SAR from ground control which would contain information on which direction the SAR should go and what type of samples to collect, etc. But the individual path decisions would have to be made by the SAR. The vehicle must have capabilities to "remember" some information about where it has been. Not all obstacles need to be remembered. Only that information which involves the vehicle's path and those which lead to dead ends.

One example of present capabilities is a robot developed by S.R.I. International. This system uses a strobe and a camera to pick up reflected light. Other systems use a camera on a sliding rail to get the images from several perspectives. Most systems available now cannot work on a real-time basis. The "cart" project done in the Stanford Artificial Intelligence laboratories uses a sliding rail imaging system. It takes approximately 10-15 minutes of computing time to decide on its next 1 meter move. As the above information indicates, a fully autonomous system that operates in real-time is a difficult objective.

One of the problems which researchers are working on now is the fact that as they try to feed a rover more and more information about its environment in order to help it make better decisions, they are creating another problem which involves the time needed to process and continually update that information. Research is pointing to the direction of sorting out data which is not needed. This will allow the rover to come closer to real-time system responses rather than well-reasoned plans. The use of parallel processing could also be a possible stop towards a solution to some of the problems of data analysis on a real-time basis.

Most of the imaging systems in use today have major drawbacks. The system used in the "cart" project could distinguish obstacles such as trees, chairs, garbage cans, and large rocks, but it could not "see" a smooth wall in front of it. The strobe system used by the S.R.I. robot only works well on specific geometric shapes. It will be necessary to find new methods of sensing the environment or a better combination of the present methods. One possible method of sensing is the use of ultra-sound.

Martin Marietta is working on an autonomous land vehicle for the military which uses a laser scanner and can follow a paved road at approximately 5 km/hour. This version has a projected test date of 1987. This vehicle will use two high-resolution color T.V. cameras and a laser scanner to get environmental information.

The conclusion of the Ground Systems group concerning the use of a fully autonomous system is that the state of the art at present and in the near future is not adequate to fill the needs of a fully autonomous SAR.

The next system considered was a fully remote controlled system. This system would be as described in the above paragraphs on short range and medium range systems. The major advantages of this system would be simplicity, and complete control of the system by ground control. The drawbacks are the time lag between when a message is sent from Earth to

Mars or vice versa and the time when it is received at the other end, the difficulty of planning for all possible problems for a path, and total breakdown of the system if communication is interrupted or if noise in communication causes erroneous information to be fed to the SAR. The ground system group came to the conclusion that these problems were not insurmountable and therefore a fully remote controlled system should be further investigated.

The option of a semi-autonomous system was also considered. As a baseline, this system was defined as able to avoid obstacles directly in its path and to have some capability of memory which would allow it to backtrack out of a dead end situation in which communication with ground control was lost or interrupted. This system would seem to be in line with present technology and seems to be a viable alternative to either a fully autonomous system or a completely remote control system.

A breakdown of possible degrees of autonomy along with features and drawbacks are included in the following section.

4.3.2 Mobility of the Rover

Since there may be different types of soil at each landing site, it may be possible to use different devices depending upon soil characteristics. For example, wheels seem appropriate to use on smooth soil, whereas legs seem better on rocky surfaces and tracks may be more stable on ice.

Before 1990, hopefully, the technology concerning autonomous robot vehicles will improve. As for now, some companies and laboratories have already developed some interesting prototypes:

- 1) 6-wheeled prototypes: MARS V (Standard Manufacturing Co.)
PROWLER (Robot Defense Systems)
ROD (Viking Energy Corp.)
- 2) 6-legged prototypes: Odex (Odetics)
OSU (MIT)
- 3) tracked prototypes: TELEMAT (Acac-Belgium)
TSR 70 (21st Century Robotics)
SURVEYOR (ARD Corporation)

The SURVEYOR appears to have characteristics closest to the requirements. Moreover, the video system is quite interesting: telescopic close-up, wide-angle, enhanced image interpretation and resolution, increased visual field size, and detection of binocular luster and scintillation. The SURVEYOR is compared to the mission requirements on the following page.

FEATURE	REQUIREMENTS	SURVEYOR
Locomotion	2 tracks/6 wheels/6 legs	2 tracks
Dimensions (LxWxH)	40x29x30	45x22x20
Weight	440 lb or 200 kg	140 kg
Communication	RF/Optical	COMVU
Data/Info Transfer	RF/Optical	
Power Supply	Battery/RTG	
Autonomy	> 5 hours	
Arm Reach	5 ft or 1.5 m	4.5 m (Telesampler)
Lift Capacity	20 lb or 9 kg	22.7 kg
Number of Axes	4-6	6
Sensors/Equipment	2-3 videos CCD/CID or ranging sensors	2 high resolution CCD black and white
Microcomputer	small, local, autonomous	computer based command computer
Slope	45°	45°
Chasms	10 in or 25 cm	
Obstacle Height	10 in or 25 cm	
Speed	0.45 mph or 0.72 km/h	1 km/h
Payload Capacity	20 kg	113 kg
Vertical Clearance	< 90 cm	< 86 cm

However, the main problem is whether or not an autonomous rover is needed. If one is needed, an Expert System could determine which way to go taking the following into consideration:

- 1) sampling requirements
- 2) existing samplings
- 3) soil analysis
- 4) atmosphere analysis
- 5) clearance
- 6) power capacity
- 7) motion capacity

Yet, the rover should not be completely autonomous; a human operator must be able to alter the rover's path in response to video transmissions to Earth by the rover. What must be determined is whether or not a human operator completely controls the rover or whether the operator can simply interrupt the rover's path and change some parameters.

ROVER ->	AUTONOMOUS Expert system choose own path	SEMI-AUTONOMOUS Ranging sensor can't choose if 2 paths available	TELEOPERATED 100% operated from Earth
OPERATOR			
MASTER	If the rover has pbs: it is lost or it has broken part of its control INCIDENT	the operator designs a path; the rover avoids the obstacles NORMAL	the rover must wait for commands from Earth NORMAL
ACTIVE SPECTATOR	Earth operator can change param. NORMAL	the rover goes thru a path until a node NORMAL	Earth commands misunderstood INCIDENT
PASSIVE SPECTATOR	Rover moves by itself NORMAL	The transmission is interrupted; rover out of control (no more commands from Earth available) INCIDENT	Rover out of order. Operator useless. INCIDENT

The distance from Mars to the Earth varies from 1 AU to 2.6 AU. This means that the time that it takes to transmit data from Mars to the Earth and to return a command from a human operator is

$$T = 2d/c + t_0$$

where t_0 is the time needed by the operator to determine a command. If it takes 5 minutes to determine a command, it takes 35 to 48 minutes for the rover to receive it. During this amount of time, the rover could travel between 583 and 800 meters. This is quite significant considering that its 0.5 m camera separation provides depth perception of only 200 meters. If the rover is not stopped, to wait for commands, it may take a hazardous path. Control of the rover is not feasible unless its position remains the same during the transmission process. The speed of the rover is a significant factor in this process. Therefore, the solutions for control of the system tend toward two limiting cases:

- 1) to control everything from the Earth (a sophisticated mobility control system is not needed in this case)
- 2) to have an autonomous rover that moves around on its own with occasional pauses to determine whether or not the Earth operator has any commands (a highly sophisticated mobility control system is necessary in this case)

4.3.3 Choice of Ranging Senors

Different types of proximity sensors were compared, and it appears that ultrasonic ranging sensors will be the best for the Rover. The ultrasonic sensor offers the following characteristics:

- 1) position/obstacle detection
- 2) reliability
- 3) insensitivity to dust, dirt, and light availability
- 4) lower cost than microwave and laser sensors
- 5) greater range than inductive and capacitive sensors
- 6) can produce either analog or digital signals

Among the best of the ultrasonic sensors is the Polaroid electrostatic ultrasonic transducer SN28827. This sensor is used by the Naval Weapons Center for its prototype sentry robot ROBARTII. This sensor is comparable with the E 200 from Massa Product but is more expensive. It has a range of up to 35 ft (10.5 m). Temperature correction is provided by another sensor.

4.3.4 Choice of Cameras

The following is a comparison of typical image sensors.

FEATURE		VIDICON		CCD		CID	
Resolution	9	3	27	2	18	2	18
Sensitivity	9	3	27	2	18	1	9
Speed	7	1	7	2	14	3	21
Bloom	8	1	8	2	16	3	24
Size	8	2	16	3	24	3	24
Reliability	8	2	16	3	24	3	24
Current Cost	1	3	3	1	1	2	2
Future Cost	8	1	8	2	16	3	24
TOTAL		112		131		146	

The CCD is a charge coupled device, and the CID is a charge injected device. In general, the CID appears to be better than the CCD except for sensitivity. The major drawback to the VIDICON camera is image distortion, 'burning,' and sensitivity to vibration and a relatively short life. For both the VIDICON and solid-state type cameras, the voltage levels are coded:

- 1) binary (2 values = 2 colors) which is not very illustrative
- 2) gray coded (256 values) which shows different shades

The problem then becomes capacity since gray code requires 256x256x256 bits to code a picture. Even worse, if real time is desired, it would have to be multiplied by 30 (1/30 s to scan a screen). Obviously, data compression is needed:

- 1) code differences between adjacent pixels
- 2) use of an index corresponding to the lower bound of pixels value for one line, and, then, for each pixel, code variations with respect to this index

Alternatively, the transmission rate could be reduced (the data will

appear line by line). Once the data is received on Earth, computer enhancement may be employed to refine the resulting imaging.

4.3.5 Communications

Objective: The Ground Systems Groups objectives in the direction of communications included three areas. The first area was communication between the initial lander and ground control on Earth. The second area of consideration was the communication link between the SAR and the initial lander. In this case, the initial lander serves as a relay between the SAR and ground control. The third area of consideration was the communication requirements of the balloon rovers. The objective in all three areas was to gather some preliminary information on what methods of communication were available and what advantages and disadvantages each had.

Options: The options to be considered were radio transmission of data and some of the general limitations involved with different wavelengths. Another option which the group is looking into with interest is the possibility of using ultrasonic waves for communication between the initial lander and the SAR.

Requirements: Each of the initial landers must be able to communicate with the orbiter. In this mission scenario, this would require telemetry to each of the individual initial landers. On top of this each of the balloon rovers must be able to transmit data to the orbiter. This results in ten separate links each in a different locations on the Martian surface. The video data transmitted must also be of a high enough resolution to enable the ground control operators to accurately program each of the SAR's.

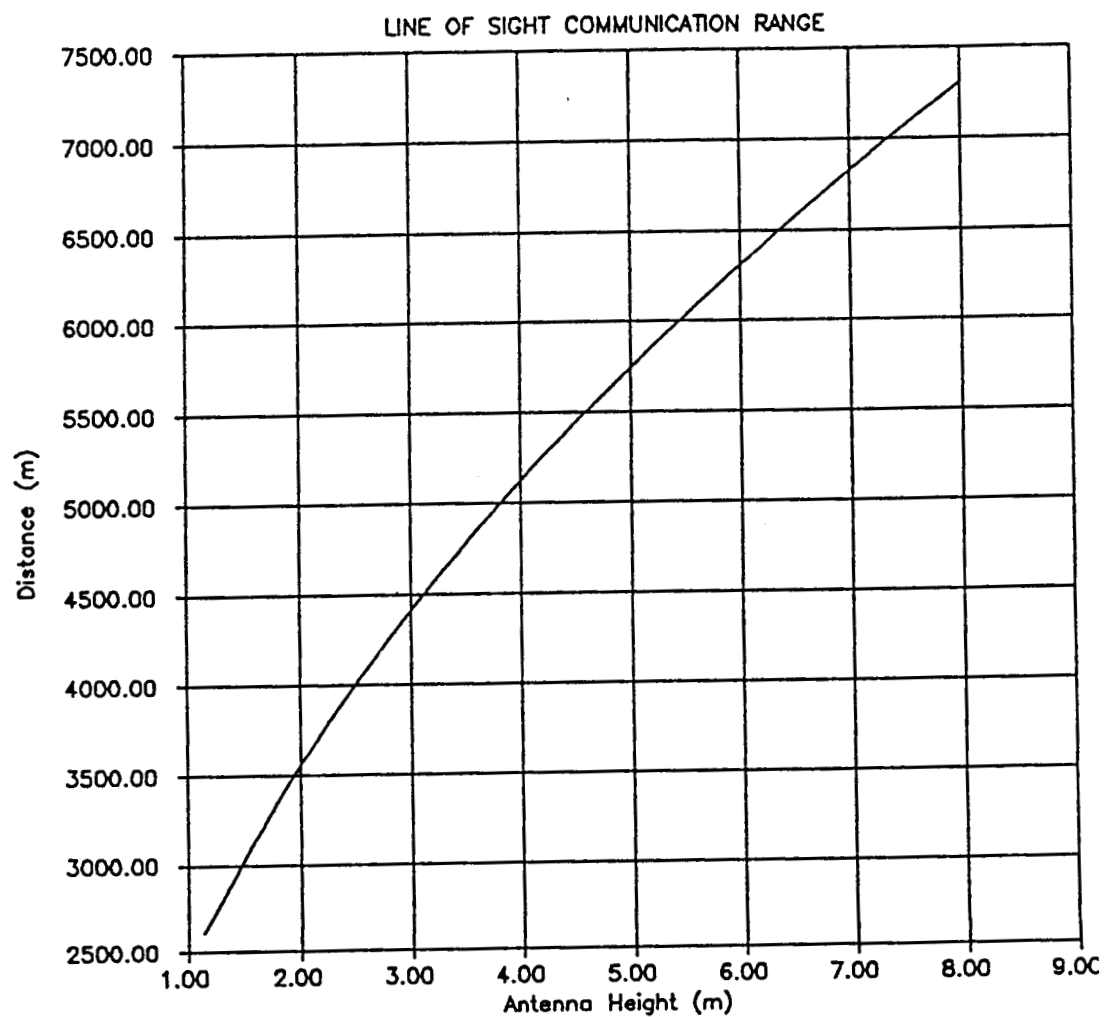
Evaluation: The first thing considered was how the curvature of the Martian surface would affect the communication range between the initial lander and either the balloon rover or the SAR. Because of the curvature of the surface, the range became a function of antenna height, assuming a smooth surface on the planet (see Appendix 4.8). Figure 4.16 indicates the line of sight communication range possible for varying antenna heights. This assumes that the antenna of the SAR is at ground level. The line of sight communication range possible from the initial lander to the balloon rover is shown in Figure 4.17. This also assumes a smooth surface. The antenna height is considered to be the vertical height of the balloon rover payload from the surface.

The 120 km range for the balloon rover, assuming a 2 km payload height, was not considered to be large enough, therefore, the balloon rovers will have to communicate directly with the orbiter.

Assuming an antenna height of 4 m, the SAR would have a maximum range of 5 km. This range would put it within the parameters set for a medium range rover system.

If the initial lander should happen to land in a depression on the surface of Mars or if the SAR were to go behind a hill and therefore no longer be within the line of sight, there would be the possibility of a communication breakdown. If the rover were semi-autonomous to the point that it could backtrack if there were a loss of communication with ground control, that problem would be partially solved, but the range of the SAR could be severely decreased. Because of this possibility, other alternatives besides line of sight radio frequencies must be considered.

One possible solution to the above problem would be to use lower



PRECEDING PAGE BLANK NOT FILMED

Figure 4.16

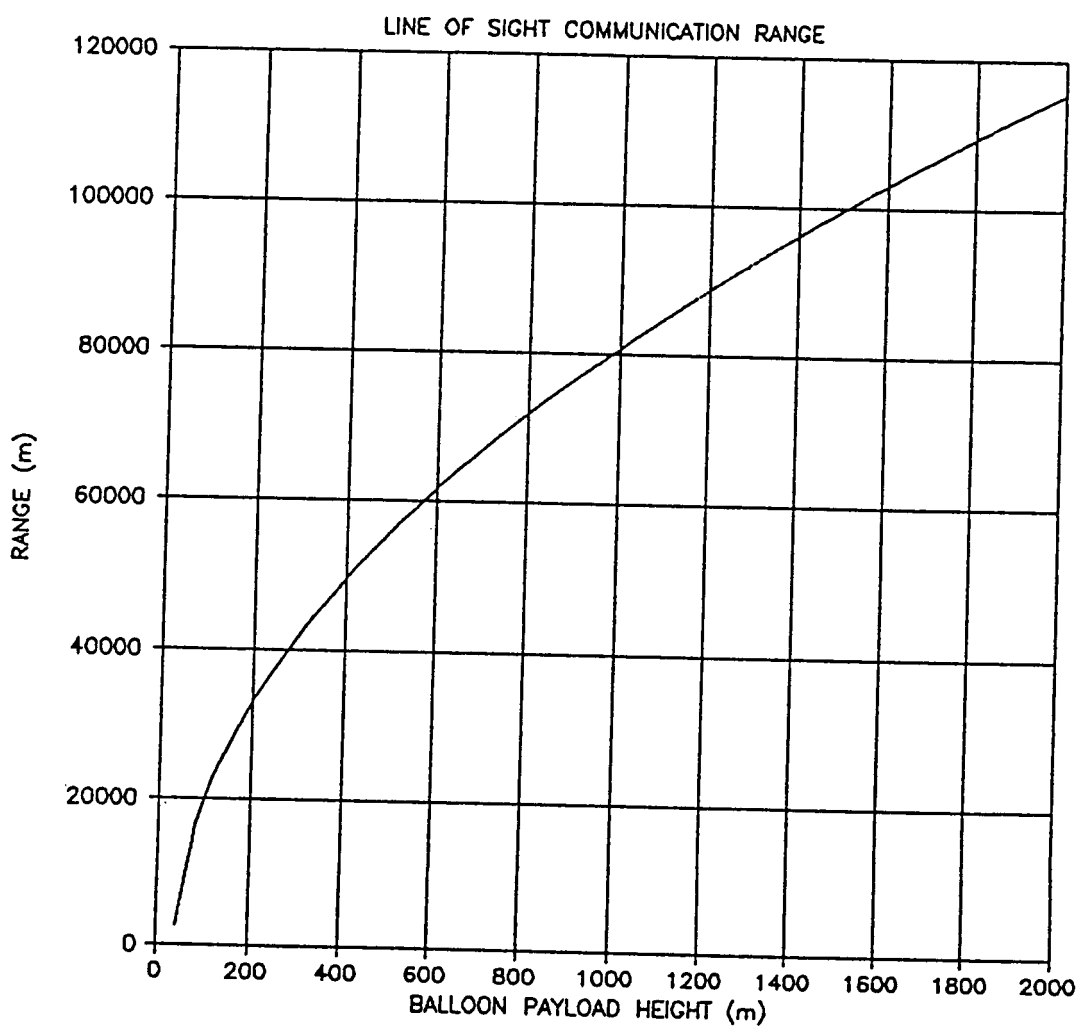


Figure 4.17

frequency radio waves, in which case, the ground could act as a carrier. In this case, the SAR would no longer be dependent upon having a clear line of sight to the initial lander. Another possible solution is direct communication with the orbiter from the SAR. A third possibility would be to use high frequency sound waves for communication. This possibility was suggested by one member of the group and is now being investigated. This may not be a viable solution to the communication problem because of the high absorption level of CO₂ to ultrasonic vibrations. Beginning at 206k-Hz, CO₂ has a decrease in reaction to the waves of a crystal vibrator as the distance to the reflector was increased beyond a few centimeters and appears to be opaque to ultrasonic frequencies above 1 M-Hz.

The problem of ten separate communication links from different areas of Mars to the orbiter could be reduced by stationing two or three orbiters in synchronous orbit above the planet. Ideally, three satellites would be used separated by an angle of 120°. If positioned correctly, two orbiters may be just as effective. This would eliminate tracking requirements on the part of the initial landers and would greatly reduce the tracking requirements of the balloon rovers.

REFERENCES

- Roark, R. J., and W. C. Young, Formulas for Stress and Strain, McGraw Hill, 5th edition.
- Klein, G., Planetary Spacecraft Systems Technology, Final Report 1986, October 30, 1986.
- Beresford, J., Mars Balloon Payload, Summer Undergraduate Research Fellowship Report, August 1986.
- Black, W. Z., and J. G. Hartley, Thermodynamics, Harper & Row, 1985.
- Byte, October 1984.
- Robotics Age, "A Multielement Ultrasonic Ranging Array," July 1985.
- Vision Technology, June 1986.
- Van Wylen and Sonntag, Fundamentals of Classical Thermodynamics, Table A.9, Wiley, 1973.
- Casasent, D. P., "Intelligent Robots and Computer Vision," SPIE, Vol. 579, September 1985.
- Moravec, H. P., Robot Rover Visual Navigation, 1981.
- Albus, J. S., Brains, Behavior, and Robotics, 1981.
- Kinsler, L. E., and A. R. Frey, Fundamentals of Acoustics, 1950.

5.0 Balloon System

The Balloon Systems Group's task has been to perform preliminary design analysis on a suitable balloon rover system for the Mars Lander/Rover. Included in the design analysis is sizing of the balloon, determining available lift for payloads, operating conditions, and heat transfer. This section presents the results to date of this study, as well as recommendations for further research.

5.1 Balloon Design

5.1.1 Balloon Physics

In order to understand the balloon's dynamics, the basic theory of balloons is examined, and the forces that affect them are presented. Then, it will be shown that under certain circumstances a balloon's gas temperature becomes important.

Archimedes' principle is applied here to non-extensible and zero pressure balloons and equations are derived by which their performance in the atmosphere of any planet can be analyzed. For convenience, Archimedes' principle is repeated here:

A body wholly or partly immersed in a fluid is buoyed up with a force equal to the weight of the fluid displaced by the body.

By Archimedes' principle, the buoyant force (F_B) of a balloon in the atmosphere is

$$F_B = V_{bal} (D_{air} - D_{gas}) - A_{bm} D_{bm} \quad (5.1)$$

where V_{bal} is the balloon volume, D_{air} is the air density, D_{gas} is the balloon gas density (evaluated from ideal gas law), A_{bm} is the surface area of the balloon, and D_{bm} is the area density of the balloon's material. It should be noted that at zero buoyant force, the balloon will not rise or fall, and it is floating at a given altitude.

For the lower atmosphere of Mars, the exponential density model will work, which is based on a constant atmospheric temperature of 220 K, based on Viking mission data [1]. The density of the air can be expressed as

$$D_{air} = D_0 e^{(H/SH)} \quad (5.2)$$

where D_0 is the density at mean elevation ($.0143 \text{ kg/m}^3$), H is the altitude in km, and SH is the scale height (11.3 km). In order to evaluate the pressure (P) and gas density, the ideal gas law is applied

$$P = D_{air} R T_{air}/MW_{air} \quad (5.3)$$

$$D_{gas} = P MW_{gas}/ R/ T_{gas} \quad (5.4)$$

where R is the universal gas constant, MW_{air} is the molecular weight of the air, and MW_{gas} is the molecular weight of the gas. The combination of Equations 5.3 and 5.4 yields

$$D_{gas} = D_{air} (MW_{gas} / MW_{air})(T_{air} / T_{gas}) \quad (5.5)$$

This equation suggests that the $MW_{\text{gas}} / MW_{\text{air}}$ needs to be as low as possible. Since 94% of the Mars atmosphere consists of CO_2 , the molecular weight of Mars is assumed to be 44 gr/mole. Also, the third term on the right side of Equation 5.5 suggests that the higher the inside temperature, the lower the gas density, resulting in greater lift. Figure 5.1 represents the temperature difference between balloon gas (hydrogen) and air (Mars) vs. the lift for different balloon radii. As expected, for low $MW_{\text{gas}} / MW_{\text{air}}$, all four curves have a gradual slope. This figure shows that in order to provide significant lift due to the temperature difference, the balloon radius should exceed 27 meters and ΔT (Difference between ambient and balloon gas temperature) must be greater than 350 K. Considering payload mass limitations (to be discussed later), it appears that a lighter-than-air gas balloon is preferable when compared to a hot air balloon.

5.1.2 Balloon Design Computer Program

A computer program has been developed to evaluate balloon performance in the Martian atmosphere based upon Archimedes' principle. Input parameters include balloon fabric density, balloon gas, gas equilibrium temperature, and the cruising altitude. Output consists of total mass, fabric mass, and payload mass as a function of radius, assuming a spherical balloon. For a given radius spherical balloon, the total buoyant force is calculated, and the fabric weight is subtracted from it. Any remaining lift is available for an external payload, including the structure, connecting system and the actual scientific payload. The simulated computer model is presented in the Appendix 5.1.

Employing the balloon analysis program, the use of a balloon to lift the whole MLR was deemed unfeasible, due to the extremely large balloon required (54 m diameter), even when assuming a 2 km cruising altitude and hydrogen as the balloon gas. In order to take advantage of the unique scientific benefits offered by a balloon rover, a smaller system (total mass of 300 kg) was designated. Upon landing of the 1,000 kg lander, a balloon would be inflated with stored gas, sealed, and together with a small payload, be detached from the mothership. After reaching cruising altitude, the balloon would stay aloft day and night, until diffusion losses force the rover to land. As soon as the rover lands, the balloon will be detached (in order to avoid payload dragging).

5.1.3 Balloon Analysis

In order to optimize the balloon design, the Balloon Systems Group identified the major design parameters that affect the balloon's performance. These parameters are: balloon gas, balloon fabric density, and cruising altitude. The temperature difference between the balloon gas and the ambient atmosphere had little effect on the balloon's lifting capability for balloon gases with low molecular weights, but has an appreciable effect on "hot-air" systems, as will be discussed later.

Due to the extremely thin Martian atmosphere, ambient density drops rapidly with altitude. Within the 300 kg mass constraint, the balloon is limited to cruising altitudes below 8 km for a helium balloon with a typical fabric density. Lift varies inversely with altitude, as can be seen in Figure 5.2. A cruising altitude of 2 km has been selected as the cruising altitude for the 300 kg rover, since it is low enough to provide

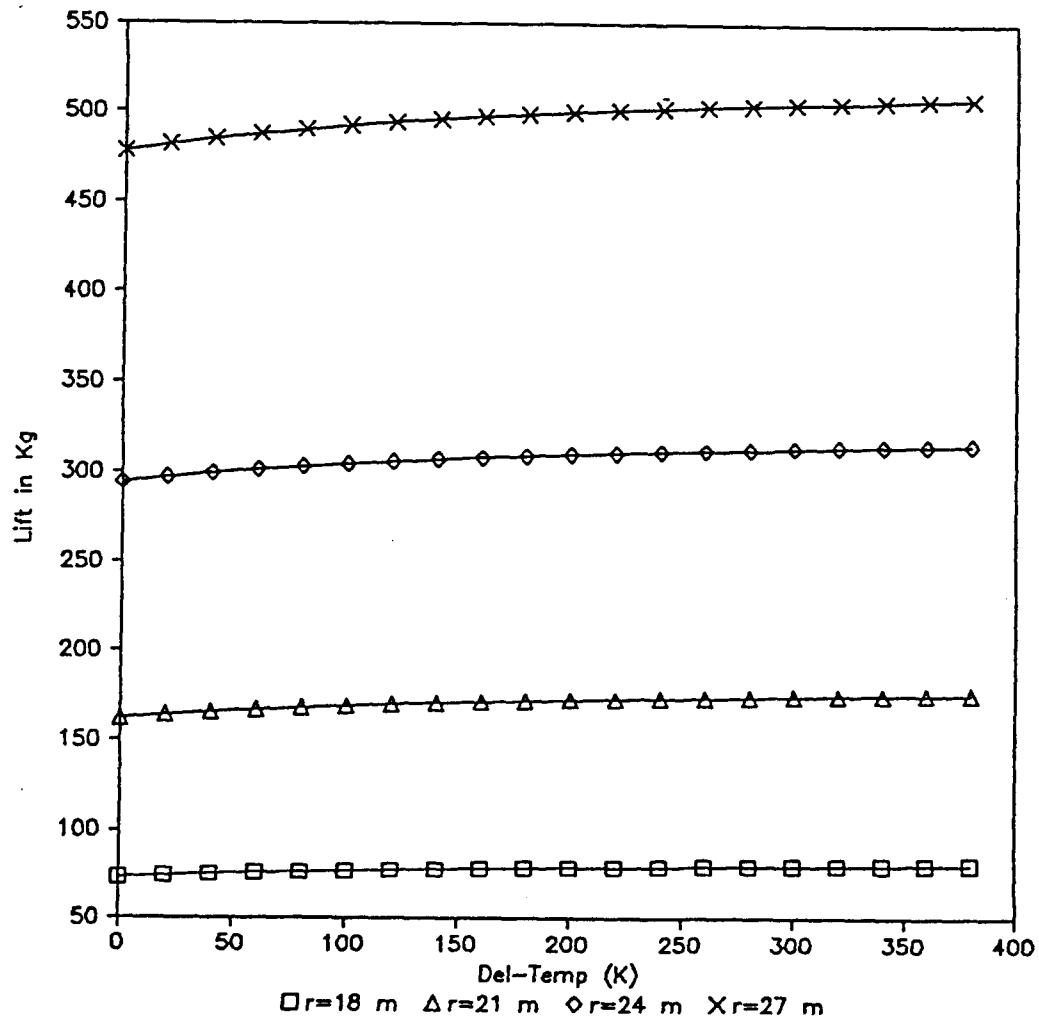


Figure 5.1 Temperature Difference vs. Lift

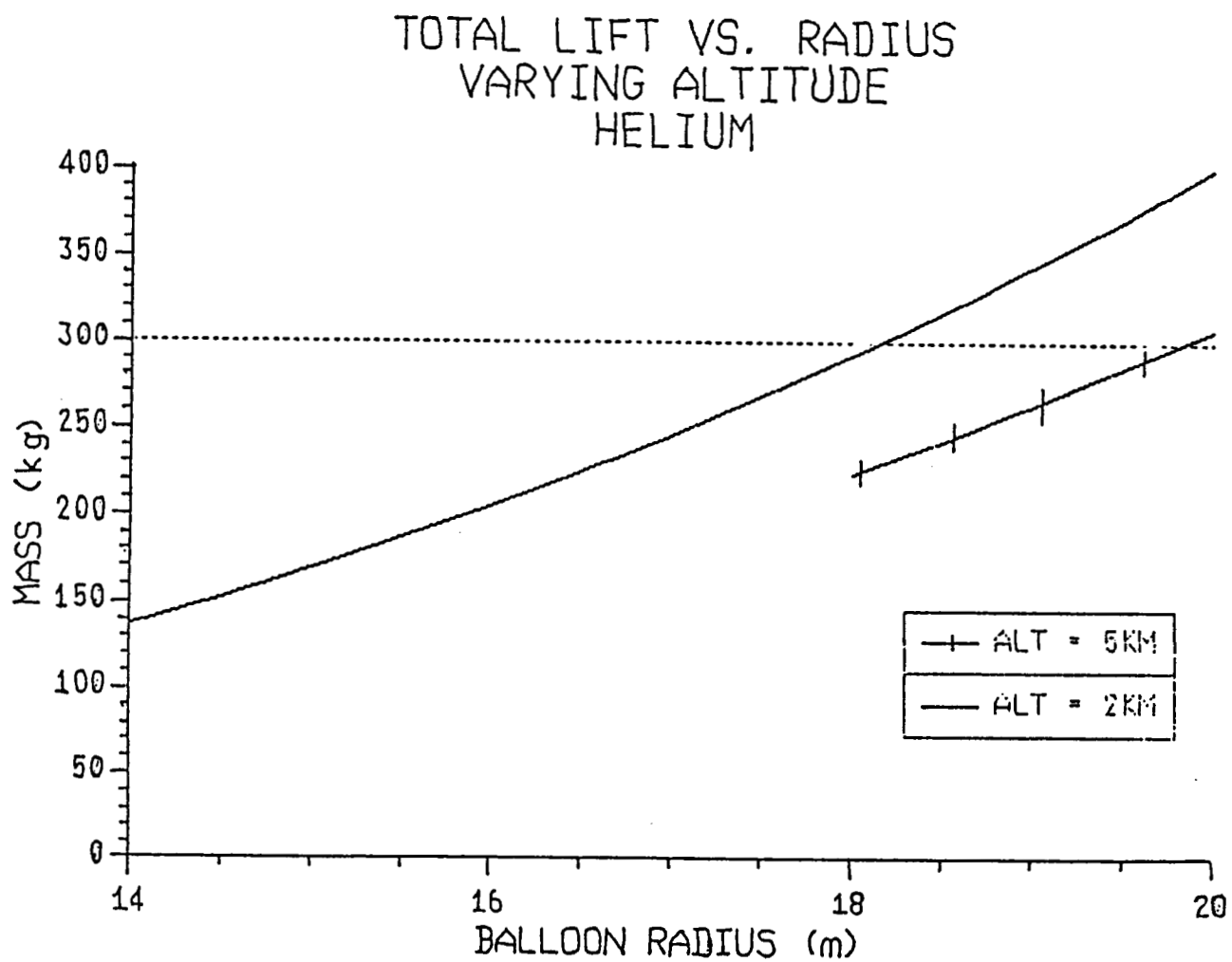


Figure 5.2

relatively good lift, but high enough to avoid surface-induced air turbulence and most surface obstructions.

As mentioned previously, a lighter balloon gas will provide more payload lift per unit volume. As shown in Figure 5.3, a 300 kg balloon filled with hydrogen can lift 80 kg of payload, a helium balloon can lift 67 kg, but a methane balloon can only lift 9 kg. The difference between hydrogen and helium is slight, and final selection between the two will depend strongly on other factors besides buoyancy, such as storability, diffusion through the balloon wall, and safety considerations. At this point, it seems that hydrogen is the most effective lifting gas.

The fabric density has a substantial effect on balloon performance as seen from Figure 5.4. While thick fabrics carry a substantial weight penalty, the fabric must be strong enough to withstand the harsh Martian environment. Based on the present day standards for Mylar weather balloons, a fabric density of 50.8 g/m^2 has been selected, corresponding to the density of a Mylar/nylon balloon with a 0.0508 mm (2 mil) fabric thickness [2].

Based upon research to date, the Balloon System group recommends using an 18 m radius, hydrogen-filled sealed balloon, which can provide lift for an 80 kg payload package (including science, structure, connecting tether, etc.) with a total system mass of 300 kg. Maximum cruising altitude is 2 km, assuming a balloon fabric density of 50.8 g/m^2 .

There is a great deal of further research that needs to be performed before a final design is proposed. More in-depth investigation of balloon materials is needed to determine realistic fabric densities, allowable temperature range, diffusion rates, and strength characteristics. Gas storage and deployment systems also need to be subjected to further investigation.

In the next section, principles of hot air balloons will be studied and compared with the lighter-than-air gas balloon.

5.2 Other Areas of Research

5.2.1 Hot Air Balloon

In principle, a hot air balloon is the same as the aforementioned balloon, but it achieves lift only through a temperature differential between the atmospheric gases inside the balloon and the air outside. The air inside is heated through solar radiation and/or a heater. Thus, the air inside is less dense than the air outside. This density difference provides lift in the same manner as the lighter-than-air gas balloon.

A major requirement for hot air balloon operation is the replacement of lost heat. Heat is lost through radiation and convection. The possibility of using a heater to heat the balloon gas is mass and power prohibitive, so heating sources are limited to direct solar radiation and that reflected from Mars' surface. During the day, the balloon will achieve a higher temperature than the surrounding air if it absorbs radiation energy.

Figure 5.5 shows the lift vs. temperature difference between the surface of the balloon and the outside (air) temperature for different balloon radii. Comparison of Figures 5.4 and 5.5 shows that in order to have the lift capability of the (high fabric density) hydrogen system, the hot air system needs to be almost eight times larger in volume.

PAYLOAD MASS VS. TOTAL MASS
ALT = 2km, $d = 50.8 \text{ g/m}^2$
VARIOUS BALLOON GASES

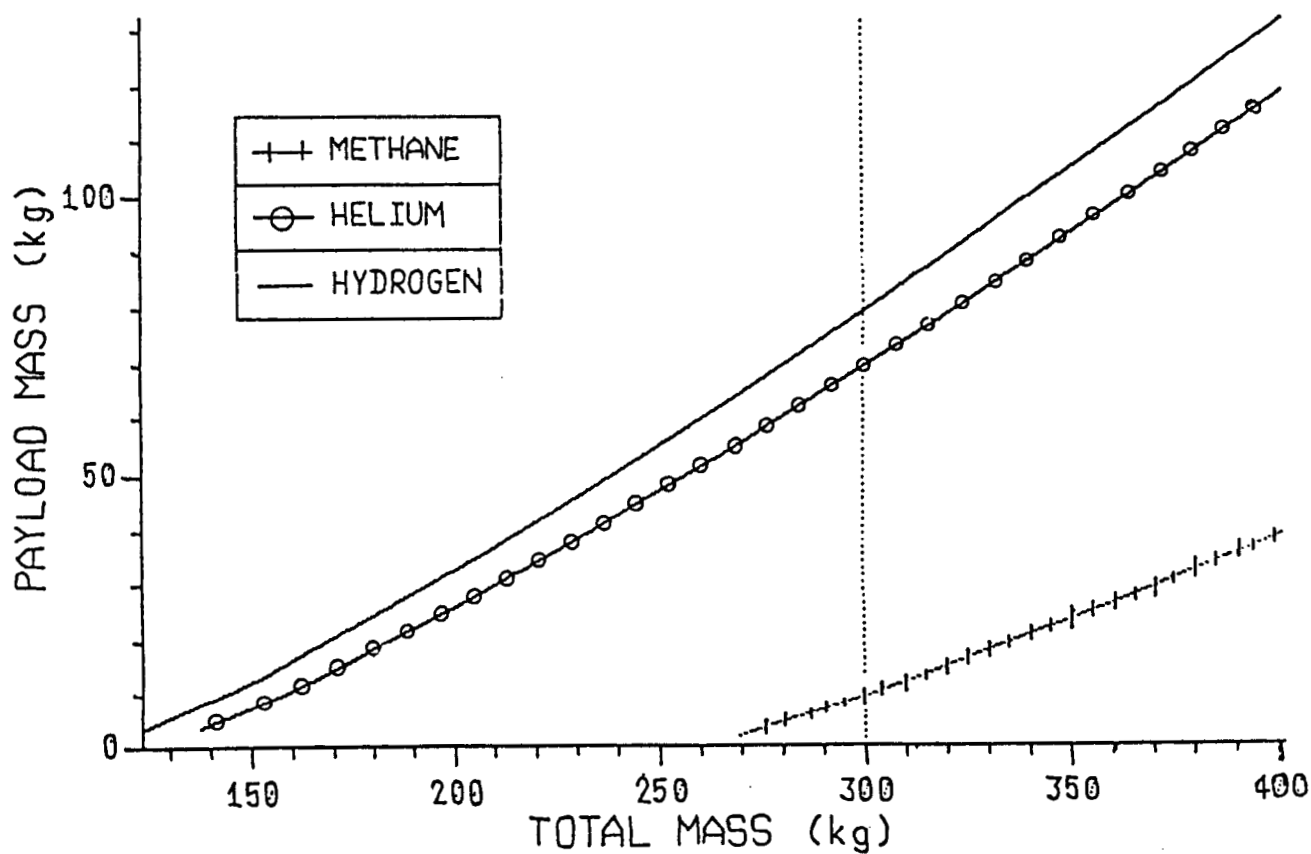


Figure 5.3

PAYLOAD MASS VS. TOTAL MASS
HYDROGEN, ALT = 2km
VARIOUS FABRIC DENSITIES

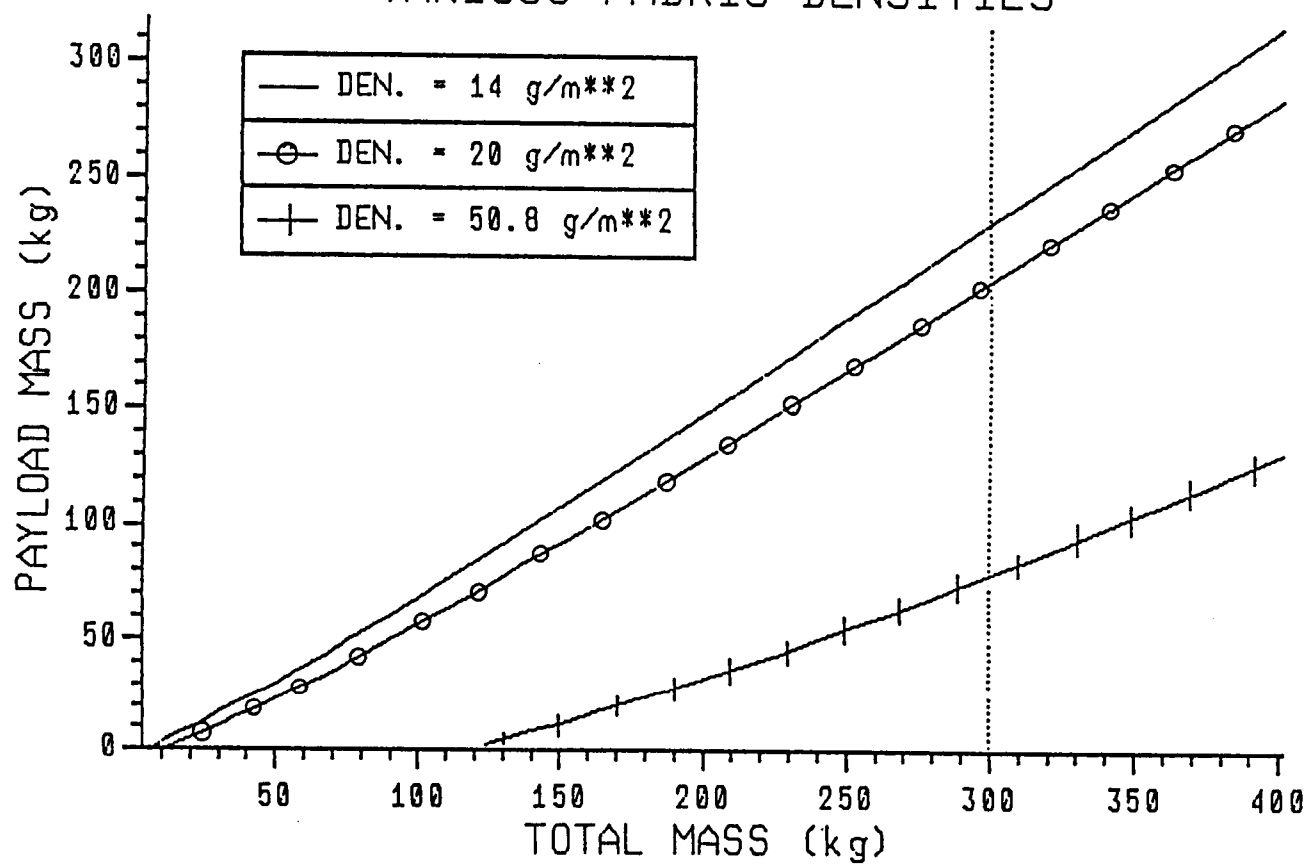


Figure 5.4

PAYLOAD/TOTAL MASS PROFILE
DEN. = 20 g/m**2, ALT = 2km
HOT AIR BALLOON

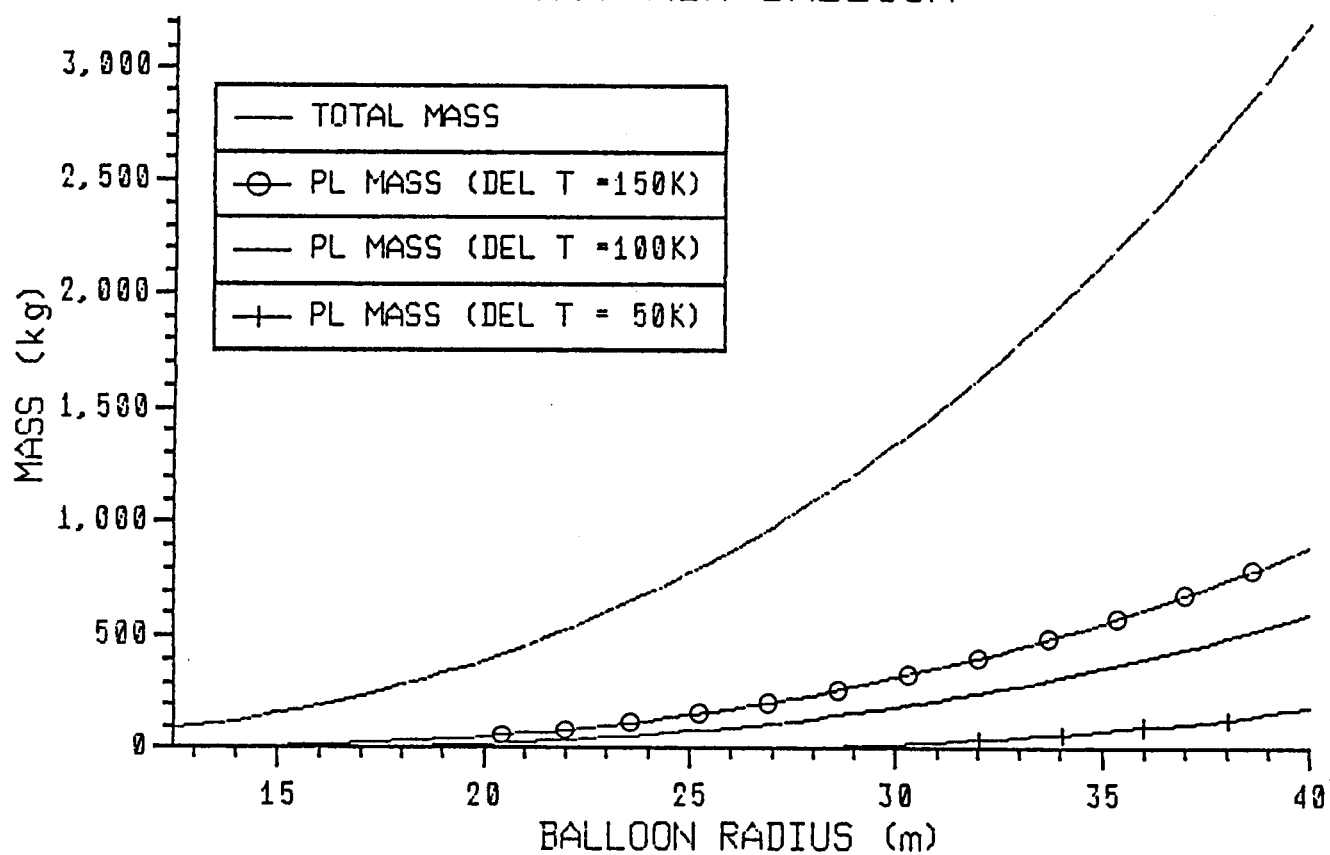


Figure 5.5

Using such a large balloon would place excessively high mass and storage volume constraints on the total lander/rover design.

5.2.2 Heat Transfer Analysis

For simplicity of the analysis, conduction heat transfer is ignored and heat transfer process is assumed to be solely due to radiation and convection. Thermal mass is assumed to be negligible (no energy stored in the balloon material), and only steady state analysis is performed.

Radiation heat transfer is treated very simply, ignoring the many complications involved in the heat transfer details. Nevertheless, the simplified model will constitute a reasonable compromise between utility and clarity of development.

Free convection heat transfer is based on the following assumptions:

- 1) Ambient temperature and pressure are 220 K and 1000 Pa, respectively
- 2) Mars atmosphere is modeled as a perfect gas consisting only of CO₂
- 3) Thermal conductivity is a function of temperature only.
- 4) No conduction heat transfer occurs inside the balloon

The steady state temperature response is determined by formulating an overall energy balance on the solid. This includes energy entering (E_{in}) and leaving (E_{out}) the surface. A general form of the energy conservation requirement may then be expressed on a rate basis as

$$E_{in} - E_{out} = 0 \quad (5.6)$$

The simplified model is represented in Figure 5.6. The analysis is based on a flat disc surface. The plate is parallel to the surface of Mars. In this figure, G_s is the solar flux (580 W/m²), e is the emissivity of the surface (0.9), Z is the Stefan-Boltzmann constant (5.67E-8 W/m²/K⁴), T_s is the material surface temperature, q_{conv} is convection heat lost, and G_m is the reflected Mars flux (70 W/m²). Note that arrows pointing into and out of the disc represent E_{in} and E_{out} , respectively.

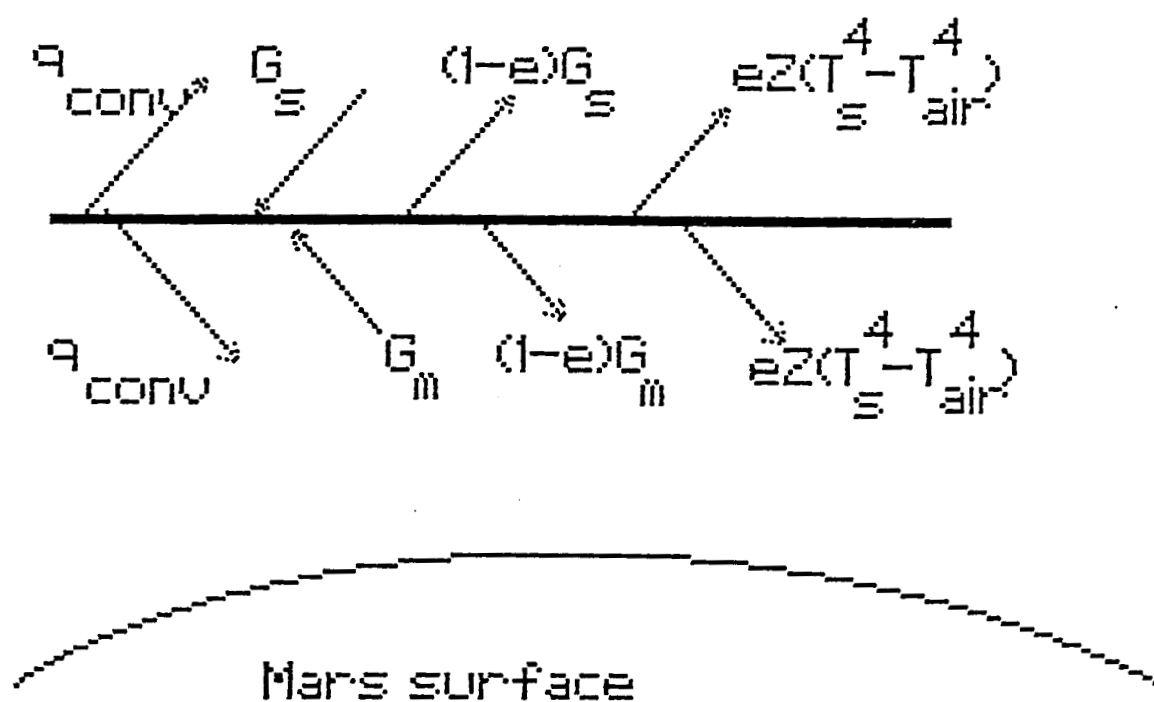
Free convection heat transfer was calculated using standard empirical techniques to determine the heat transfer coefficient (h). Initially, h was calculated for a spherical surface, but the resulting Raleigh (Ra) number was several orders of magnitude high than the upper limit of the empirical formula used. Satisfactory results were obtained by using a disc model (Figure 5.6). The equation used to define the convection heat transfer process of a disc can be expressed as

$$q_{conv} = A h (T_s - T_0) \quad (5.7)$$

where A is the surface area and h is defined as [3]:

$$h = (.0168/D) \{ [.27(3.93 \times 10^6 ((T_s - T_0)/T_s) D^3)^{.25}] + [.15(3.93 \times 10^6 ((T_s - T_0)/T_s) D^3)^{.3334}] \} \quad (5.8)$$

where D is the diameter of the disc in meters.



PRECEDING PAGE BLANK NOT FILMED

Figure 5.6 Heat Transfer Model

Based on the above assumptions, the surface temperature of the disc is calculated for different ambient temperatures (Appendix 5.2 contains the program), and the results of the simulation are shown in Figure 5.7. This figure suggests that the maximum Del-Temp is about 100 K, which corresponds to only 10 kg lift for balloon radius of 18 m.

From the heat transfer analysis of the hot air balloon, it was concluded that the hot air balloon is not suitable for missions that require a payload mass of 50 kg or more. This conclusion is based on a very simplified model and further studies in this field are needed to understand the more profound and realistic relations between the different processes defining heat transfer through the balloon material.

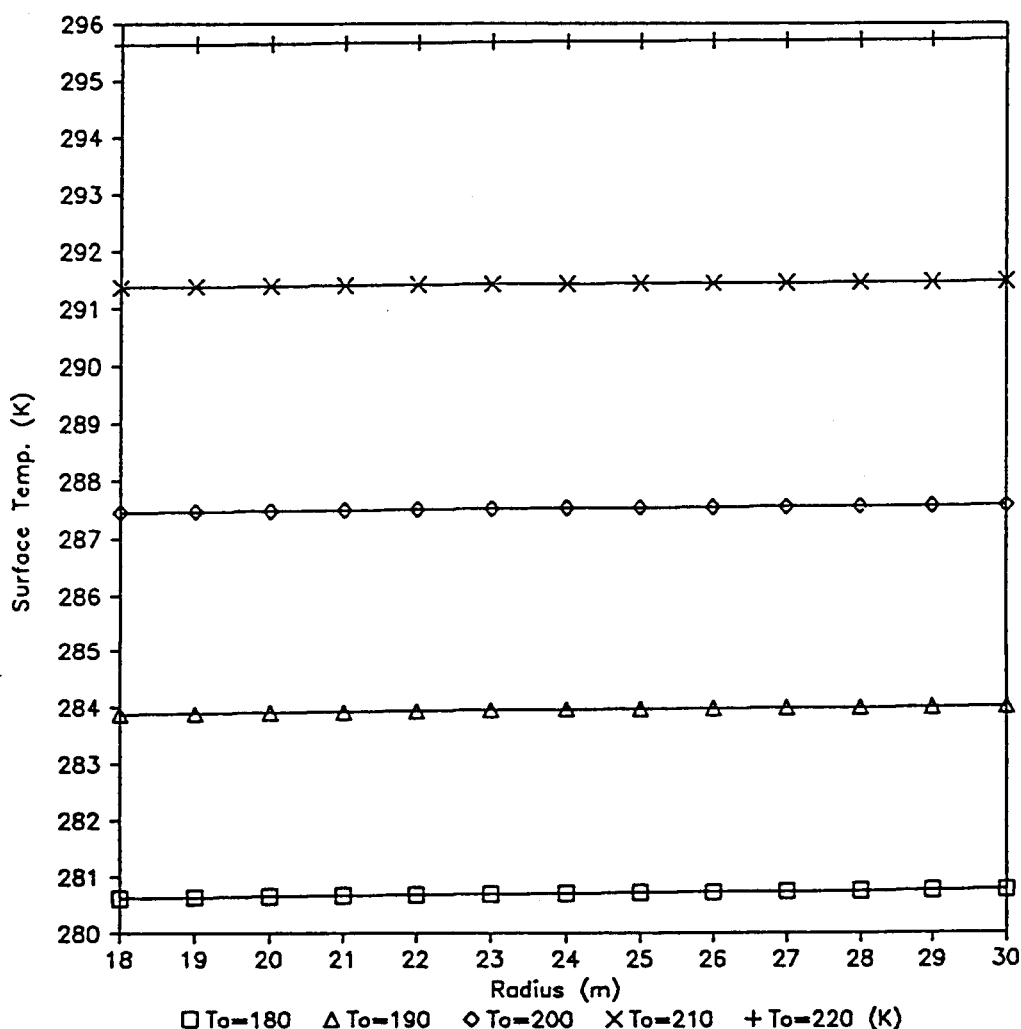


Figure 5.7 Balloon Surface Temperature vs. Balloon Radius

REFERENCES

Beresford, J., E. Gaidos, and B. Hayes, "Balloons: A Promising Option for the Surface Exploration of Mars," Report of the Cal Tech Mars SURF, 1985.

Davis, M. H., and S. M. Greenfield, "The Physics of Balloons and their Feasibility as Exploration Vehicles on Mars," RAND Corp for JPL, September 1963.

Keith, F., and W. Z. Black, Basic Heat Transfer, New York: Harper, 1980.

PRECEDING PAGE BLANK NOT FILMED

6.0 Conclusion

The Winter Quarter phase of the MLR Design process has been quite effective in more clearly defining the overall system. During Spring Quarter, one major element of this system, the Balloon Rover, will be selected for further development. In this fashion, two goals will be accomplished. First, this design course, over the academic year, will have demonstrated and taken an active part in a majority of the phases involved in the development of a project, from initial scoping to in-depth design. Second, the results from this effort will provide a valid and useful basis for further studies of Mars exploratory vehicles. Throughout this course, a philosophy of diligent source referencing and explanation of pertinent equation derivations has been followed in order to augment the utility of the final design conclusions and recommendations in further research efforts.

ORIGINAL PAGE IS
OF POOR QUALITY

APPENDICES

Note: Appendix numbering corresponds to the referrant section. As such, the numbering appears discontinuous, but is employed for ease of reference to appropriate sections within the report.

Appendix 2

Orbital Descent Modeling Program

C#####
C MLTRAJ. FOR 14 NOV 86 RUSS LAHER AND ROGER HART

THIS PROGRAM INTEGRATES THE EQUATIONS OF MOTION (PG 11 IN NOTES)
OF THE MARS LANDER, GIVING VELOCITIES AND POSITION AS A FUNCTION
OF TIME IN POLAR COORDINATES. MKS UNITS ARE USED UNLESS OTHER-
WISE SPECIFIED.

INPUT:

MO - INITIAL MASS OF LANDER (KG)
A - RADIUS OF LANDER (M)
R1 - SEMI-MINOR AXIS OF INITIAL ORBIT (M)
R2 - SEMI-MAJOR AXIS (M)
THETA0 - KEPLER ANGLE OF ENTRY RETRO-BURN (0-360 DEG)
DELT - TIME INTEGRATION STEP SIZE (SEC)
TOL - MAXIMUM ALLOWED CHANGE IN RADIAL POSITION (M)

C#####

REAL*8 RHO, NRE, CD, TEMP, MO, M, A, H, RP, RHOO, HETA, GACC, HR, HT,
> K, G, MP, E, AP, R1, R2, EC, VPOT, THETA0, RO, L, VRO, VTO, PI,
> R(3,2), T(3,2), VR(3,2), VT(3,2), DELT, TIME, HR12, HT12,
> HR21, HT21, TOL, CHANGE, HR22, HT22, HR31, HT31, DELT2,
> RHOC, CDC, GACCC, MCO2, NA, SIGMAC, RGAS, ISP, DELTV,
> RPAR, ZPAR, ZPARE, FMBR, TAU, ME, VE, VINIT, RI, RIF
INTEGER*4 I, IPFREQ

EXTERNAL HR
EXTERNAL HT
EXTERNAL GACC
EXTERNAL CD
EXTERNAL RHO

COMMON/CMARS/TEMP, MO, M, A, H, RP, RHOO, HETA, NRE, PI, G, MP, ISP,
> RPAR, ZPAR, ZPARE, FMBR, TIME, DELT2, ME, VE
COMMON/CEXT/RHOC, CDC, GACCC

CONSTANTS & INITIALIZATION

DELTAVS=0.
TEMP=220.
H=11.28D3
G=6.672D-11
MP=6.42D23
RP=3.388D6
PI=3.14159265
MCO2=4.401D-2
NA=6.022D23
SIGMAC=6.65D-19
RGAS=8.3144
ISP=235.

HETA=(MCO2/(3.*NA*SIGMAC))*SQRT(8.*RGAS*TEMP/(PI*MCO2))

RHOO=1.426E-2

INPUT

OPEN(UNIT=3, FILE='MLTRAJ. INP', FORM='FORMATTED', STATUS='OLD')
READ(3,*)MO
M=MO

```

READ(3,*)A
READ(3,*)R1
READ(3,*)R2
READ(3,*)THETA0
  IF (THETA0.LT.0.OR.THETA0.GT.360.) THEN
    STOP ' THETA0 OUT OF REQUIRED RANGE '
  END IF
READ(3,*)DELT
READ(3,*)TOL
READ(3,*)DELT V
READ(3,*)IPFREQ
READ(3,*)RPAR
READ(3,*)ZPARD
READ(3,*)ZPARE

```

OUTPUT

```

OPEN(UNIT=7, FILE='MLTRAJ. OUT', FORM='FORMATTED', STATUS='NEW')

```

COMPUT INITIAL POSITION AND VELOCITY BEFORE RETRO-BURN

```

AP=(R1+R2)/2.
K=G*MP*MO
E=-K/(2.*AP)
EC=1.-R1/AP
RO=AP*(1.-EC*EC)/(1.+EC*COS(PI*THETA0/180.))
VPOT=-K/RO
L=SQRT((1.-EC*EC)*MO*K*AP)
  IF (THETA0.EQ.0..OR.THETA0.EQ.180.) THEN
    VRO=0.
  ELSE
    VRO=SQRT(2.*(E-VPOT-L*L/(2.*MO*RO*RO))/MO)
  END IF
  IF (THETA0.GT.180.) VRO=-VRO
VTO=L/(MO*RO)

```

LOAD INITIAL POSITION AND VELOCITY VALUES INTO
PREDICTOR-CORRECTOR TIME INTEGRATION ARRAYS

```

R(1,2)=RO
T(1,2)=THETA0*PI/180.
VR(1,2)=VRO
VT(1,2)=VTO

```

PRINT COMPUTED DATA

```

WRITE(7,90)
90 FORMAT(30X, 'MARS LANDER SIMULATION')
WRITE(7,91)
91 FORMAT(1X)
WRITE(7,*) ' INITIAL LANDER MASS (KG) = ', MO
WRITE(7,*) ' LANDER RADIUS (M) = ', A
WRITE(7,*) ' SEMI-MINOR AXIS OF INITIAL ORBIT (M) = ', R1
WRITE(7,*) ' SEMI-MAJOR AXIS OF INITIAL ORBIT (M) = ', R2
WRITE(7,*) ' KEPLER ANGLE OF ENTRY RETRO-BURN (DEG) = ', THETA0
WRITE(7,*) ' TIME INTEGRATION STEP SIZE (SEC) = ', DELT
WRITE(7,*) ' PREDICTOR-CORRECTOR ERROR BOUND (M) = ', TOL
WRITE(7,*) ' RETROGRADE BURN DELTA V (THETA) = ', DELT V
WRITE(7,*) ' PARACHUTE RADIUS (M) = ', RPAR
WRITE(7,*) ' PARACHUTE DEPLOYMENT ALT. (KM) = ', ZPARD

```

```

WRITE(7,*)' CHUTE EJECT & DESCENT PROPULSION ALT. (KM)=' , ZPARE
WRITE(7,91)
WRITE(7,95)
95 FORMAT(1X, 'TIME (SEC)', 3X, 'ALT (KM) ', 1X,
> 'THETA (DEG) VR (M/SEC) ',
> 'VTHETA (M/SEC) RHOC', 8X, 'GRAY ACCEL',
> 2X, 'NRE', 7X, 'MASS (KG)', 'TOTAL ACCEL')

RHOC=RHO(R(1,2))
GACCC=GACC(R(1,2))

WRITE(7,100) TIME, (R(1,2)-RP)/1000., T(1,2)*180./PI, VR(1,2),
> VT(1,2), RHOC, GACCC, RHOC*A*SQRT(VR(1,2)**2+VT(1,2)**2)/HETA,
> M, GACCC
100 FORMAT(1X, F10.1, 1P, 9D12.3)

DEORBIT RETROGRADE BURN - FROM INPUTTED DELTA V

VINIT=SQRT(VR(1,2)**2+VT(1,2)**2)
VR(1,2)=VR(1,2)-DELT*VR(1,2)/VINIT
VT(1,2)=VT(1,2)-DELT*VT(1,2)/VINIT
CALL DORBIT(DELT)

WRITE(7,100) TIME, (R(1,2)-RP)/1000., T(1,2)*180./PI, VR(1,2),
> VT(1,2), RHOC, GACCC, RHOC*A*SQRT(VR(1,2)**2+VT(1,2)**2)/HETA, M

USE THE SECOND-ORDER MODIFIED EULER METHOD TO ITERATE ONE
STEP IN TIME FOR THE PREDICTOR-CORRECTOR TIME INTEGRATION

DELT2=DELT/2.
TIME=DELT

R(2,1)=R(1,2)+DELT2*VR(1,2)
T(2,1)=T(1,2)+DELT2*VT(1,2)/R(1,2)
HR12=HR(R(1,2), T(1,2), VR(1,2), VT(1,2))
VR(2,1)=VR(1,2)+DELT2*HR12
HT12=HT(R(1,2), T(1,2), VR(1,2), VT(1,2))
VT(2,1)=VT(1,2)+DELT2*HT12

R(2,2)=R(1,2)+DELT*VR(2,1)
T(2,2)=T(1,2)+DELT*VT(2,1)/R(2,1)
HR21=HR(R(2,1), T(2,1), VR(2,1), VT(2,1))
VR(2,2)=VR(1,2)+DELT*HR21
HT21=HT(R(2,1), T(2,1), VR(2,1), VT(2,1))
VT(2,2)=VT(1,2)+DELT*HT21

PRINT COMPUTED DATA

WRITE(7,100) TIME, (R(2,2)-RP)/1000., T(2,2)*180./PI, VR(2,2),
> VT(2,2), RHOC, GACCC, RHOC*A*SQRT(VR(2,2)**2+VT(2,2)**2)/HETA, M

BEGIN PREDICTOR-CORRECTOR TIME INTEGRATION

IFLAG1=0

I=0
10 I=I+1
20 TIME=TIME+DELT

PREDICTOR STEP

```

```

R(3,1)=R(2,2)+DELT2*(3.*VR(2,2)-VR(1,2))
T(3,1)=T(2,2)+DELT2*(3.*VT(2,2)/R(2,2)-VT(1,2)/R(1,2))
HR22=HR(R(2,2), T(2,2), VR(2,2), VT(2,2))
VR(3,1)=VR(2,2)+DELT2*(3.*HR22-HR12)
HT22=HT(R(2,2), T(2,2), VR(2,2), VT(2,2))
VT(3,1)=VT(2,2)+DELT2*(3.*HT22-HT12)

```

CORRECTOR STEP

```

R(3,2)=R(2,2)+DELT2*(VR(3,1)+VR(2,2))
T(3,2)=T(2,2)+DELT2*(VT(3,1)/R(3,1)+VT(2,2)/R(2,2))
HR31=HR(R(3,1), T(3,1), VR(3,1), VT(3,1))
VR(3,2)=VR(2,2)+DELT2*(HR31+HR22)
HT31=HT(R(3,1), T(3,1), VR(3,1), VT(3,1))
VT(3,2)=VT(2,2)+DELT2*(HT31+HT22)

```

ERROR MANAGEMENT: RADIAL POSITION IS NOT ALLOWED TO CHANGE MORE THAN THE VALUE TOL; USING THE PREDICTOR-CORRECTOR ERROR CONDITION ON THE R-POSITION EQUATION...

```

CHANGE=ABS(VR(3,2)-VR(2,2))/(6.*DELT)
IF (CHANGE.GT.TOL) THEN
  TIME=TIME-DELT
  DELT=DELT2
  DELT2=DELT/2.
  WRITE(7,*)' TIME STEP HALVED - DELT (SEC) =',DELT
  WRITE(*,*)' TIME STEP HALVED - DELT (SEC) =',DELT
  GOTO 20
END IF

```

PRINT COMPUTED DATA

```

IF ((R(3,2)-RP)/1000. .LT. 80.) IPFREQ=INT(1./DELT)
RI=DFLOAT(I)
RIF=DFLOAT(IPFREQ)
IF (RI/RIF.EQ. INT(RI/RIF)) THEN
  WRITE(7,100)TIME, (R(3,2)-RP)/1000., T(3,2)*180./PI, VR(3,2),
> VT(3,2), RHOC, GACCC, NRE, M, SQRT(((HR31+HR22)/2. )**2+((HT31+
> HT22)/2. )**2)
> VT(3,2), RHOC, GACCC, RHOC*A*SQRT(VR(3,2)**2+VT(3,2)**2)/HETA, M
END IF

```

```

IF ((R(3,2)-RP)/1000. .LT. ZPARD .AND. IFLAG1.EQ.0) THEN
  IFLAG1=1
  WRITE(7,*)' EJECT AEROSHELL & DEPLOY PARACHUTE'
  M=M-192.
  DELT=0.01
  DELT2=DELT/2.
END IF

```

```

IF ((R(3,2)-RP)/1000. .LT. ZPARE) THEN
  WRITE(7,*)' EJECT PARACHUTE'
  M=M-50.
  GOTO 200
END IF

```

PREPARE FOR NEXT TIME STEP

```

R(1,2)=R(2,2)
R(2,2)=R(3,2)
T(1,2)=T(2,2)
T(2,2)=T(3,2)
VR(1,2)=VR(2,2)
VR(2,2)=VR(3,2)
VT(1,2)=VT(2,2)
VT(2,2)=VT(3,2)
HR12=HR22
HT12=HT22
GOTO 10
STOP ' NEED MORE DO LOOP STEPS TO FINISH'

```

```

GET DESCENT PROPULSION BURN RATE

```

```

200 ME=M
VE=VR(3,2)
CALL DESCEN(TAU)
WRITE(7,*) ' FUEL MASS BURN RATE (KG/SEC) =', FMBR
WRITE(7,*) ' DESCENT PROPULSION BURN TIME (SEC) =', TAU
WRITE(7,*) ' MASS OF FUEL USED (KG) =', TAU*FMBR
M=M-TAU*FMBR
WRITE(7,*) ' FINAL MASS OF LANDER ON MARTIAN SURFACE (KG) =', M
WRITE(7,*) ' IMPACT VELOCITY (M/SEC) =',
> VE-GACC(RP+ZPARE*1000./2.)*TAU+ISP*9.81*LOG(ME/(-FMBR*TAU
> +ME))

```

```

STOP
END

```

```

=====
C MLTRAJSB.FOR      19 NOV 86      ROGER HART AND RUSS LAHER
C
C THE FOLLOWING SET OF SUBROUTINES ARE USED WITH PROGRAM
C MLTRAJ.FOR TO SIMULATE THE ENTRY OF SPACECRAFT INTO
C THE MARTIAN ATMOSPHERE.
=====
C FUNCTION HR(R, THETA, VR, VT)
=====
C
C HR COMPUTES THE RADIAL COMPONENT OF ACCELERATION OF A
C SHPERICAL VEHICLE. THIS COMPONENT INCLUDES BOTH DRAG AND
C GRAVITY TERMS.
C
C REAL*8 MO, M, A, H, RP, RHOO, HETA, NRE, PI, THETA, TEMP
C REAL*8 DENS, BETA, HR, CD, GACC, V, VR, VT, R, RHO, G, MP, ISP
C REAL*8 TIME, RPAR, ZPARD, ZPARE, FMBR, DELT2
C
C COMMON/CMARS/TEMP, MO, M, A, H, RP, RHOO, HETA, NRE, PI, G, MP, ISP,
C > RPAR, ZPARD, ZPARE, FMBR, TIME, DELT2
C
C DENS=RHO(R)
C V=SQRT(VR**2+VT**2)
C BETA=0.5*PI*CD(VR, VT, DENS)*A**2*DENS/M
C GACCC=GACC(R)
C HR=-BETA*V*VR-GACCC+VT*VT/R
C
C PARACHUTE DECELERATION TERM
C
C Z=(R-RP)/1000.
C IF (Z.GT.ZPARD) GOTO 99
C IF (Z.GT.ZPARE) THEN
C   HR=HR-0.5*0.55*DENS*V*VR*PI*RPAR**2/M
C END IF
C
C 99 RETURN
C END
=====
C FUNCTION HT(R, THETA, VR, VT)
=====
C
C HT COMPUTES THE COMPONENT OF ACCELERATION OF THE VEHICLE IN
C THE VT DIRECTION. THIS COMPONENT IS DUE TO DRAG ALONE.
C
C REAL*8 MO, M, A, H, RP, RHOO, HETA, NRE, PI, G, MP, ISP
C REAL*8 TEMP, R, THETA, VR, VT, HT, BETA, RHO, CD, V, DENS
C REAL*8 RPAR, ZPARD, ZPARE, FMBR, TIME, DELT2
C
C COMMON/CMARS/TEMP, MO, M, A, H, RP, RHOO, HETA, NRE, PI, G, MP, ISP,
C > RPAR, ZPARD, ZPARE, FMBR, TIME, DELT2
C
C DENS=RHO(R)
C V=SQRT(VR**2+VT**2)
C BETA=0.5*PI*CD(VR, VT, DENS)*A**2*DENS/M
C HT=-BETA*V*VT-VR*VT/R

```

PARACHUTE DECELERATION & TERMINAL DESCENT PROPULSION DECELERATION TERMS

Z=(R-RP)/1000.

IF (Z.GT.ZPARD) GOTO 99

IF (Z.GT.ZPARE) THEN

HT=HT-0.5*0.55*DENS*V*VT*PI*RPAR**2/M

ELSE

HT=HT-ISP*9.81*FMBR*VT/V/M

M=M-DELT2*FMBR

END IF

99 RETURN

END

=====

FUNCTION RHO(R)

=====

RHO.FOR 11/18/86

RHO RETURNS THE DENSITY AT THE INPUT ALTITUDE IN THE MARTIAN
ATMOSPHERE. THE MODEL USES A CONSTANT SCALE HEIGHT (T=220K)
AND IS VALID TO ABOUT 100KM.

INPUT: R, ALTITUDE (M)

OUTPUT: RHO, DENSITY IN KG/M**3

REAL*8 TEMP, ISP, MO, M, A, H, RP, RHOO, R, HETA, NRE, PI, G, MP, RHO

REAL*8 RHOC, CD, GACC

COMMON/CMARS/TEMP, MO, M, A, H, RP, RHOO, HETA, NRE, PI, G, MP, ISP

COMMON/CEXT/RHOC, CD, GACC

RHO=RHOO*EXP((RP-R)/H)

RHOC=RHO

RETURN

END

=====

FUNCTION GACC(R)

=====

GACC.FOR 11/18/86

GACC RETURNS THE GRAVITATION ACCELERATION FOR THE INPUT ALTITUDE
ABOVE MARS.

INPUT: R, ALTITUDE (M)

OUTPUT: GACC, ACCELERATION (M/S/S)

REAL*8 TEMP, ISP, MO, M, A, H, RP, RHOO, HETA, NRE, PI, G, MP,

> GACC, R, GM, RHO, CD, GACCC

COMMON/CMARS/TEMP, MO, M, A, H, RP, RHOO, HETA, NRE, PI, G, MP, ISP

COMMON/CEXT/RHO, CD, GACCC

GM=G*MP

GACC=GM/R**2

GACCC=GACC

RETURN

END

#####

LANDER DRAG FUNCTION

#####

FUNCTION CD(VR, VT, RHO)

```

REAL*8 CD, VR, VT, RHO
CD=0.5
RETURN
END
FUNCTION CD(VR, VT, RHO)
REAL*8 VR, VT, RHO, NRE, CD, T, MO, M, A, H, RP, RHOO,
< HETA, PI, CDS(20), NRS(20), Y1, Y2, X1, X2, SLOPE, YINT, Y, X
COMMON/CMARS/T, MO, M, A, H, RP, RHOO, HETA, NRE
DATA CDS/8.5, 6.2, 5.8, 4.5, 3.0, 1.9, 1.6, 1.2, 1.1, .8,
< .6, .48, .45, .44, .4, .43, .45, .43, .42, .4/
DATA NRS/4., 6., 8., 10., 20., 40., 60., 80., 100., 200.,
< 400., 600., 800., 1000., 10000., 20000., 40000., 80000.,
< 100000., 200000. /
NRE=SQRT(VR*VR+VT*VT)*A*RHO/HETA
IF (NRE.GT.2.D5) THEN
CD=0.4
RETURN
END IF
IF (NRE.EQ.0.) THEN
CD=0.
RETURN
END IF

IF (NRE.LT.1.0) THEN
CD=24./NRE
RETURN
END IF
DO 10 I=2, 20
IF (NRE.GT.NRS(I)) GO TO 10
IHI=I
ILO=I-1
GO TO 20
10 CONTINUE
STOP 'INTERPOLATION ERROR'
20 X=LOG10(NRE)
Y1=LOG10(CDS(ILO))
Y2=LOG10(CDS(IHI))
X1=LOG10(NRS(ILO))
X2=LOG10(NRS(IHI))
SLOPE=(Y2-Y1)/(X2-X1)
YINT=Y1-SLOPE*X1
Y=SLOPE*X+YINT
CD=10.**Y
RETURN
END

SUBROUTINE DORBIT(DELT V)
REAL*8 DELT V, TEMP, MO, M, A, H, RP, RHOO, HETA, NRE, PI, G, MP, ISP
REAL*8 RPAR, ZPARD, ZPARE, FNBR, TIME, DELT2

COMMON/CMARS/TEMP, MO, M, A, H, RP, RHOO, HETA, NRE, PI, G, MP, ISP,
> RPAR, ZPARD, ZPARE, FNBR, TIME, DELT2

M=MO*EXP(-DELT V/(ISP*9.81))
RETURN
END

TERMINAL DESCENT PROPULSION -- COMPUTE THE FUEL BURN RATE

```


AND BURN TIME.

SUBROUTINE DESCEN(TAU)

REAL*8 XE, RE2, VEXH, ME, GACC, TAU, VE

REAL*8 TEMP, MO, M, A, H, RP, RHOO, HETA, NRE, PI, G, MP, ISP,

> RPAR, ZPARD, ZPARE, FMBR, TIME, DELT2

COMMON/CMARS/TEMP, MO, M, A, H, RP, RHOO, HETA, NRE, PI, G, MP, ISP,

> RPAR, ZPARD, ZPARE, FMBR, TIME, DELT2, ME, VE

VEXH=9.81*ISP

XE=ZPARE*1000.

RE2=RP+XE/2.

TAU=0.

DO 20 N=1, 50

X=-(GACC(RE2)*TAU-VE)/VEXH

F=XE+(VE+VEXH)*TAU-0.5*GACC(RE2)*TAU**2

> -X*VEXH*TAU*(EXP(X)/(EXP(X)-1.))

DXDTAU=-GACC(RE2)/VEXH

Z=EXP(X)/(EXP(X)-1.)

DZDX=Z*(-1./(EXP(X)-1.))

DERTRM=Z*(2.*GACC(RE2)*TAU-VE)+(GACC(RE2)*

> TAU**2-VE*TAU)*DZDX*DXDTAU

FP=VE+VEXH-GACC(RE2)*TAU+DERTRM

TAU=TAU-F/FP

WRITE(*,*) 'N, TAU=', N, TAU

20 CONTINUE

FMBR=(ME/TAU)*(EXP(-(GACC(RE2)*TAU-VE)/VEXH)-1.)

WRITE(*,*) 'VE, TAU, FMBR=', VE, TAU, FMBR

FMBR=-FMBR

RETURN

END

Appendix 3

Descent Propulsion Subsystem Sizing

SIZING OF THE USU MARS/LANDER

DESCENT PROPULSION SUBSYSTEM

Oscar Monje

The descent propulsion subsystem is to provide a smooth landing (5m/s) on the surface of Mars. The propellant of choice is Hydrazine-40% NH₃. The Environment and Trajectory Group has determined that 98 kg of fuel will be necessary to land the Lander/Rover. The purpose of this section is to size the masses and volumes occupied by the propulsion components. The information used can be found in Section 4 of the USU Little Dipper Design study.

Fuel properties:

Name	Isp	Density	Tcombustion
Hydrazine-40% NH ₃	235 (96% eff.)	1002 kg/m ³	2442 K

Hydrazine-40% NH₃ is a monopropellant that will explode at high temperatures and reacts with aluminum vessels, thus a tank made of steel or titanium is suggested. The density of titanium is 4632 kg/m³.

Sizing of Propellant Tank Volume and Mass

The tank volume can be approximated with the following equation:

$$V_{\text{tank}} = V_{\text{pu}} + V_{\text{pl}} + V_{\text{u}}$$

where V_{tank} = tank volume
 V_{pu} = volume of propellant used
 V_{pl} = volume of fuel not used (safety margin)
 V_{u} = ullage volume (volume of fuel in piping)
= 1% V_{pu}

The individual volumes are calculated from the fuel mass needed to accomplish the mission. The fuel used = 98 kg, and a safety margin of 12kg of unused fuel is allotted. This means that there will be 110 kg of hydrazine fuel which will require a minimum volume of $V_{\text{tank}} = 0.11 \text{ m}^3$.

The mass of a 3mm thick Titanium spherical tank has been calculated for a 29 cm radius, $M_{\text{tank}} = 18.5 \text{ kg}$. Another manner of storing the fuel would be to use two spherical tanks, each weighing 9.3 kg and having a 11 cm radius. The masses and volumes of the propulsion subsystem are listed in Table 1. Table 2 shows a preliminary mass budget for the mission.

TABLE 1 : Mass, Volume Budget of Propulsion Subsystem

#	System	Mass(kg)	Volume(m3)
1	Fuel Tank (empty) Radius = 29cm	18.5	.11 (Titanium,3mm)
1	Fuel Tank (full)	128.5	.11
2	Fuel Tanks(empty) Radius = 11 cm	9.3(ea.)	.055(ea.)
2	Fuel Tanks (full)	64.3(ea.)	.055(ea.)
	Hydrazine Fuel	110	.11
1	Large Thruster	2	.0004
2	Small Thrusters	1	.0008
3	Solenoid Valves	1.4	.0001
	Fuel Lines (2 m)	0.6	.0002

Propulsion Subsystem: 134 kg -- 0.122 m3
Prior to Landing.

Propulsion Subsystem 36 kg -- 0.122 m3
After Landing.

TABLE 2. Preliminary Mass Budget of Subsystems

Total Landed Mass/Landing site: 1000 kg

Balloon Rover: 300 kg

Surface Science/
Computers/Data : 155 kg

Descent Propulsion: 36 kg

Subtotal 491 kg

Remainder 509 kg
to be used for
Ground Systems

Appendix 4.1

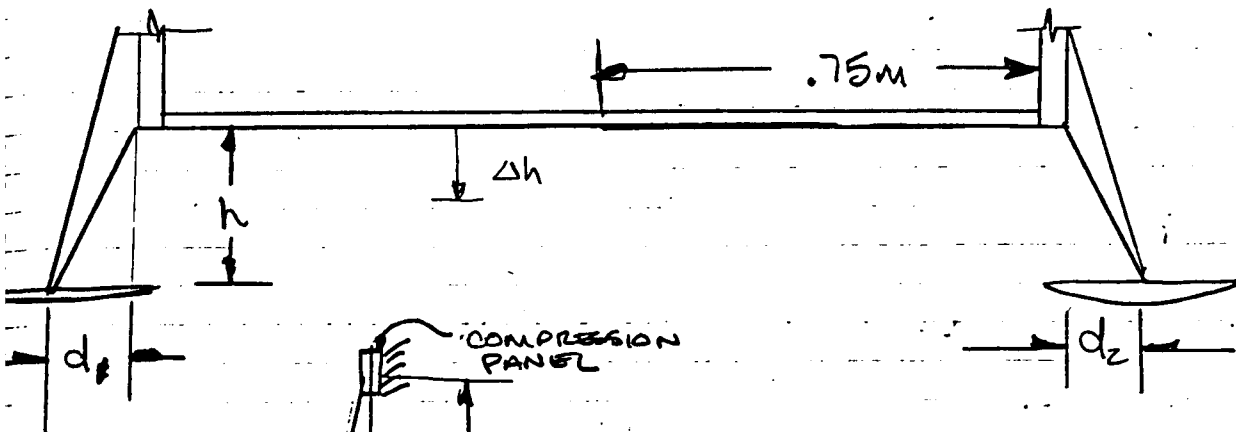
Lander Leg Design/Mass Fraction

LANDER SYSTEM

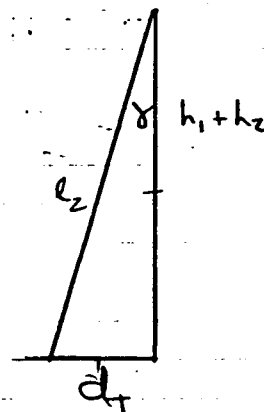
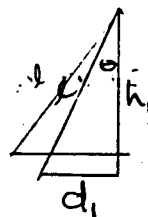
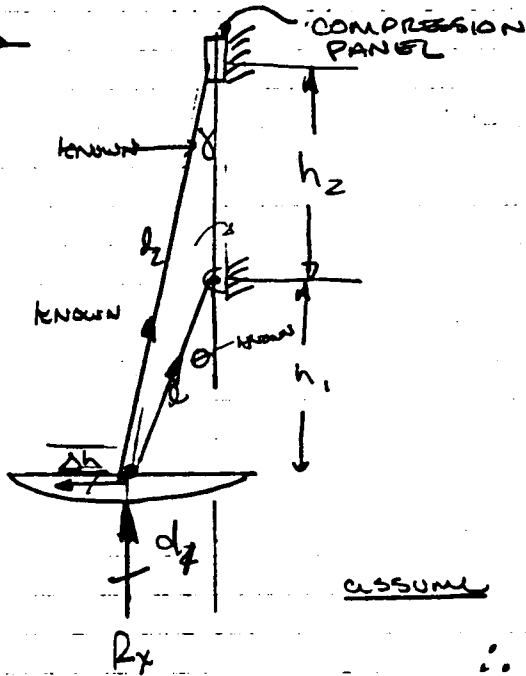
J. CANTRELL

$$A = 3.37 \text{ m}^2$$

MODEL



FBD 1



assume $d_1 = .25 \text{ m}$
 $h_1 = .5 \text{ m}$
 $\therefore l_1 = .56 \text{ m}$
 $\theta_1 = 26.56^\circ$
 $h_2 = h_1$

FIND $\Delta l_2 < \theta < \Delta h_1$

$$\theta_1 = \sin^{-1} \frac{d_1}{l_1}$$

$$l \cos \theta_1 = h_1$$

$$l \cos \theta_2 = h_1 - \Delta h_1$$

$$\Delta h = h_1 - l \cos \theta_2$$

$$\Delta h = l (\cos \theta_1 - \cos \theta_2)$$

SOLVE FOR θ_2

$$.051 = .56 (\cos 26.56^\circ - \cos \theta_2)$$

$$\cos \theta_2 = .8034$$

$$\theta_2 = 36.54^\circ$$

$$d_2 = l_2 \sin 36.54 = .333 \text{ m}$$

ORIGINAL PAGE IS
OF POOR QUALITY

IMPACT ENERGY

$$E_i = \frac{1}{2}(1000)(5)^2 = 12500 \text{ J}$$

$$E_i = F \cdot d$$

$$\bar{a} = \frac{V^2}{2d}$$

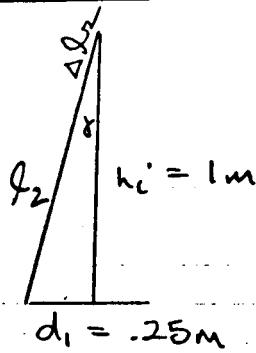
$$a_{\text{peak}} = \frac{F_{\text{max}}}{m} \quad (\text{IN NEWTONIAN COORDINATE SYSTEM})$$

$$\text{design for } \bar{a} = 25(9.81) = 245.25 \text{ m/s}^2$$

$$245.25 \frac{\text{m}}{\text{s}^2} = \frac{25 \frac{\text{m}^2}{\text{s}^2}}{2 \Delta h}$$

$$\underline{\Delta h = .051 \text{ m} = 51 \text{ mm}}$$

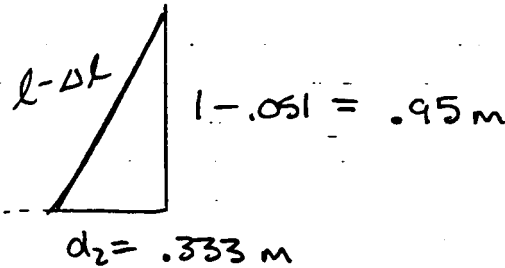
LANDER DESIGN CONT



$$\gamma = 14^\circ$$

$$l_2 = 1.0308$$

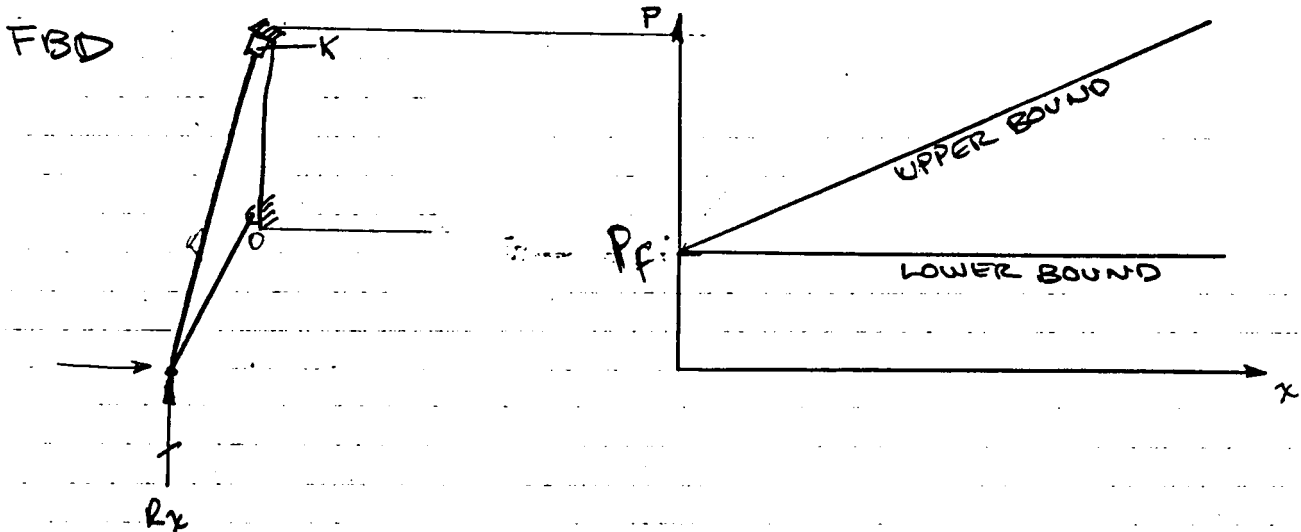
$$\Delta h = .051 \text{ m}$$



ORIGINAL PAGE IS
OF POOR QUALITY

$$l_2 - \Delta l_2 = 1.0068 \text{ m}$$

$$\Delta l_2 = 1.0308 - 1.0068 = 24 \text{ mm}$$



$$\frac{1}{2} m V^2 = 3 \int_0^{.024} k x dx \quad (\text{Upper bound})$$

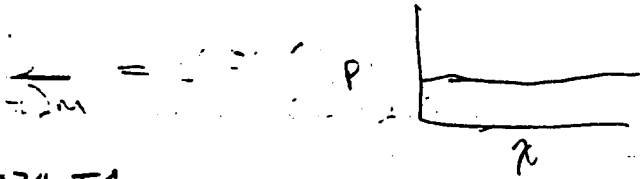
$$k = \frac{2 m V^2}{3(2) x^2} = \frac{m V^2}{3 x^2} =$$

$$\frac{1}{2} m V^2 = 3 P_f A_x(x) \quad (\text{Lower bound})$$

$$A_x = \frac{1}{6} \frac{m V^2}{P_f x} = \frac{1000(25)}{6(1.72 \times 10^6)(.024)} = .1009 \text{ m}^2 \checkmark$$

USE LOWER BOUNDLANDER SYSTEM CONT

$$P_F = 85.5 \text{ MPa}$$

USE UPPER BOUND

$$P_F < 330 \times 10^6 \text{ Pa } 2024\text{-T4}$$

$$\text{assume } P_{\text{fail}} = 290 \times 10^6 \text{ Pa } (87\% \text{ of capacity}) 2024\text{-T4}$$

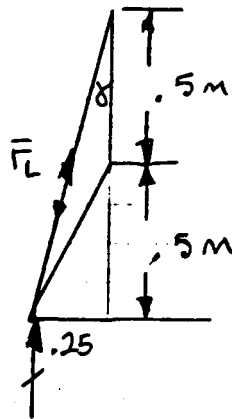
$$A_x = \frac{1000(25)}{6(290 \times 10^6)(.024)}$$

Mass of link

$$V = (6 \times 10^{-4} \text{ m}^2)(1.038) \text{ m} = 6.23 \times 10^{-4} \text{ m}^3$$

$$\rho_{2024\text{-T4}} = 2770 \text{ kg/m}^3$$

$$m = 2770 (6.23 \times 10^{-4}) = \underline{1.73 \text{ kg}}$$

STRUCTURE ANALYSIS

$$\begin{aligned} F_L &= 290 \times 10^6 \text{ Pa} (6 \times 10^{-4} \text{ m}^2) \\ &= 174000.0 \text{ N} \\ &= 174 \text{ kN} \end{aligned}$$

$$\delta = 14^\circ$$

$$\theta = 26.56^\circ$$

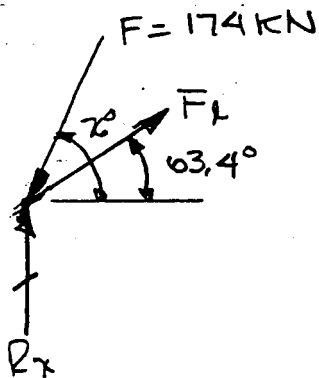
$$168831.5 \text{ N } (3)$$



$$\begin{aligned}\gamma &= 14^\circ \\ \theta &= 26.56^\circ \\ F_L &= 174 \text{ kN} \\ d &= .25 \text{ m} \\ h_1 &= .50 \text{ m} \\ h_2 &= .50 \text{ m}\end{aligned}$$

ORIGINAL PAGE IS
OF POOR QUALITY

FBD #1



LOWER BOUND

$$[\sum F_y = 0]$$

$$174 \cos 14^\circ = R_x + F_L \sin 63.4^\circ$$

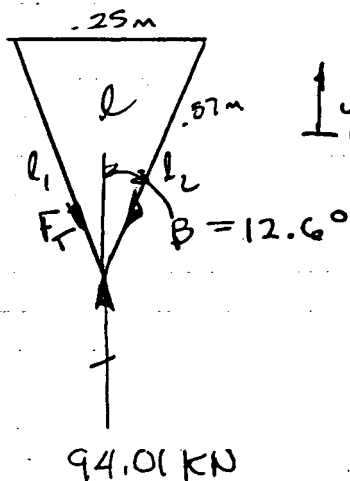
$$R_x = \underline{89.94 \text{ kN}}$$

$$[\sum F_x = 0]$$

$$174 \sin 14^\circ = F_L \cos 63.4^\circ$$

$$\underline{F_L = 94.01 \text{ kN}}$$

TOP VIEW FBD



$$\uparrow y \quad l_1 = l_2 = .56 \text{ m}$$

$$\beta = \tan^{-1} \frac{.125}{.56} = 12.6^\circ$$

$$[\sum F_y = 0] \quad 94.01 = 2 F_T \cos 12.6^\circ$$

$$F_T = 48.16 \text{ kN}$$

Use 2024 T-4 A1 SF = 2

DESIGN LOWER LINES

2024 T-4 Al

$$\sigma_{max} = 330 \times 10^6 \text{ Pa}$$

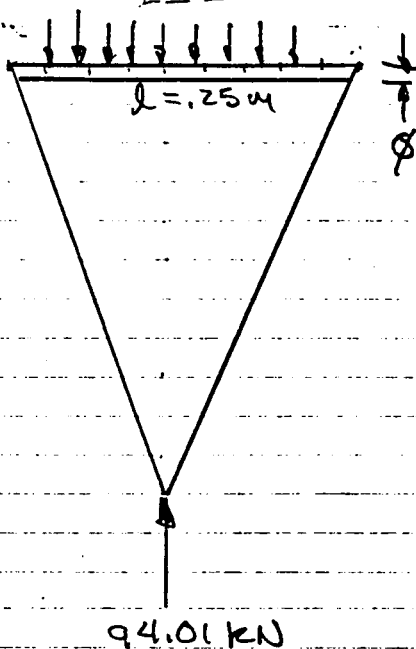
$$A = \frac{2(48.16 \times 10^3)}{330 \times 10^6 \text{ Pa}} = 2.92 \times 10^{-4} \text{ m}^2$$

$$R = \sqrt{\frac{A}{\pi}} = \sqrt{\frac{2.92}{\pi}} = 0.96 \text{ cm}$$

$$\phi = 2(0.96) = \underline{1.93 \text{ cm}}$$

$$\rho = 2770 \text{ kg/m}^3$$

DESIGN SHEAR LINK



THIS PAGE IS
OF POOR QUALITY

2024 T-4 Al

$$\sigma_{max} = 330 \times 10^6 \text{ Pa}$$

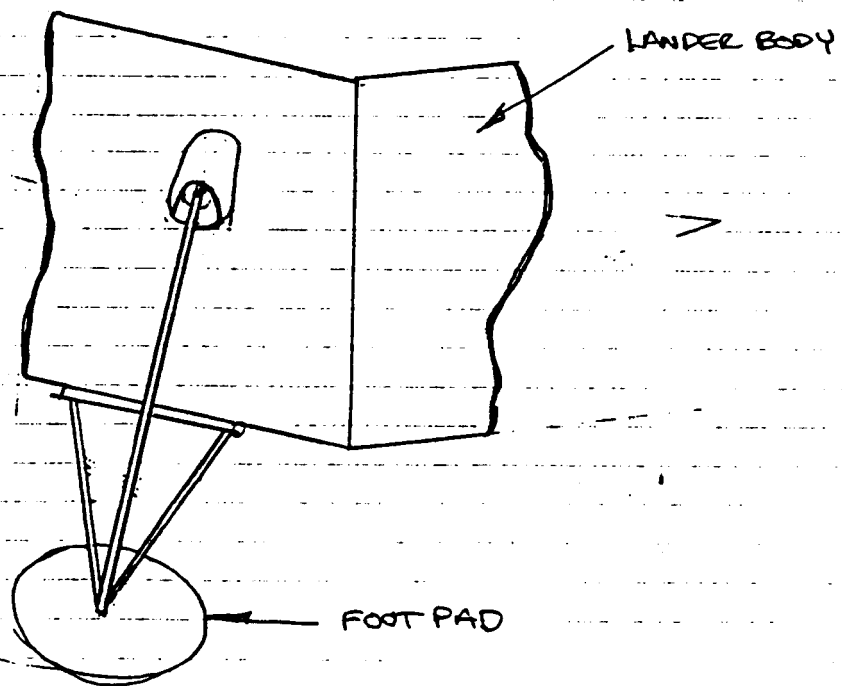
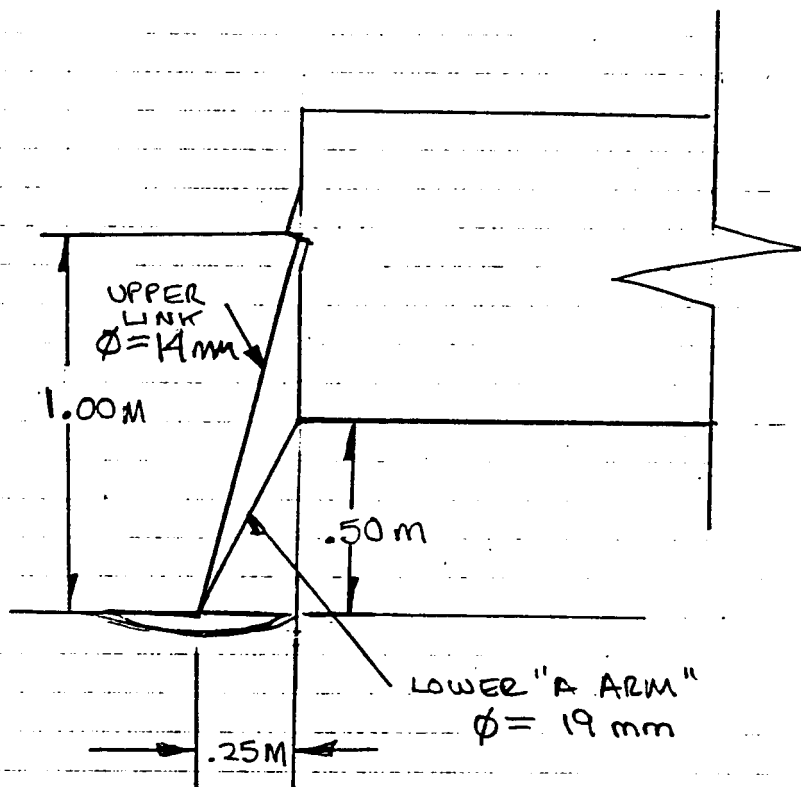
$$\tau = \frac{94.01}{\pi(\phi/2)^2}$$

$$\phi = 2 \sqrt{\frac{94010}{\pi(220 \times 10^6)}} = 23 \text{ mm}$$

$$\text{Mass of link} = \rho V$$

$$= 2770 \text{ kg/m}^3 \left[\pi(0.012)^2(0.25) + (57)(2) \pi(0.0096)^2 \right]$$

$$\approx 1.25 \text{ kg}$$



LANDER MASS FRACTION

		MASS	X	#
+	mass of A-arm (ea)	=	1.25 kg	3
	mass of links (ea)	=	1.73 kg	3

TOTAL MASS FOR (3) above 8.94 kg

MASS OF PODS (ea) \approx * 4.01 kg

* based on a computer program developed by formula 16 on page 366 in [ref. 1] and the use of 2024-T4 alum.

Appendix 4.2

Crushable Lander Volume

APPENDIX 1.2

ANTRECC

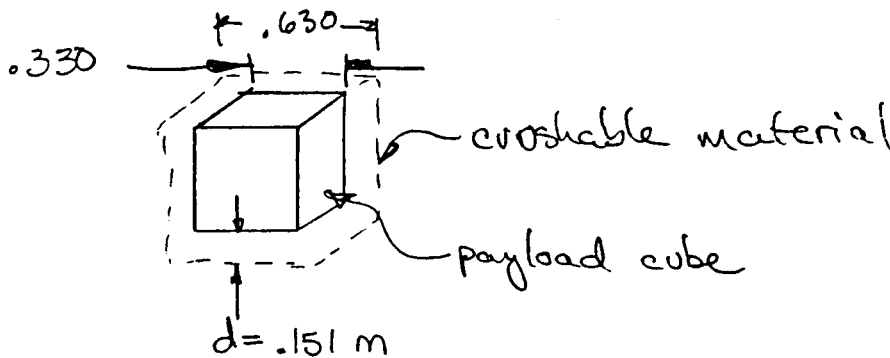
$$V^2 = 2as$$

$$s = \frac{V^2}{2a}$$

a is max. deceleration average
V is landing velocity
s is deflection distance

$$s = \frac{25}{2(9.81)(25)} = 51 \text{ mm}$$

using a safety factor of three:
d for material becomes .151 meters



$$\text{Volume} = (.630)^3 - (.330)^3 = .25 \text{ m}^3 = .25$$

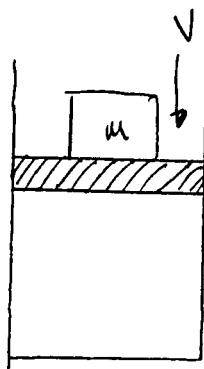
Appendix 4.3

Pressure Bladder Design

CONSIDER THE SYSTEM:

$$K_e = \frac{1}{2} m V^2$$

$$W_{12} = P_1 V_1 \ln \frac{V_2}{V_1} \quad (1a)$$



OBJECTIVE: COMPARE the work done on an ideal gas where $PV = \text{const.} = nRT$ with the first law of thermodynamics

FIRST LAW OF THERMODYNAMICS: (GENERAL FORM)

$$\dot{Q} = \dot{W}_{\text{out}} + \int_{A_c} e(pV dA) - \int_{A_i} e(pV dA) + \frac{d}{dt} \int e p dV$$

FOR A CLOSED SYSTEM F.L.T. becomes:

$$Q_{12} = W_{12} + m(u_2 - u_1)_{\text{sys}} \quad (1.b)$$

CONSIDER AN ADIABATIC SYSTEM (IDEALIZED)

$$W_{12} = m_g(u_1 - u_2)_{\text{sys}} \quad (1c) \quad \begin{matrix} m = 50 \text{ kg} \\ V = 5 \text{ m/s} \end{matrix}$$

$$W_{12} = -\frac{1}{2}(50)(25) = -625 \text{ J}$$

assume: ideal gas (unknown)

compare with the $PV = nRT$

$$P_1 V_1 = nRT_1$$

start with $P_1 = 56.37 \text{ kPa}$
 $V_1 = .7 \text{ m}^3$

$$V_1 - V_2 = .011 \text{ m}^3$$

$$56370.57(.7) = nRT_1 = 39459.4$$

assume $T_1 = T_{\text{ambient}} \approx 250 \text{ K}$

C-2

Use H_2 $R = 2077$

$$(P_{\text{atm}}) 39459.4 = m \left(2077 \frac{\text{Pa m}^3}{\text{kg K}} \right) (250 \text{ K}) \quad \checkmark$$

Mass = .076 kg (independent quantity)

$$mRT_2 = P_2 V_2$$

$$\left(.076 \times 2077 \frac{\text{Pa m}^3}{\text{kg K}} \right) T_2 = P_2 V_2 = P_2 (.7 - .011) \text{ m}^3 \quad (2a)$$

$$= P_2 (.689)$$

two unknowns and one equation

consider the closed system - First law eqn 1.b & 1.c

$$W_{12} = M_{\text{gas}} (U_1 - U_2)_{\text{sys}} = 625 \text{ J} \quad \text{(kinetic energy of payload is equal to the work done on the sys.)}$$

(work is neg. if done on system)

$$-625 = .076 (C_p T_1 - C_p T_2) = .076 C_p (T_1 - T_2)$$

$$-625 \text{ J} = (.076) \left(\text{kg} \right) \left(5,192.6 \frac{\text{J}}{\text{kg K}} \right) (250 \text{ K} - T_2)$$

$$\underline{T_2 = 251.58 \text{ K}}$$

according to first law of thermo
using $W_{12} = 625 \text{ J}$ (payload K_c)FIND P_2 with $P_2 V_2 = mRT_2$

$$\text{kg} \left(.076 \right) \left(2077 \frac{\text{Pa m}^3}{\text{kg K}} \right) (251.58 \text{ K}) = P_2 (.689) \text{ m}^3$$

$$P_2 = 57637.75 \text{ Pa by } P_2 V_2 = mRT_2 \quad \text{(actual by F.L.T.)}$$

check P_2 by $P_2 V_2 = P_1 V_1$ and find error

$$P_2 (\text{ideal}) = \frac{P_1 V_1}{V_2} = \frac{(56370.57)(.7)}{(.7 - .011)} = 57270.54$$

$$\% \text{ error} = \left(100 \right) \left(1 - \frac{P_2 \text{ actual}}{P_2 \text{ ideal}} \right) = 100 \left(1 - \frac{57637.75}{57270.54} \right)$$

$$\% \text{ err} = .64 \%$$

CONSIDER SIMILAR SYSTEM, DEVELOP SEQUENCE:

- 1. BLADDER EXISTS AT P_1, T_{amb} , mass initially
- 2. equating payload kinetic energy with an amount of work done by the pressure bladder.
- 3. in any case of impact, pressure will increase and volume will decrease with a rigid containment therefore the product PV may very well remain close to const.

PROBLEM STATEMENT: find the % error in the final pressure of the pressure bladder system given arbitrary initial and Boundary conditions

SOLUTION: assume Air as gas, a small initial volume, and a corresponding initial pressure, initial temp is a boundary condition for the final volume. Find the ideal final pressure by $P_1 V_1 = \text{const} = P_2 V_2$ and compare with the actual final pressure by the first law of thermodynamics.

GOVERNING EQUATIONS:

First Law for closed system

$$Q_{12} = W_{12} + m(U_2 - U_1)_{\text{sys}} \quad (1-1)$$

Q_{12} becomes zero as heat transfer is most likely to be negligible during $\Delta t = 0.047 \text{ sec}$ in which the event takes place.

First Law becomes:

$$W_{12} = m(U_2 - U_1) \quad (1-2)$$

for air $c_p = \text{const}$

$$W_{12} = m(c_p)(T_2 - T_1) \quad (1-3)$$

the ideal P_2 is:

$$P_1 V_1 = nRT = \text{constant} = P_2 V_2 \quad (2-1)$$

$$P_2 = \frac{P_1 V_1}{V_2} \quad (2-2)$$

SOLUTION:

solve for q actual:

initial conditions

$$V_1 = .5 \text{ m}^3 \quad T_1 = T_{\text{amb}} \approx 200 \text{ K}$$

$$V_2 = .5 \text{ m}^3 - .011 \text{ m}^3 = .489 \text{ m}^3$$

$$P_1 = 101 \text{ kPa}$$

$$P_1 (.5 \text{ m}^3) = m_g \left(\frac{287 \times 10^3 \text{ (N.m)}}{\text{kg K}} \right) (200 \text{ K})$$

$$m_g = .88 \text{ kg} = \text{constant}$$

F.L.T. equation (1-3) $U_k = W_{12}$

$$625 \text{ J} = .88 \left(\frac{1005 \text{ J}}{\text{kg K}} \right) (T_2 - 200 \text{ K})$$

$$\underline{T_2 = 200.707 \text{ K}}$$

$$P_2 (.489 \text{ m}^3) = .88 \text{ kg} \left(\frac{287 \text{ N.m}}{\text{kg K}} \right) (200.707 \text{ K})$$

$$P_2 = 103661.67 \text{ Pa}$$

solve for P_2 ideal

$$P_2 V_2 = P_1 V_1 \quad P_2 = \frac{P_1 V_1}{V_2}$$

$$P_{2 \text{ ideal}} = \frac{101000 (0.5 \text{ m}^3)}{.489 \text{ m}^3} = 103271.98$$

$$\begin{aligned} \text{d}^\circ \text{error} &= 100 \left(1 - \frac{P_{2 \text{ actual}}}{P_{2 \text{ ideal}}} \right) \\ &= 100 \left(1 - \frac{103661.7}{103272} \right) \end{aligned}$$

$$\boxed{= .37 \%}$$

CONCLUSION:

given an arbitrary example, the temperature difference encountered is not significant to induce significant error in the final pressure and therefore the final work from the ideal conditions. Therefore a workable equation for the pressure bladder would be:

$$W_{12} = P_1 V_1 \ln \frac{V_2}{V_1}$$

For any ideal or perfect gas

PRESSURE BLADDER DESIGN

J. KANTRELL

MODEL



KINETIC ENERGY OF PAYLOAD -

$$\frac{1}{2} M V_i^2 = U$$

V_i = impact velocity
 M = mass payload

WORK DONE BY PRESSURE BLADDER

$$W_{12} = \int_1^2 \delta W = \int_1^2 P dV$$

if one assumes an ideal/perfect gas:

$$PV = mRT \rightarrow PV = \text{constant}$$

during the $\approx .047$ second compression interval,
the temperature change $\approx 0\%$ therefore:

$$W_{12} = \int_1^2 \frac{C dV}{V} = C \ln \frac{V_2}{V_1} = P_1 V_1 \ln \frac{V_2}{V_1}$$

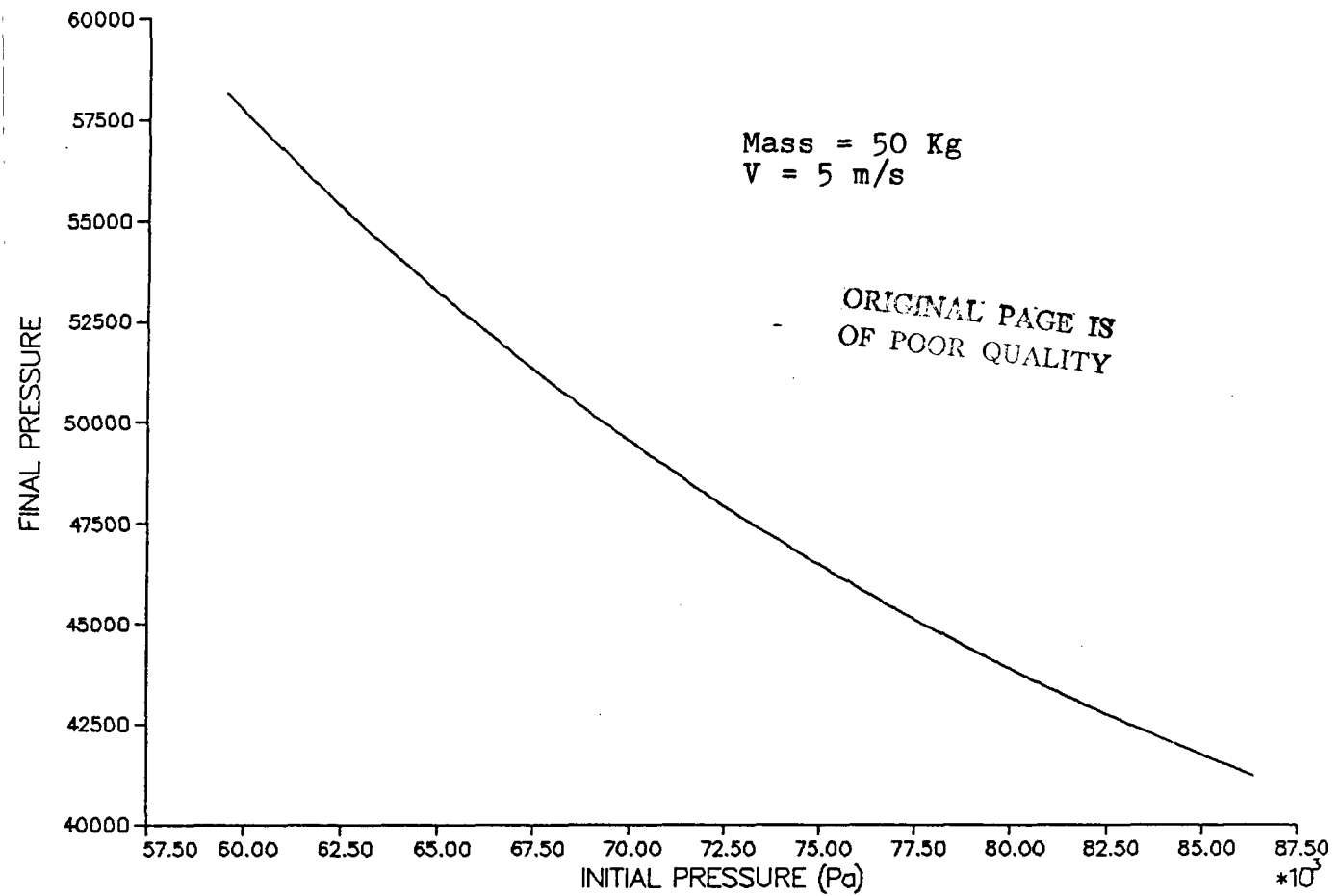
so by the P.G. Law

$$P_1 V_1 = P_2 V_2 \quad \text{it can be shown that;}$$

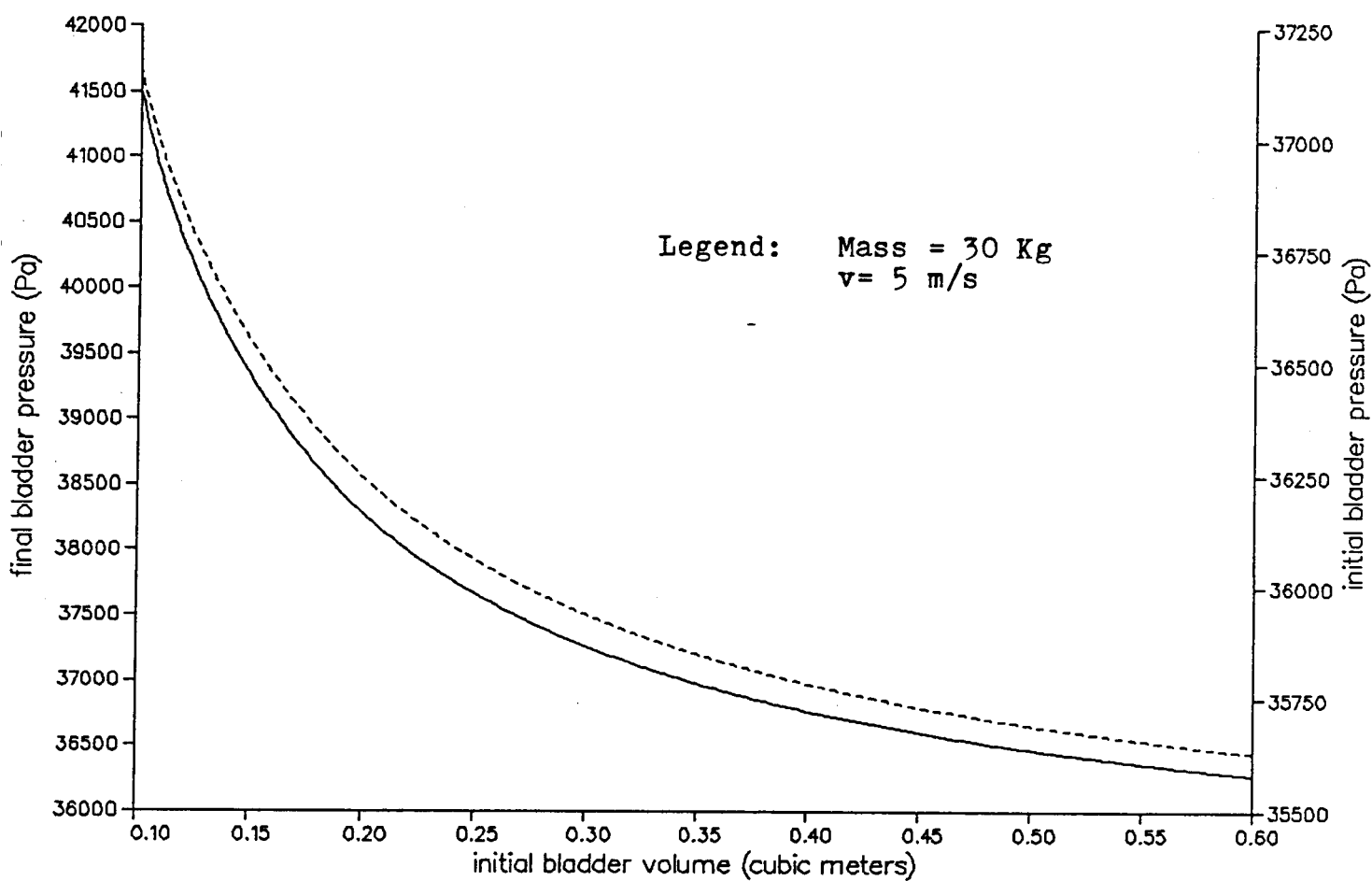
$$P_1 = \frac{U}{2 V_1 \ln \left(\frac{V_1 + DV}{V_1} \right)} \quad \text{where } V_2 - V_1 = DV$$

* see appendix for further analysis on this important assumption

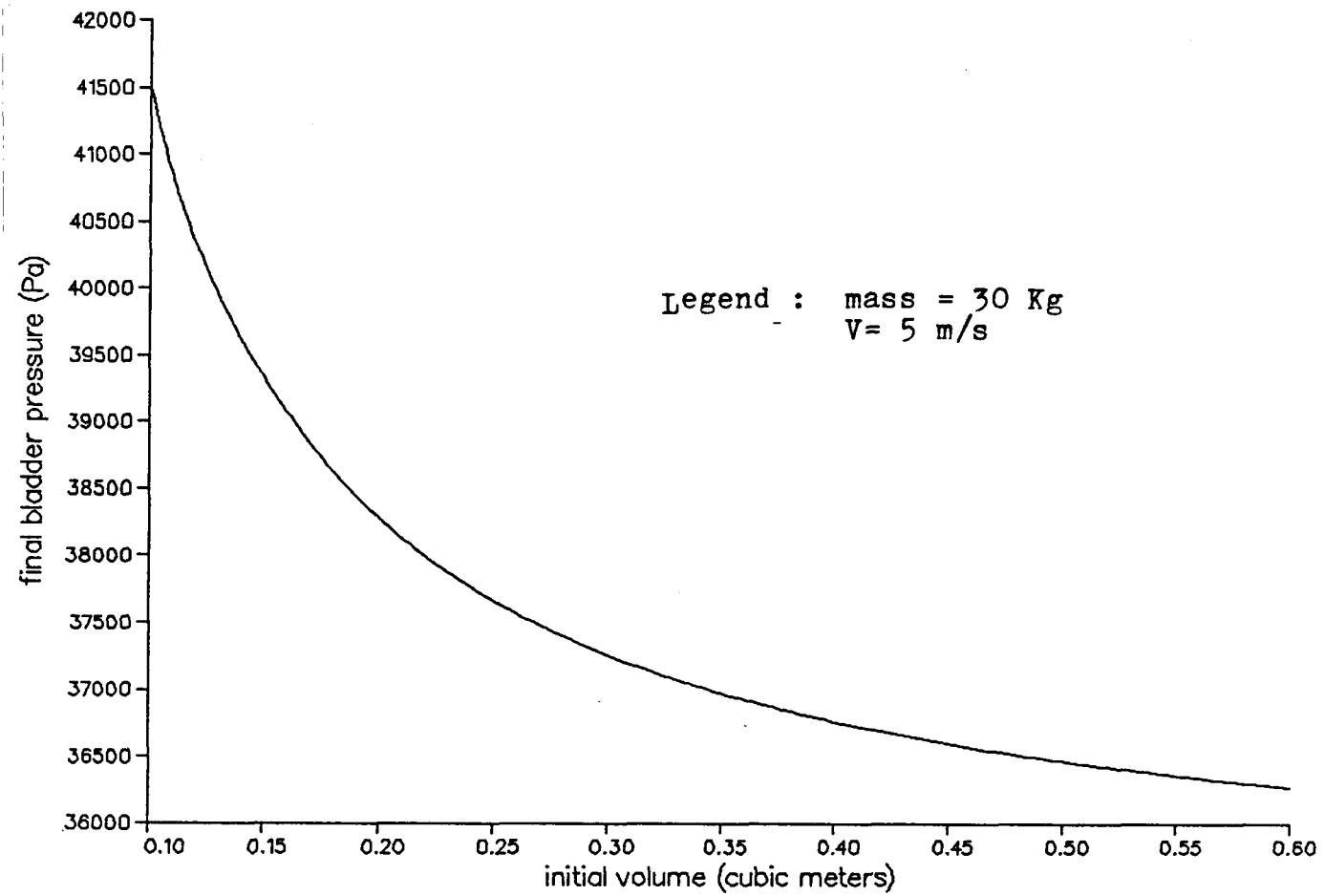
PRESSURE BLADDER P1-P2



Pressure Bladder P1-P2-V1

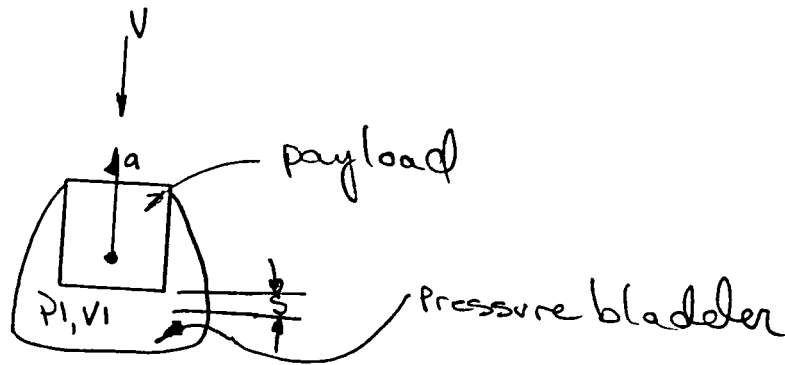


Pressure Bladder P1-V1



Appendix 4.4

Payload Deceleration



where
 a_{max} = payload deceleration limit
 m = payload mass
 V = impact velocity
 δ = bladder deflection during impact
 a = payload deceleration
 A_x = payload cross section area

from Appendix 4.3) $\frac{1}{2} m V^2 = P_1 \cdot V_1 \cdot \ln(V_2/V_1) = P_1 \cdot V_1 \cdot \ln(V_1 - DV/V_1)$

where $DV = \frac{A_x (V^2)}{2(A_{MAX})}$

$$P_1 \cdot V_1 = P_2 \cdot V_2 \Rightarrow P_2 = \frac{P_1 \cdot V_1}{V_1 - DV}$$

then solving for payload deceleration
 $[F=ma]$ (valid for Newtonian coordinate system shown)

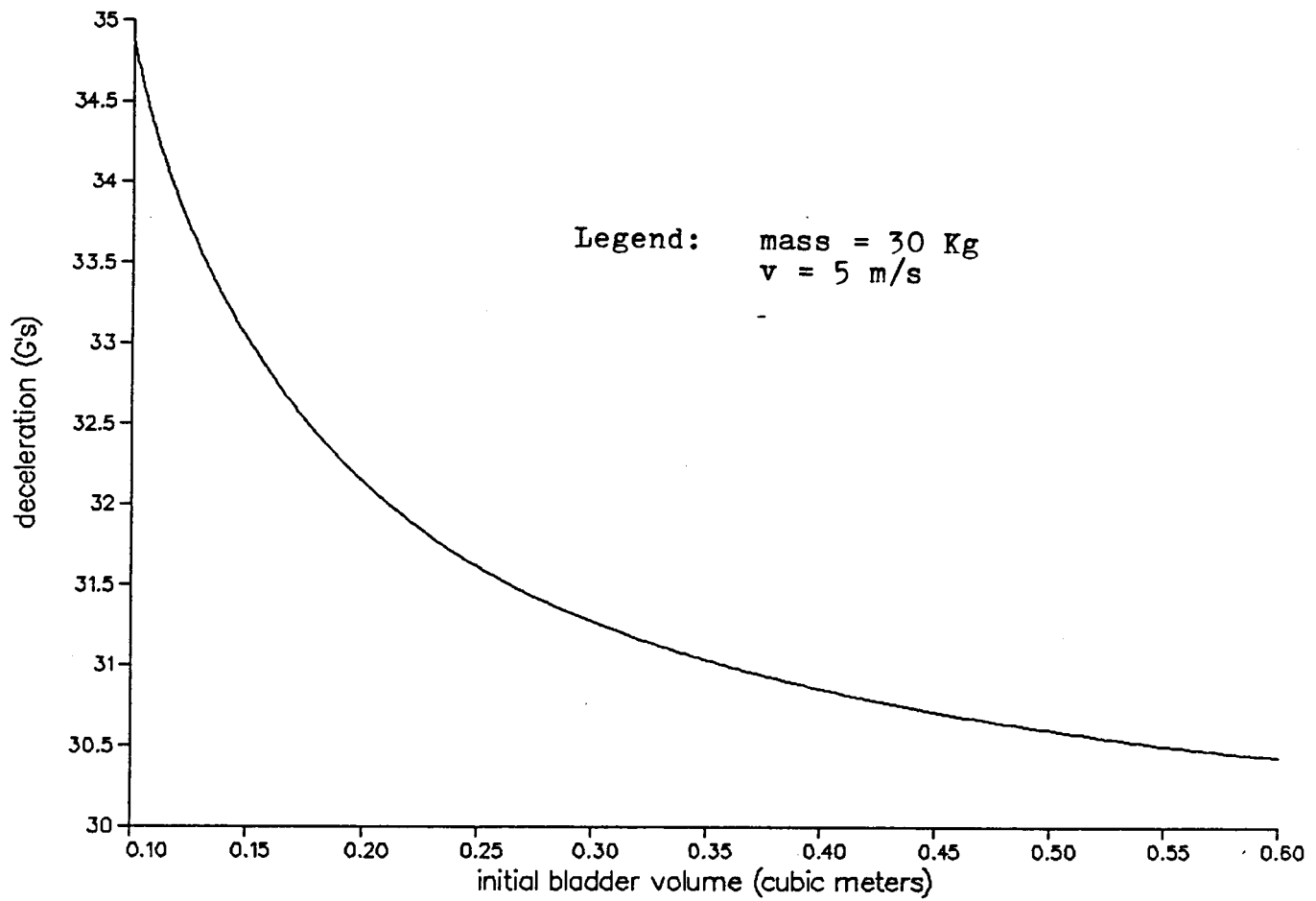
$$F_2 = P_2 A_x = m a$$

a becomes:

$$a = \frac{P_1 \cdot V_1 \cdot A_x}{\left[V_1 - \frac{A_x V^2}{2 A_{MAX}} \right] m}$$

ORIGINAL PAGE IS
OF POOR QUALITY

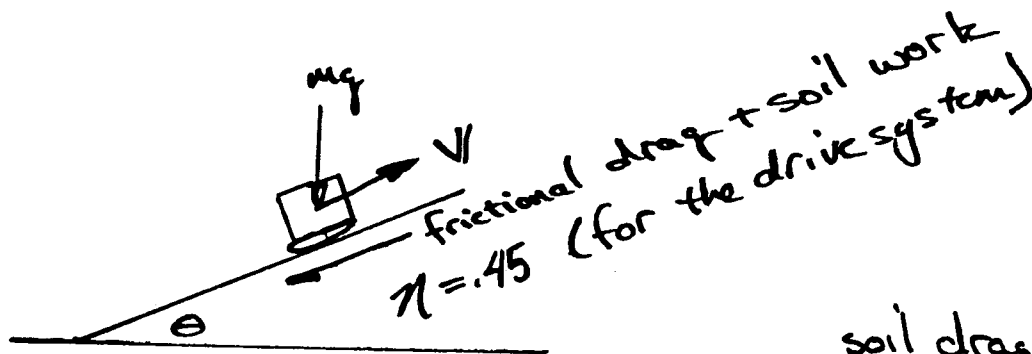
Pressure Bladder Deceleration



Appendix 4.5

Rover Locomotion Requirements

POWER LOCOMOTION REQUIREMENTS:



soil drag term *

$$\text{Power } \left(\frac{\text{N} \cdot \text{m}}{\text{s}} \right) = \frac{m \cdot g \cdot V (\sin \theta)}{.45} + \frac{V}{.45} (6) e^{\frac{\lambda m g}{6}}$$

of wheels

From Planetary spacecraft systems: [Ref. 2]

<u>slope</u>	<u>% of dist. covered</u>
0	9.5
1	10.8
3	12.4
5	12.4
10	11.0
15	2.7
20	0.8
35	0.2

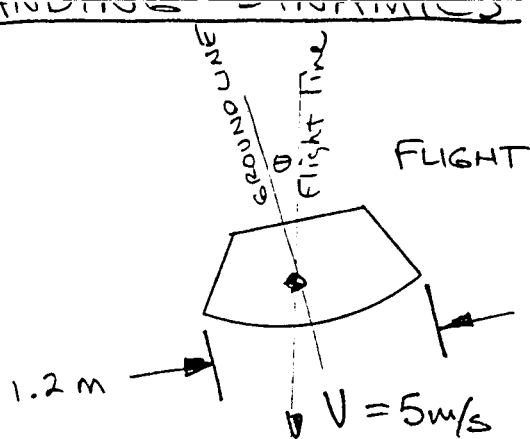
the average slope (for the average power req'd) was chosen as 5°

the largest slope, for peak power, was not expected to exceed 35°, this slope was chosen as max. slope

from motion resistance chart in [Ref. 2] appendix B-7, where λ is a curve-fit variable = .02025 for a 40 in x 10 in wheel, and assuming a six wheeled mobility system.

Appendix 4.6

Shell Lander Dynamics



assume:

$$m = 300 \text{ kg}$$

$$h = .5 \text{ m}$$

$$V_i = 5 \text{ m/s}$$

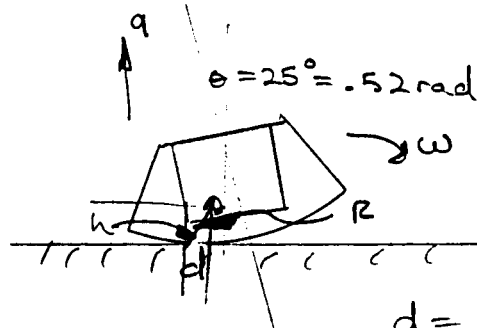
$$\theta_i - \theta_f = 25^\circ$$

$$a = -5(9.81) \text{ m/s}^2 \text{ (a low estimate)}$$

$$U = \frac{1}{2} m V^2 = \frac{1}{2} (300)(5)^2$$

$$= 3750 \text{ J}$$

LANDING



$$I \approx \text{const} \approx 300(.5)^2 = 75 \text{ kg m}^2$$

* $h \approx \text{constant}$ over θ rotation

$$d = .5 \text{ m} \sin 25^\circ = .21 \text{ m}$$

$$\begin{aligned} \uparrow d\theta &= m a(r) \int_0^{.52} \sin \theta d\theta \\ &= m a r (-\cos \theta) \Big|_0^{.52} \end{aligned}$$

$$[\sum F_{cg} \uparrow = m a]$$

$$= m a r (1 - .87) = m a r (.13)$$

$$= 300(5)(9.81)(.13)(.5)$$

$$= 956.5 \text{ J}$$

ORIGINAL PAGE IS
OF POOR QUALITY

translation into rotational energy

$$956.5 \text{ J} = \frac{1}{2} (75) \omega^2 \quad \omega = 5.05 \text{ rad/s}$$

$$956.5 = m g h = 300(3.73) \Delta h_{cg}$$

$$\Delta h_{cg} = .85 \text{ m}$$

CONCLUSION: for a spherical bottom shell:

Δh_{cg} is too much to properly counter the rotational energy, thus the lander will roll over with only moderate decelerations and no side friction on the payload, and no horizontal velocity.

Appendix 4.7

Speed of Sound in Martian Atmosphere

SPEED OF SOUND ON MARS

ATMOSPHERE : 95.32 % CO2 N=48
 2.7 % N2 N=4
 1.6 % ARG N=39.94

The speed of sound in any atmosphere is given by $c = \sqrt{g k R T}$ (2)
 in feet/s = 1/3.28 m/s .

g: gravitacionnal constant

k: ratio of specific heat

R: gas constant

T: temperature (degre Rankine = Farenheit + 460)

- gravitation : $g = g(\text{earth})/3 \rightarrow g = 10.77 \text{ ft/sec}$

- ratio of specific heat : CO2 N2
 1.285 1.4 (1)

considering only these 2 major elements we have 98% of the atmosphere .

$$k(100\%) = (1.285 \times 0.953 + 1.4 \times 0.027) / 0.98 = 1.2882$$

- gas constant : CO2 N2
 35.1 55.15

$$R(100\%) = (35.1 \times 0.953 + 55.15 \times 0.027) / 0.98 = 35.65$$

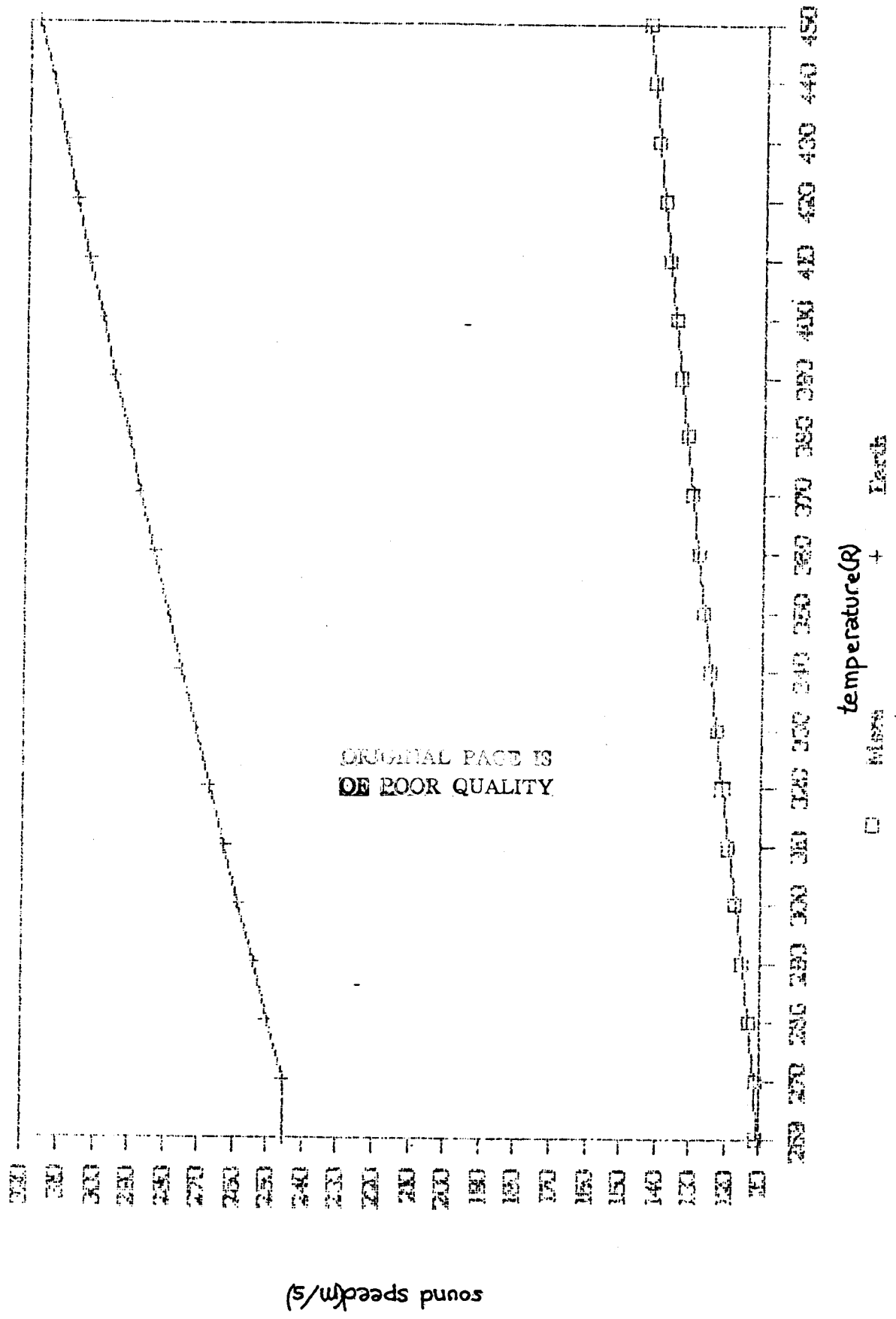
---> so we get $c = 22.24 \sqrt{T}$ feet/s = $6.78 \sqrt{T}$ m/s

comparaison	Earth	Mars
g	32.2	10.77
k	1.4	1.29
R	53.3	35.65
C	49.08	22.24

- Temperature : -24 degrees F \rightarrow -191 F
 that is 436 R \rightarrow 269 R

ref: (1) Fundamentals of Classical Thermodynamics. Van Wylen, 1973. Table A.9.

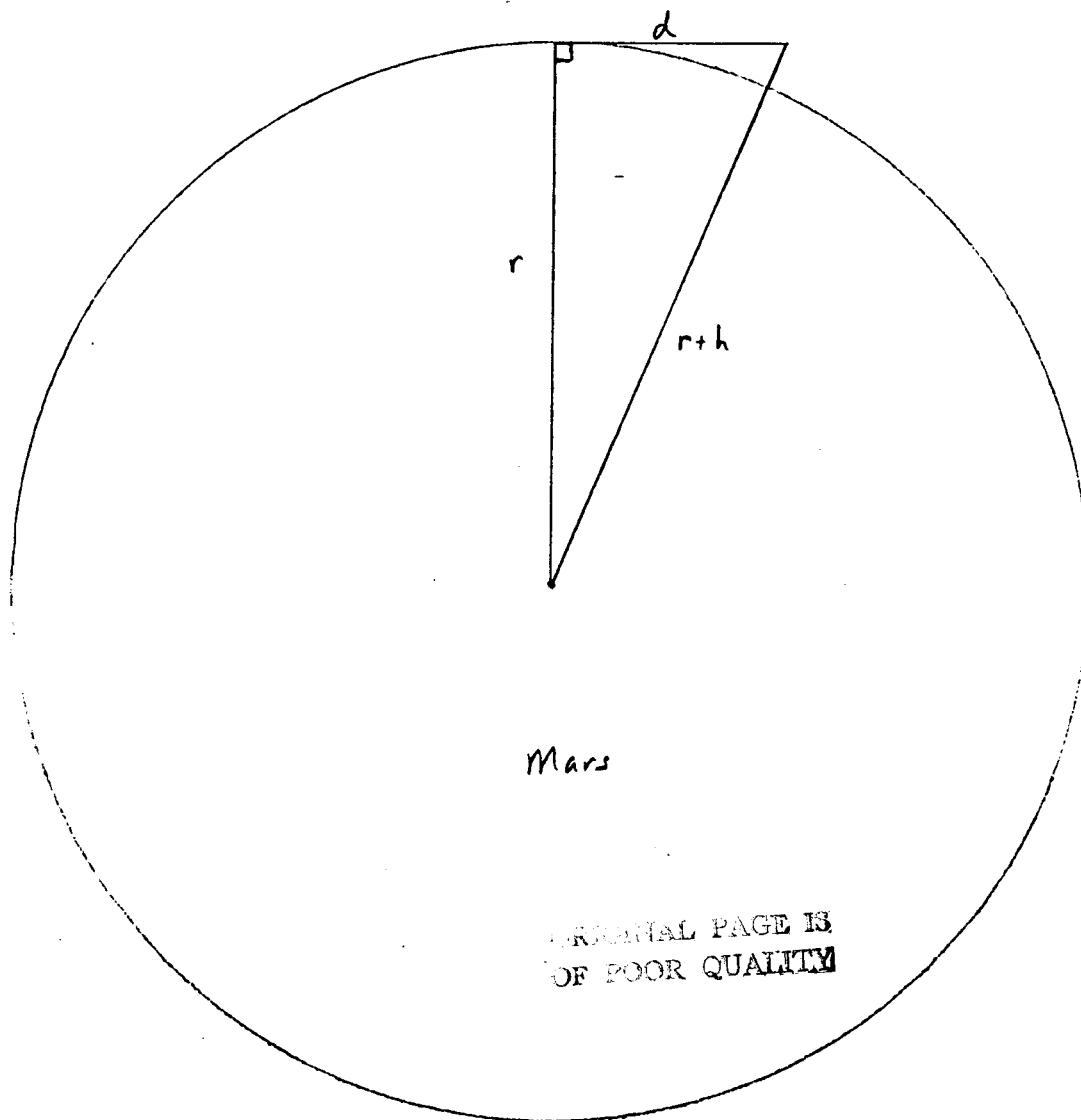
(2) magazine : Robotics Age ,7/85, " A Multielement Ultrasonic Ranging Array."



Appendix 4.8

Line of Sight Distances on Mars

Approximate Line of Sight distances on Mars



$$(r+h)^2 = r^2 + d^2$$

$$d = [(r+h)^2 - r^2]^{\frac{1}{2}}$$

r = mean radius of mars (3400 km)

h = antenna height

d = line of sight distance to surface from top of antenna

Appendix 5.1

Balloon Lifting Force Program Code

C PROGRAM BALON2.FOR BY GRANT WILLIAMS & S. ALI SIAHPUSH 3-20-87

C THIS PROGRAM WILL CALCULATE THE BALLOON'S LIFT FORCE.
C $P_{in}=P_{out}$. THIS PROGRAM IS ALSO CAPABLE OF EVALUATING A
C HOT AIR BALLOON LIFT.

PROGRAM BALON

REAL MWGAS,MWOUT,LIFT
CHARACTER*1 ANS,OUTPUT*8
ARDEN=.0508 !area density of the balloon material (kg/m²)
WRITE(*,*)'ENTER GAS T (K), MOLAR WT., ALTIT. (KM)'
READ(*,*)TIN,MW,ALT
MWGAS=2. ! molecular weight of the balloon gas (Hydrogen)
MWOUT=44. ! molecular weight of the Mars atmosphere
ALT=2.0 ! cruising altitude (km)

GCON=(ATM-GR/MOLE)/(LIT-ATM/MOLE-K)/K

GCON=.0821 ! ideal gas constant

WRITE(*,101)

101 FORMAT(1X,'R BAL. (M)',2X,'BAL.MAS. (KG)',2X,'GAS MAS. (KG)',2X,
+'PAYLOAD',4X,'TOTAL',3X,'% PAY/TOT')

WRITE(*,102)

102 FORMAT(40X,'MASS (KG)',2X,'MASS (KG)')

DENSITY PROFILE OF THE MARS ATMOS.

PI=3.14159

DMAR=(1.43E-2)*EXP(-ALT/11.3) ! Mars density (kg/m³)

TOUT=220. ! ambient temperature (K)

P=DMAR*GCON*TOUT/MWOUT ! pressure (N/m²)

DO 10 I=18,27,3

WRITE(*,*) 'ENTER THE NAME OF THE OUTPUT FILE (<=8 CHAR.)'

READ(*, '(A)')OUTPUT

OPEN(12,FILE=OUTPUT,STATUS='NEW')

R=I ! radius of the balloon (m)

TIN=220. ! balloon gas temperature (K)

BALMAS=4.*PI*R**2*ARDEN ! balloon material mass (kg)

VOLUME=4.*PI*R**3/3.

DO 20 J=1,20

DGAS=P*MWGAS/GCON/TIN ! density of the balloon gas (kg/m³)

LIFT=VOLUME*(DMAR-DGAS)-BALMAS ! (kg)

TOTAL=LIFT+BALMAS+VOLUME*DGAS ! total mass of the system (kg)

PERCE=LIFT/TOTAL

DELT=TIN-TOUT

WRITE(12,*)DELT,lift

WRITE(*,*)R,DELT,lift

TIN=TIN+20.

WRITE(*,100)R,BALMAS,VOLUME*DGAS,LIFT,TOTAL,PERCE

20 CONTINUE

10 CONTINUE

100 FORMAT(1X,F4.1,4(7X,F6.2),3X,F6.3)

STOP

END

Appendix 5.2

Balloon Convection and Radiation Analysis Program Code

C PROGRAM BALON5.FOR BY S. ALI SIAHPUSH 2-10-87

C CONVECTION & RADIATION ANALYSIS
C H=CONVECTION HEAT TRANSFER COEF. (W/m²/K)
C THIS PROGRAM IS BASED ON THE 'H' BEING ONLY FUNCTION OF RADIUS
C OF THE DISC

PROGRAM BALON4

CHARACTER*10 NAME

TO=180. !ambient temperature (K)

E=0.9 !emissivity of the surface

Z=5.67E-8 !Stefan-Boltzmann constant (W/m²/K⁴)

GS=580. !Solar flux (W/m²)

GM=70. !reflected Mars flux (W/m²)

DO 10 I=1,5

WRITE(*,*)'ENTER THE OUTPUT FILE NAME'

READ(*, '(A)')NAME

OPEN(12,FILE=NAME,STATUS='NEW')

DO 20 J=18,30

TS=320. !surface temperature (K)

R=J !radius of the disc

H=.0168/(2.*R)*(13.75*R**(.75)+28.36*R)

NUMERICAL SOLUTION (NEWTON METHOD)

DO 30 K=1,50

FTS=E*(GM+GS)-2.*E*Z*(TS**4-TO**4)-2.*H*(TS-TO)

DFTS=-8.*E*Z*TS**3-2.*H

TS=TS-FTS/DFTS

CONTINUE

WRITE(*,*)R,TO,TS

WRITE(12,*)R,TS

CONTINUE

TO=TO+10.

CONTINUE

STOP

END